NASA TECHNICAL MEMORANDUM

NASA TM X-73,114

NASA TM X-73,114

A PRIMER OF BASALTIC AND STRATIFORM IGNEOUS ROCKS AND THEIR EXTRATERRESTRIAL ANALOGS

T. E. Bunch

Ames Research Center
Moffett Field, California 94035

April 1976

1. Report No.	2. Government Accession No.	3. Recipient's Catalog No.
NASA TM X-73,114		

4. Title and Subtitle	5. Report Date
A PRIMER OF BASALTIC AND STRATIFORM IGNEOUS ROCKS AND THEIR EXTRATERRESTRIAL ANALOGS	6. Performing Organization Code

7. Author(s)	8. Performing Organization Report No.
T. E. Bunch	A-6495
	10. Work Unit No. 195-21-04
9. Performing Organization Name and Address	11. Contract or Grant No.
NASA Ames Research Center Moffett Field, California 94035	
	13. Type of Report and Period Covered
12. Sponsoring Agency Name and Address	Technical Memorandum
National Aeronautics and Space Administration Washington, D. C. 20546	14. Sponsoring Agency Code

15. Supplementary Notes

16. Abstract

The material presented in this article attempts to convey basic textural, chemical, and mineralogical information to people with limited geological knowledge who are interested in basaltic rocks. Basaltic and stratiform igneous rocks are extremely important for understanding the origin and evolution of the terrestrial planets, their satellites, and asteroids. Comparative planetology studies over recent time show that basaltic rocks have formed by total or partial melting of pre-existing materials through geologic time. Differentiation of terrestrial planets as shown by research on lunar, meteoritic, and terrestrial basalts, was probably initiated very early in their history. The moon and possibly the achondritic meteorite parent body generated basalts for at least IAE after their formation; the earth is still an evolving planet and basalts flow somewhere in or on the earth every day.

Much of the contents of this article deal with textural interpretation and mineralogy of terrestrial basalts and cumulate rocks, and similarities with extraterrestrial analogs are presented.

17. Key Words (Suggested by Author(s))	18. Distribution Statement
Basalts, Stratiform igneous rocks, Cumulate rocks, Basalt textures, Lunar basalts, Meteorite basalts, Phase petrology, Origin of basaltic rocks, Tholeiitic basalts, Basaltic pyroxenes, Mineral calculations, Phase diagrams	Unlimited STAR Category – 42

19. Security Classif. (of this report)	20. Security Classif. (of this page)	21. No. of Pages	22. Price*
Unclassified	Unclassified	79	$4.75

*For sale by the National Technical Information Service, Springfield, Virginia 22161

PREFACE

Perhaps the most valuable result of all education is the ability to make yourself do the thing you have to do when it ought to be done whether you like it or not. This is the first lesson to be learned.

T. Huxley

This primer is concerned with a basic description of basaltic and layered intrusive rocks with emphasis on textures. In general, texts on basaltic rocks devote little attention to the needs of the beginning student or the lay person. Throughout the early years of research on lunar rocks, many nongeological scientists were perplexed by the "strange" terminology used by geologists to describe basalts. During my tenure as a visiting professor to two colleges, I found that many aspects of basaltic textures and nomenclature are not easily understood by most students nor are source books that provide an insight into basaltic and stratiform igneous rocks (cumulates) readily available.

Although this effort is not complete, even on the simplistic approach, it does offer the reader limited information about these rocks; references to the scientific literature are included to cover the gaps that may exist in this presentation.

TABLE OF CONTENTS

1. TERRESTRIAL BASALTS

It often occurs to me to envy the future for what it will know about the past.

B. Berenson

1.1 INTRODUCTION

Basaltic and layered intrusive rocks are formed by the cooling and solidification of a hot mobile liquid called magma. The magma forms through partial or total melting of preexisting rocks in response to a heat source. The kinds of mineral phases that form during cooling of the magma, their composition, and resulting rock textures depend primarily on the bulk composition of the magma, temperature, pressure (total), partial pressure of O_2 or fO_2, cooling rate, H_2O, and gaseous contents. Basaltic rocks are formed from magmas that result from the partial melting of mafic or ultramafic rocks (mafic refers to a rock consisting mainly of mafic or ferromagnesian minerals; ultramafic refers to a mafic rock that contains >70 percent mafic or ferromagnesian minerals). Layered intrusive rocks typically form through the action of crystal settling from tholeiitic basaltic magmas.

An initially homogeneous magma may divide into fractions of different compositions by a process known as differentiation. Commonly, differentiation occurs through fractional crystallization of the magma. As the solid phases form and separate from the magma, the equilibrium between succeeding phases and liquid shifts to accommodate the chemical changes. To maintain equilibrium as temperature drops, each formed crystal reacts with the liquid and changes in composition. A continuous series of homogeneous reaction products may be produced that is slightly different in composition from the earlier formed products; for example, each formed calcic plagioclase changes progressively with reaction and falling temperature to form more sodic varieties, thus a *continuous reaction* series. Ferromagnesian minerals form on cooling, and continued reaction may transform these products at particular temperatures into other minerals of different crystal structure; for example, olivine may be transformed into hypersthene (pyroxene). Changes of this type constitute a *discontinuous reaction* series. An illustration of these two series reactions was devised by Bowen (1928). Differentiation may

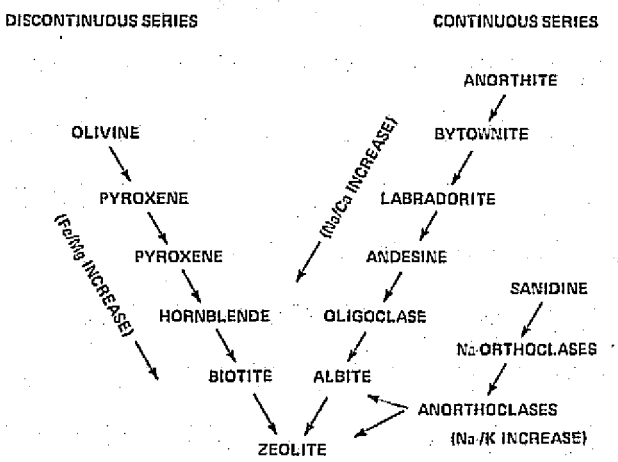

be achieved by crystal settling whereby early formal crystals are physically separated from the magma; consequently, these early formed, separated minerals cannot react and are preserved. The liquid, of course, is also different in composition and further crystallization will result in somewhat different mineral phases and bulk chemistry.

This chapter deals with chemical and textural characteristics of some basaltic rocks with consideration given to experimental methods, petrology, and petrogenesis.

1.2 TEXTURE

It requires a very unusual mind to make an analysis of the obvious.

A. N. Whitehead

1.2.1 Textures of Basalts and Gabbros

Texture refers to the degree of crystallinity, grain size, and fabric or geometrical relationships among the constituents of a rock. Textural features are probably the most important aspect of an igneous rock for they are a necessary aid in understanding the conditions under which igneous rocks crystallize (rate and order of crystallization) that in turn depend on initial composition, temperature, pressure, gaseous contents, and viscosity of the magma. In addition, texture is important in determining the post-solidification history and whether a rock is cumulate or noncumulate in origin.

Degree of crystallinity- Rocks composed wholly of crystals are called *holocrystalline*; those composed entirely of glass are *holohyaline*. Rocks containing both crystals and glass are *hypocrystalline*. *Microlites* are extremely small crystals in glass; crystallites are smaller rod-shaped isotopic forms.

Grain size– Generally, there is a distinction between the grain size of rocks that have crystallized at depth and are medium- to coarse-grained (e.g., gabbros) and those that crystallized at shallow depths, or were effusive, and are fine grained (e.g., basalts). If most of the constituents of a rock are so small as not to be visible to the unaided eye, the rock is *aphanitic*. Coarser-grained textures are *phaneritic*. Extremely small crystals that cannot be defined even with the aid of a microscope are *cryptocrystalline*. Grain sizes are defined as follows:

fine-grained, < 1 mm
medium-grained, 1-5 mm
coarse-grained, 5 mm-3 cm
very coarse-grained, > 3 cm

The cutoff grain-size between basalt and gabbro is commonly placed at 2 mm.

Rock fabric– Fabric is the shape and mutual relationships among the constituents of a rock.

1. Euhedral, idiomorphic, or automorphic – grains completely bounded by crystal faces. Subhedral or hypidiomorphic – grains bounded by crystal faces.

2. Anhedral, allotrimorphic or xenomorphic – grains devoid of crystal faces.

Order of crystallization– Three rules may be applied to determine the order of crystallization:

1. When one mineral is surrounded by another, the enclosing mineral is younger.

2. Early crystals are commonly euhedral.

3. If both large and small crystals occur together, the larger ones are the earliest to crystallize.

Because many exceptions to these rules can be found, caution should be exercised in their application. Mineral compositions may be used as a guide to the order of crystallization, although, again, many exceptions are found. Magnesium-rich olivine in basaltic and gabbroic rocks commonly crystallizes first followed by Mg-rich pyroxenes and calcic plagioclase. However, in many basalts, calcic plagioclase may crystallize before pyroxenes or even before olivine. Iron-rich minerals, quartz, and alkali-bearing minerals are usually late in the crystallization order together with Fe-Ti oxides and phosphates.

1.2.2 Essential Textural Terms

Definitions would be good things if we did not use words to make them.

J. Rousseau

granular – most of the grains are equant.

panidiomorphic- or *automorphic-granular* – major minerals are mostly euhedral.

allotriomorphic- or *xenomorphic-granular* – major minerals are mostly anhedral.

holocrystalline – composed entirely of crystals; no glass is present.

hypidiomorphic- or *hypautomorphic-granular* – most common granular texture in which a mixture of euhedral, subhedral, and anhedral grains are present (fig. 1).

amygdules – vesicles filled with deuteric or secondary minerals.

axiolites – same as *spherulitic*, except minerals are elongated along central axis (fig. 2).

corona structures – early mineral of the discontinuous reaction series (olivine) surrounded by a later member (pyroxene) thus forming an incomplete reaction relationship (fig. 3).

cumulate – igneous rock formed by the accumulation of crystals that settled out from a magma by the action of gravity (figs. 4 and 5).

hyaloophitic – angular interstices filled with glass instead of pyroxene. Proportion of glass greater than in *intersertal* (fig. 6).

intergranular – angular interstices between feldspars occupied by ferromagnesian granules or iron oxides (fig. 7).

intersertal – interstices filled with glass and/or secondary alteration minerals (fig. 8).

kelyphitic rims – corona structure of concentric shells with a fibrous texture.

matrix groundmass or mesotasis – fine-grained or glassy medium in which large grains are set.

megaphenocrysts – phenocrysts recognized by the unaided eye.

microphenocrysts – phenocrysts must be determined by a hand lens or microscope; texture is called *microphyritic*.

ophitic – laths of plagioclase lie in a matrix of coarse pyroxene so that the average length of the laths does not exceed that of pyroxene and the pyroxene tends to enclose plagioclase (figs. 9, 10, and 11). *Glomerocrysts* – phenocrysts are gathered in clusters (figs. 12 and 13).

phyric or *porphyritic* – larger grains (phenocrysts) set in a fine-grained matrix (figs. 14 and 15).

pilotaxitic – holocrystalline rocks in which feldspar lath microlites are arranged in a glass-free (felty) matrix in a flow oriented fashion (fig. 16).

poikilitic – small grains of one mineral completely enclosed in another; the latter being optically continuous (figs. 17-19).

relic texture – original texture that remains after replacement. *Relic grains* are original grain boundaries preserved after replacement by another mineral (fig. 20).

spherulites – radial aggregates of acicular and fibrous minerals (fig. 21).

subophitic – average length of plagioclase laths are equal to or exceed that of pyroxene and the plagioclase partly encloses pyroxene (figs. 22 and 23).

variolitic (varioles) – divergent plagioclase fibers or laths with interstitial glass or intergrown with pyroxene granules or iron oxides (fig. 24).

vesicles – cavities from expanded gases.

vitrophyric – phenocrysts set in glass matrix (fig. 25).

Additional examples of textures and basalt characteristics are shown in the supplementary figures 26-33.

Figure 1.– Hypidiomorphic – granular texture; cumulate rock, crossed Nicols (XN), field width = 3 mm.

Figure 2.– Axiolitic growth along feldspar laths; ocean ridge basalt (pillow), leg 34, plane light (PL), field width = 3 mm.

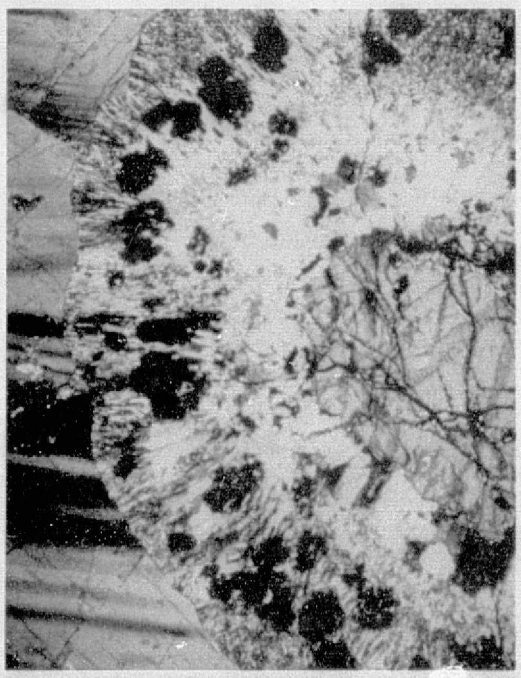

Figure 3.– Corona structure; continuous reaction and growth of olivine core → opx → mica + sphere, glacial erratic ultramafic, crossed Nicols (XN), field width = 3 mm.

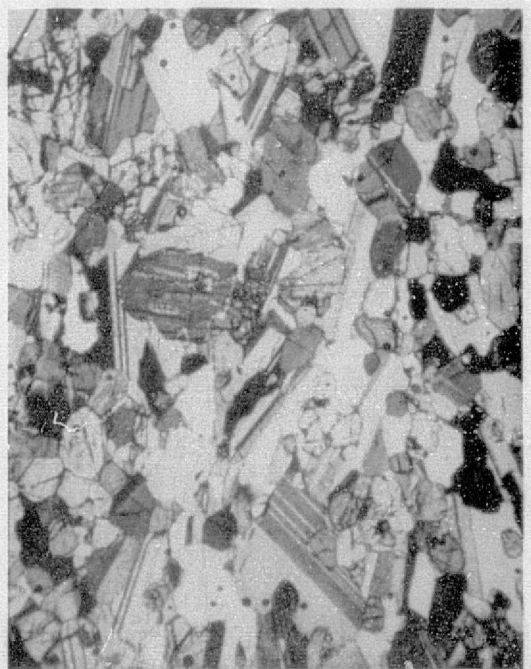

Figure 4.– Cumulus plagioclase, olivine, and pyroxene; Bushveld layered series, plane light (PL), field width = 3 mm.

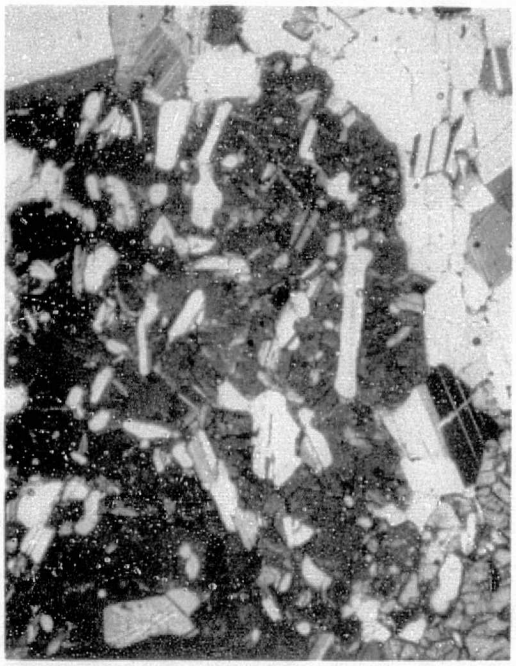

Figure 5.– Cumulate texture; large pyroxene crystal enclosing smaller plagioclase grains, Bushveld layered series, crossed Nicols (XN), field width = 3 mm.

Figure 6.– Hyaloophitic texture; oceanic basalt, leg 34, crossed Nicols (XN), field width = 3 mm.

Figure 7.– Intergranular texture; oceanic basalt, leg 34, plane light (PL), field width = 1.1 mm.

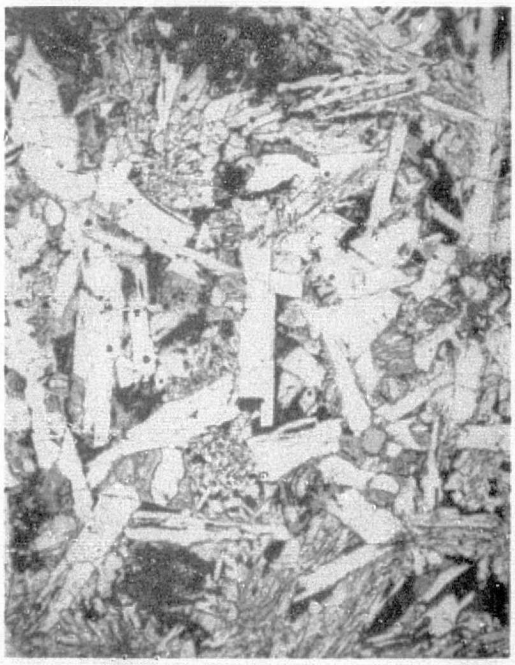

Figure 8.– Intersertal to intergranular matrix oceanic basalt; leg 34, plane light (PL), field width = 3 mm.

Figure 9.– Optically continuous augite enclosing plagioclase laths; ophitic texture, oceanic basalt, leg 34, plane light (PL), field width = 3 mm.

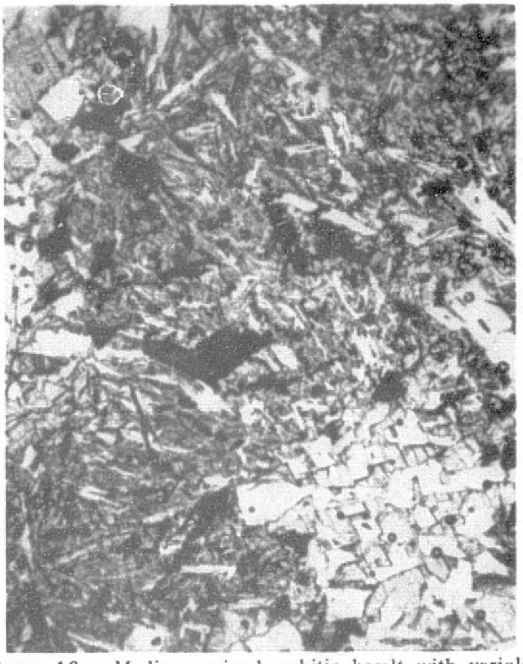

Figure 10.– Medium-grained ophitic basalt with variolitic matrix; oceanic ridge basalt, leg 34, plane light (PL), field width = 1.1 mm.

Figure 11.– Ophitic basalt (oceanic); leg 34, crossed Nicols (XN), field width = 3 mm.

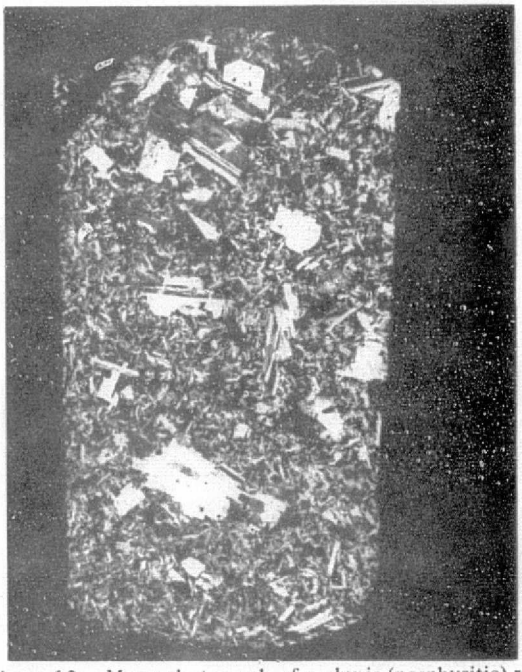

Figure 12.– Macrophotograph of a phyric (porphyritic) rock var. *glomerocrystic*, oceanic ridge basalt, leg 6, crossed Nicols (XN), field width = 3 mm.

Figure 13.– Glomerocrysts of olivine and plagioclase Hawaiian olivine basalt; West Maui, crossed Nicols (XN), field width = 3 mm.

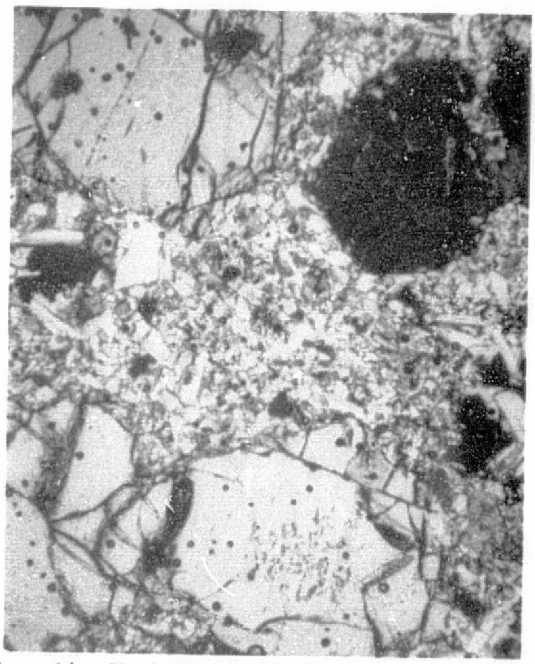

Figure 14.– Phyric (porphyritic) basalt; picrite, West Maui, crossed Nicols (XN), field width = 1.1 mm.

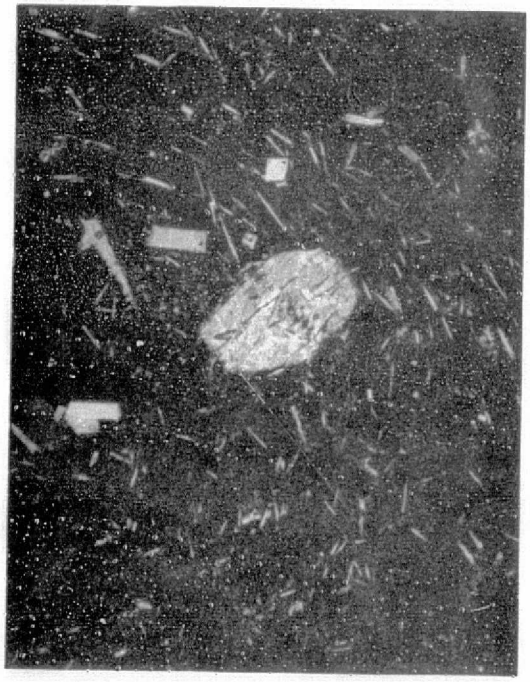

Figure 15.– Phyric (porphyritic) basalt; pilotaxitic matrix, oceanic ridge basalt, leg 34, crossed Nicols (XN), field width = 1.1 mm.

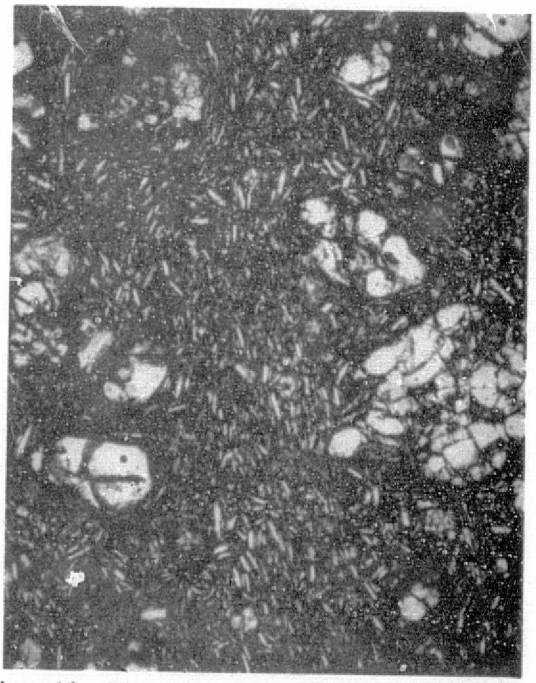

Figure 16.– Pilotaxitic matrix; olivine basalt, ophiolite complex, Panoche Valley, CA, crossed Nicols (XN), field width = 1.1 mm.

Figure 17.– Poikilitic augite enclosing plagioclase laths; oceanic ridge basalts, leg 34, crossed Nicols (XN), field width = 1.1 mm.

Figure 18.– Poikilitic augite enclosing plagioclase laths; oceanic ridge basalts, leg 34, crossed Nicols (XN), field width = 1.1 mm.

Figure 19.– Poikilitic augite enclosing plagioclase laths; oceanic ridge basalts, leg 34, crossed Nicols (XN), field width = 1.1 mm.

Figure 20.– Relic olivine, replaced by secondary alteration minerals in vitrophyric oceanic basalt; leg 16, crossed Nicols (XN), field width = 1.1 mm.

Figure 21.– Spherulites in glass matrix, pillow basalt, oceanic ridge; plane light (PL), field width = 1.1 mm.

Figure 22.– Subophitic basalt (oceanic ridge); leg 34, crossed Nicols (XN), field width = 3 mm.

Figure 23.– Fine-grained subophitic basalt (oceanic ridge); leg 34, crossed Nicols (XN), field width = 3 mm.

Figure 24.– Variolitic matrix texture; oceanic ridge basalt, leg 34, crossed Nicols (XN), field width = 3 mm.

Figure 25.– Vitrophyric basalt (glass matrix, dark; plagioclase phenocrysts, light); plane light, field width = 2 mm.

Figure 26.– Zoned titanoaugite phenocryst and olivine microphenocrysts in alkali olivine basalt; plane polarized light, field width = 2 mm.

Figure 27.– Nepheline basalt (Ixtapalpa, Mexico) with large nepheline grains (white arrow), zoned titanoaugite (dark), and abundant small euhedral to lath-shaped apatite (black arrow); plane polarized light, field width = 2 mm.

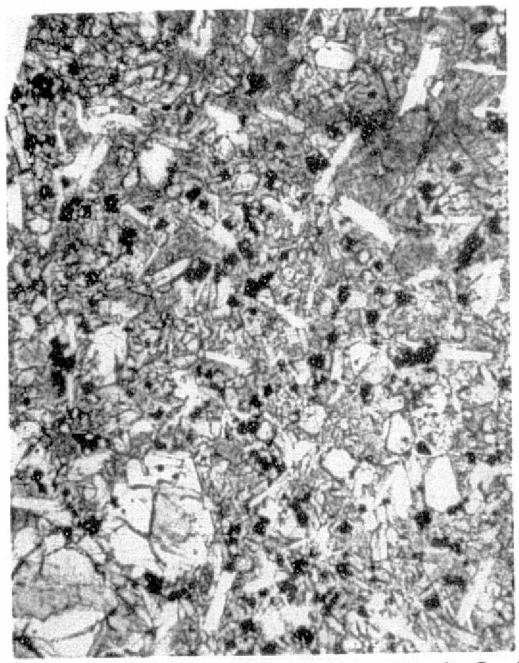

Figure 28.– Alkali olivine basalt (Banska Stiavnia, Czech.); olivine microphenocrysts in a glassy, granular groundmass, plane polarized light, field width = 2 mm.

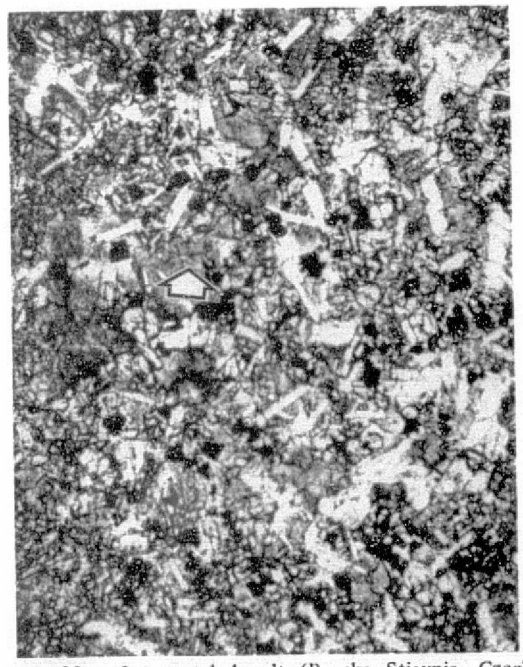

Figure 29.– Intersertal basalt (Banska Stiavnia, Czech.); plane polarized light, field width = 2 mm.

Figure 30.– Large euhedral titanoaugite crystal with small olivine inclusions (black arrow); poikilitic texture, plane polarized light, field width = 2 mm.

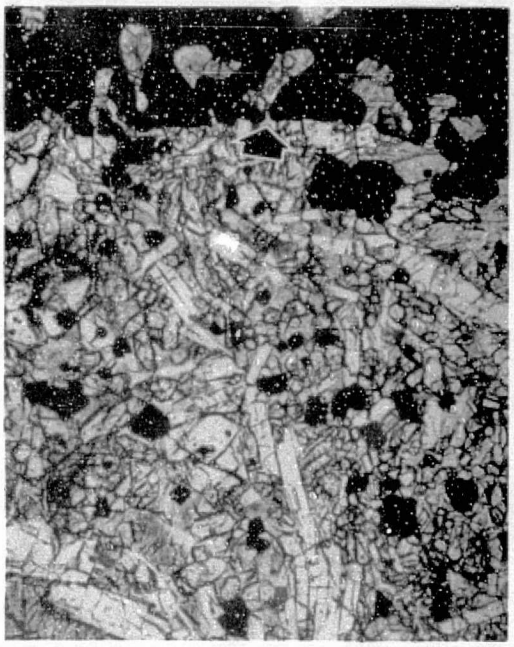

Figure 31.– Alkali olivine basalt with large titanomagnetite phenocrysts with embayment by groundmass during late stage crystallization; plane polarized light, field width = 0.8 mm.

Figure 32.– Hourglass zoning structure; differential distribution of Ti and Al in clinopyroxene causing difference in color and optical properties, plane polarized light, field width = 2 mm.

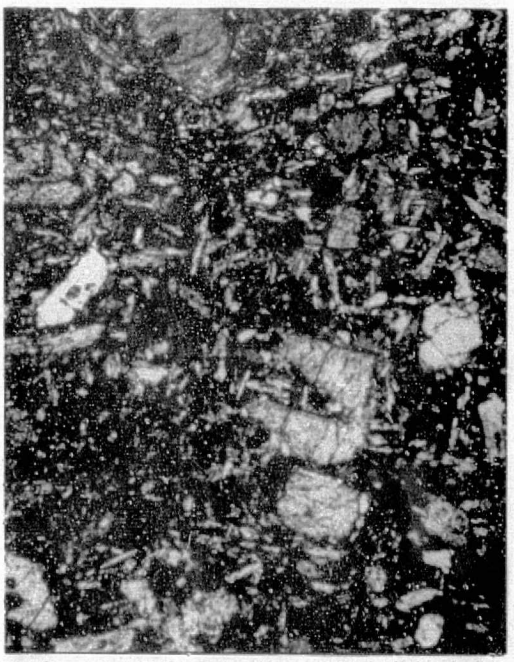

Figure 33.– Poikilitic texture in an alkali olivine basalt (El Pedigal, San Angel, Mexico); K-feldspar (dark field) enclosing grains of pyroxene and olivine, crossed polarized light, field width = 0.08 mm.

1.3 CLASSIFICATION

Nomenclature and classification of basalts have been rather confusing over the years because of attempts to define and classify basaltic rocks on a variety of parameters (bulk chemistry, silica or alkali-contents, color index, nature of feldspars or dark minerals, etc.). Several convenient classification systems are useful for general purposes and these, together with a detailed system, are presented below.

1.3.1 General (Color Index)

The proportion of light (felsic) minerals (quartz, feldspars, feldspathoids, white mica, etc.) to dark (mafic) minerals (ferromagnesians). Four rock classes have been distinguished according to volume content of dark minerals:

1. leucrocratic rocks, < 30 percent mafics
2. mesocratic rocks, 30-60 percent mafics
3. melanocratic rocks, 60-90 percent mafics
4. hypermelanic rocks, > 90 percent mafics

1.3.2 Specific Chemical Classifications

SiO_2 content– Rocks that contain free, primary silica also contain minerals that are compatible with silica under equilibrium conditions. Minerals in this category are called saturated and consist of feldspars, amphiboles, micas, pyroxenes, fayalite, spessartine, almandine, sphere, zircon, apatite, magnetite, and ilmenite. Minerals that are never associated with free silica, are called unsaturated and consist of leucite, nepheline, sodalite, hauyne, nosean, cancrinite, analcite, Mg-olivine, melanite, pyrope, perovskite, melilite, corundum, calcite, and spinel.

Rocks are classified according to free silica presence or absence as:

1. oversaturated rocks: contain free silica (primary)
2. saturated rocks: contain neither free silica nor unsaturated minerals
3. undersaturated rocks: consist wholly or in part of unsaturated minerals

a. nonfeldspathoid division: alkalis are saturated and deficiency of silica affects only mafic materials

b. feldspathoid division: alkalis are at least partly unsaturated, whereas mafics may or may not be saturated. These rocks never contain low-Ca pyroxenes, but can contain olivine or Ca-pyroxenes, or both.

Al_2O_3 saturation–

1. peraluminous rocks: molecular proportion of alumina exceeds the proportion of Σ Na_2O, K_2O and CaO. Excess Al_2O_3 combines as micas, tourmaline, topaz, or Fe-Mg garnets (low temperature rocks).
2. metaluminous rocks: proportion of alumina exceeds $Na_2O + K_2O$ only. Some Al_2O_3 goes into amphiboles, epidote, and melilite.
3. subaluminous: little or no excess of alumina over that required to crystallize feldspars and feldspathoids. Dark minerals are olivine, Ca-poor, and Ca-pyroxenes (relatively hot and dry magmas).
4. peralkaline rocks: proportion of alumina is less than that of $Na_2O + K_2O$. Dark minerals are Na-amphiboles and Na-pyroxenes. TiO_2 may substitute for Al_2O_3 (soda-rich magmas).

$CaO/(Na_2O + K_2O)$ ratio–

1. Calcic – when $Na_2O + K_2O$ wt percent = CaO and $SiO_2 > 61$ wt percent. Basalt-andesite-dacite-rhyolite series.
2. Calc-alkalic – same; SiO_2 = 56-61 percent. Basalt-andesite-dacite-rhyolite series.
3. Alkali-calcic – same; SiO_2 = 51-56 percent. Basalt-trachytephonolite series.
4. Alkalic – same; $SiO_2 < 50$ percent. Basalt-trachyte-phonolite series.

1.3.3 Normative Classification

A general classification based on normative composition has been devised by Yoder and Tilley (1962). Their simple basalt system, represented by normative components pl (plagio-

clase), cpx (clinopyroxene), opx (orthopyroxene), ol (olivine), ne (nepheline), and qz (quartz) is shown in figure 34.

1. Tholeiite (oversaturated) normative hy (hypersthene) and qz.

2. Tholeiite (saturated; hypersthene basalt): normative hy.

3. Olivine tholeiite (undersaturated): normative hy and ol.

4. Olivine basalt: normative ol.

5. Alkali basalt: normative ol and ne.

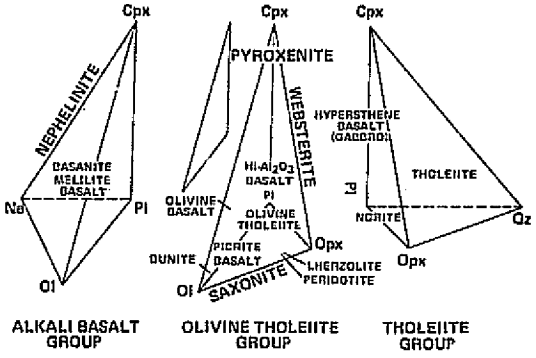

Figure 34.– Generalized simple basalt system of Yoder and Tilley (1962). Normative phases of each rock are contained in their respective tetrahedron. Underlined names are within the tetrahedron.

The separation between tholeiite and olivine tholeiite is taken as the plane of silica saturation (En-Di-Ab; fig. 35), and the separation between olivine tholeiite and alkali basalt as the critical plane of silica undersaturation (Fo-Di-Ab; fig. 35).

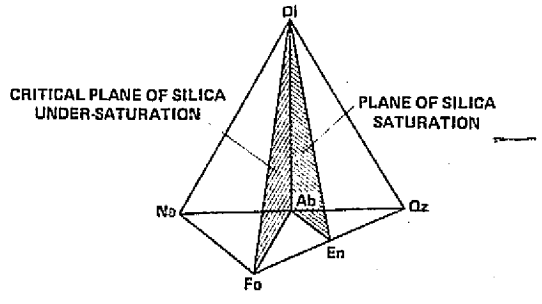

Figure 35.– Schematic visualization of the system Di-Fo-Ne-Qz (diopside-forsterite-nepheline-quartz) showing the plane of silica saturation (Di-En-Ab or diopside-enstatite-albite) and the critical plane of saturation (Di-Fo-Ab).

1.3.4 Modal and Mineralogical Classification of Hawaiian Basalts (Modified from MacDonald and Katsura (1964))

Tholeiitic suite– Rocks with tholeiitic mineral composition, falling below boundary line in figure 36.

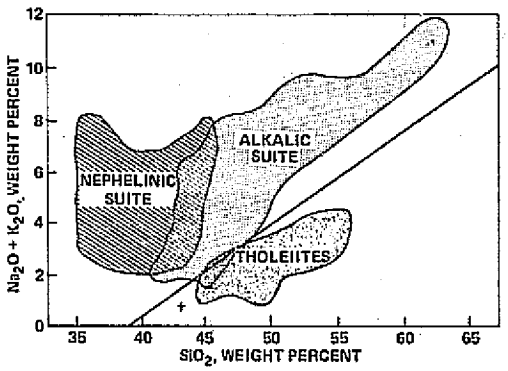

Figure 36.– Variation diagram showing arbitrary boundary for tholeiitic and alkalic rocks of Hawaii (modified from MacDonald 1968).

1. Tholeiitic basalt – <5 percent olivine (modal).

2. Tholeiitic olivine basalt – >5 percent olivine (modal).

3. Oceanite (picrite basalt of oceanic type) – containing very abundant phenocrysts of olivine and <30 percent feldspar.

Alkalic suite– Rocks with alkalic mineral composition, falling above the boundary line of figure 36.

1. Alkalic basalt – <5 percent modal olivine

2. Alkalic olivine basalt – >5 percent modal olivine and <5 percent normative nepheline.

3. Ankaramite – very abundant olivine and augite phenocrysts and <30 percent feldspar

4. Hawaiite – normative and model feldspar is labradorite and $Na_2O/K_2O > 2:1$

5. Mugearite – similar to Hawaiite but groundmass feldspar is andesine.

Nephelinic suite–

1. Basanite – >5 percent normative nepheline and with both modal nepheline and feldspar.

2. Basanitoid – > 5 percent normative nepheline, but no modal nepheline.

3. Nephelinite – > 5 percent normative nepheline, contains modal nepheline and no feldspar.

1.3.5 Oceanic Basalts

At the present time there is no detailed classification for oceanic basalts. Various terms have been used (oceanic tholeiite, abyssal basalts; Ol- or plagioclase tholeiites, depending on liquidus mineral). The presently accepted term for these basalts is *ocean-ridge tholeiitic basalt*. They differ from most continental, oceanic island, and upper seamount basalts in potassium content, usually less than 0.3 wt percent K_2O. In addition, oceanic-ridge basalts have low concentrations of P, U, Pb, Ti, and Th.

1.3.6 General Classification and Member Characteristics

Subalkaline (tholeiitic magmas)– These contain no alkali minerals other than minor alkali feldspars. Examples of intrusive subalkaline rocks are: Bushveld Complex, S. Africa; Skaergaard, E. Greenland; Great Dyke, S. Rhodesia; Stillwater Complex, Montana; and Rhum, Inner-Hebrides. These intrusions are characterized by rhythmic layering and by having dunites, harzburgites and pyroxenites in the lower positions of the intrusion with associated bands of chromite and magnetite. Troctolites, norites, anorthosites, and gabbroic rocks may be present above the ultramafic rocks.

Examples of extrusive rocks are: the great flood basalts of the world, including the Indian Deccan, Columbia Plateau, and the Hawaiian Islands, and oceanic-ridge basalts. Tholeiitic basalts are characterized by the presence of abundant calcic plagioclase and pyroxene and contains little or no olivine. If olivine is present, the rock is called *olivine tholeiite*.

Alkaline– These contain alkalis in excess of that needed to form plagioclase and are typically undersaturated with respect to SiO_2.

Examples of intrusive alkaline rocks are: Lugar sill, Scotland; Garbk Eilean sill, Shiant Isles; and the Black Jack sill, New South Wales. Examples of extrusive rocks are mainly confined to oceanic island and some continental areas.

Alkali olivine basalt is the most abundant member of this group and is often associated with trachytes and other alkalic basalts. Olivine is abundant (10-20 percent) and an increase in olivine content leads to the development of oceanites and ankaramites.

1.4 MINERALOGY

The obscure we see eventually, the completely apparent takes longer.

E. R. Murrow

The four most important minerals in basaltic rocks are plagioclase, calcic pyroxene, olivine and Fe-Ti oxides. Relatively minor minerals, which may be present as accessories or, in rare cases, as a major constituent, include silica (quartz, tridymite, and cristobalite), feldspathoids (nepheline, leucite, analcite, melilite and kalsilite), zeolites, amphiboles, micas, carbonates, serpentines and micas, phosphates and sulphides. Only the four major mineral groups will be discussed in detail.

Petrographic characteristics of the various minerals, mineral chemistry, and mineral compositions typical of Hawaiian, oceanic ridge, and continental basalts are discussed in this section.

1.4.1 Feldspars

Mineral chemistry– Plagioclase composition is expressed in terms of molecular anorthite ($CaAl_2Si_2O_8$), or An, and molecular albite ($NaAlSi_3O_8$), or Ab, which are end components of the isomorphous series (fig. 37). Analyses are usually given in terms of SiO_2, Al_2O_3, CaO,

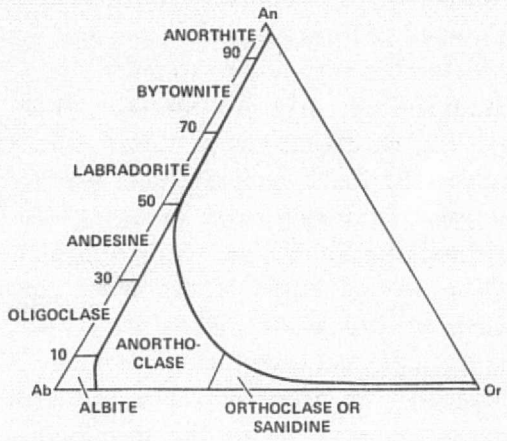

Figure 37.– Nomenclature of ternary feldspars (molecular basis). Solid line gives boundary of the two-feldspar region.

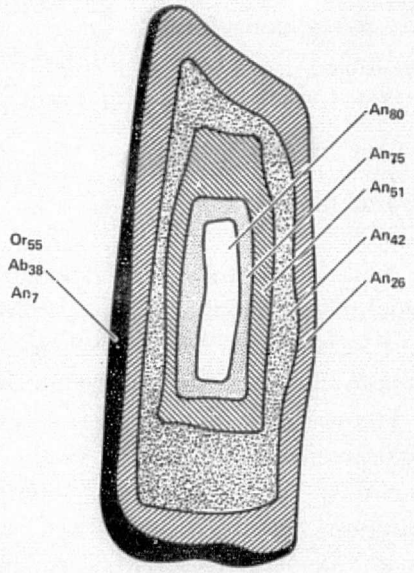

Na_2O, and K_2O with trace amounts of Fe_2O_3 and MgO. K-feldspar is present mostly as anorthoclase or sanidine and is rare in occurrence in most basalts. K-feldspar is expressed in terms of molecular orthoclase ($K AlSi_3O_8$) or Or (fig. 37).

Petrographic characteristics– Zoning in feldspars is common in basaltic rocks and is the result of nonequilibrium conditions from rapid cooling. Earliest formed crystals are Ca-rich and as crystallization proceeds with falling temperature, Ca is depleted in the surrounding liquid and Na begins to enter the structure. Thus, the magmatic history of the rock, in terms of T and $Ca \rightleftharpoons Na$ exchange can be studied by unraveling the various compositional zones. A typically zoned plagioclase crystal would have a Ca-rich core (An_{75-90}) with successive zones of decreasing Ca content until the grain margins (last crystallization stage) become very sodic in accordance with the changing liquid composition (An_{5-20}). The outermost zone (rim) is commonly enriched in both Na and K to the extent that it is consistent with K-feldspar composition.

Grain size is a very important feature and commonly indicates various crystallization stages of the magma.

1. Phenocrysts – nucleate and grow at some depth before extrusion (represented by highly calcic, rather homogeneous cores). As the magma is extruded, cooling rate increases, T drops, and bulk composition of the magma continually changes towards alkali- and Fe-rich residium (Ca and Mg being depleted). Phenocrysts continue to grow on extrusion with composition changing to more sodic varieties.

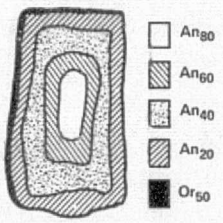

2. Microphenocrysts – commonly nucleate and grow on extrusion. Zoning is not nearly as complicated as phenocrysts and growth commonly overlaps with late stage phenocryst development.

3. Groundmass laths – small, late crystallization stage products. Composition and growth may overlap with microphenocrysts.

4. Interstitial laths and glass – very small (< 0.02 mm) components that are usually distinct from groundmass laths and are nearly always more alkalic. Interstitial material is the last feldspar component to crystallize.

All or some of the above may be present in basaltic rock. Whereas they may be transitional, one to the other in composition, they may also show compositional gaps that may imply distinct crystallization periods.

Mineral compositions of various basalts–

1. Hawaiian rocks. Hawaiian basalts are categorized into tholeiitic, alkalic and nephelinic suites. A very detailed study of plagioclase compositions in three rock suites was made by Keil et al. (1972) and is summarized as follows:

a. In all rock types, An decreases and Or increases from phenocrysts to microphenocrysts to groundmass feldspar to interstitial feldspar material (figs. 38-40).

b. Phenocrysts occur in tholeiitic and alkalic rocks and overlap in composition (figs. 38-40).

c. Groundmass in tholeiitic and nephelinic rocks are similar in composition; the highly differentiated alkalic suite has groundmass feldspar that ranges in composition from labradorite to sanidine (high CaO bulk content = higher An content and high K_2O = higher Or content).

d. Hawaiites contain labradorite, not andesine as by definition. Mugearite contains andesine and not oligoclase groundmass feldspar.

e. Rocks of the three suites can be distinguished on the basis of Or and An in groundmass feldspar (figs. 38-40).

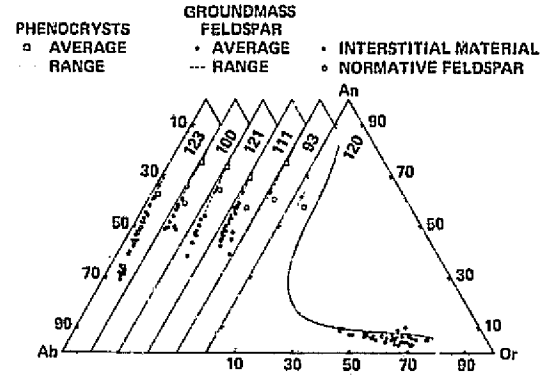

Figure 38.– Compositions of feldspars in Hawaiian tholeiitic rocks (Keil et al. 1972).

f. Rocks transitional between tholeiitic and alkalic are characterized by transitional mineral compositions.

2. Oceanic ridge tholeiitic basalts (based on examples from the JOIDES – Deep Sea Drilling Program)

a. Leg 6 (Parece Vela Basin, Philippine Sea; fig. 12). Compositional zoning in phenocrysts of plagioclase phyric rocks is normal and continuous from An_{84} to An_{25}. Phenocryst grain size varies from 4 mm to 0.8 mm. In this feature, the porphyritic nature of these rocks (large single grains or glomerocrysts) is quite distinct and unlike that of most other oceanic-ridge basalts. Microphenocrysts range in composition from An_{75} to An_{44} (a few have rims of oligoclase composition).

b. Leg 34 (Nazca Plate, S. E. Pacific). Compositional zoning in normal and continuous from cores of An_{84}-An_{81} to rims of An_{35}-An_{9}. At least three generations of plagioclase can be observed in most samples: (1) phenocrysts; (2) microphenocrysts; and (3) groundmass laths. Compositions of all three commonly overlap. Very small interstitial grains of K-feldspar may be present in the matrix.

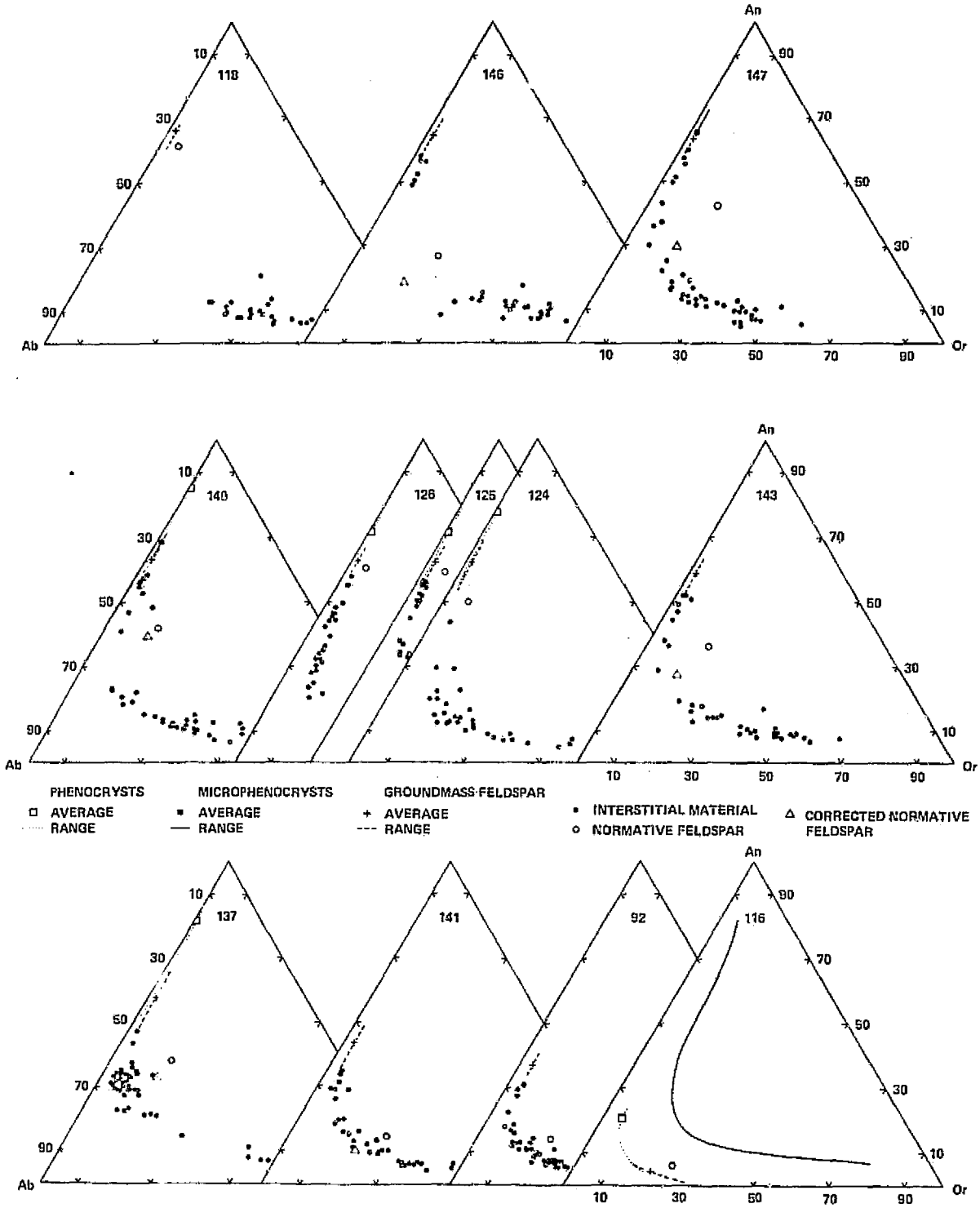

Figure 39.– Compositions of feldspars in Hawaiian alkalic rocks (Keil et al. 1972).

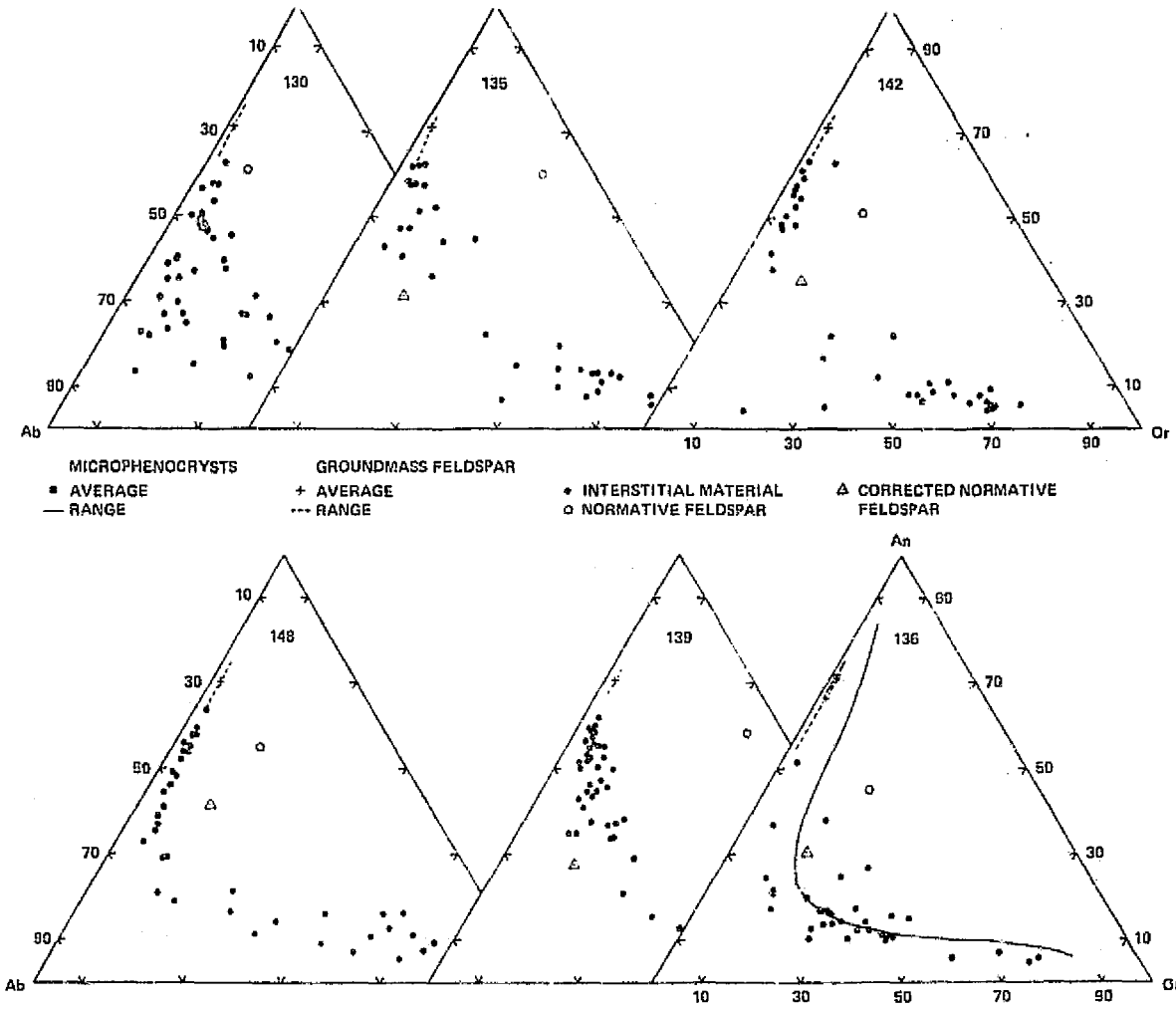

Figure 40.– Compositions of feldspars in Hawaiian nephelinic rocks (Keil et al. 1972).

1.4.2 Pyroxene

Mineral chemistry and fractionation trends– The general formula for pyroxenes can be written:

$X_{I-P}\ Y_{I+P}\ Z_2\ O_6$

X = Ca, Na

Y = Mg, Fe^{2+}, Mn, Ni, Li, Al, Fe^{3+}, Cr, and Ti

Z = Si, Al

For Ca-rich, monoclinic basaltic pyroxenes, the most important substitutions are $Mg \rightleftharpoons Fe^{2+} \rightleftharpoons Ca$ and $Si \rightleftharpoons Al^{IV}$; Ti, Al^{VI} and Na may also be present in significant amounts. Orthorhombic pyroxenes (enstatite to ferrohypersthene) contain essentially Mg, Fe^{2+}, and Si with few other major elements.

For the purposes of this chapter, discussion of pyroxenes will be limited to pyroxenes found in abundance in the major basaltic rocks. These pyroxenes consist essentially of solid solutions

of $CaSiO_3$, $MgSiO_3$ and $FeSiO_3$. Pyroxene compositions and fractionation trends are commonly illustrated in the pyroxene quadrilateral diagram (*Di* = diopside; *Hd* = hedenbergite; *En* = enstatite; and *Fs* = ferrosilite), which is a portion of the ternary system $CaSiO_3$ - $MgSiO_3$ - $FeSiO_3$. Relationships among basaltic pyroxenes (other than those that contain large amounts of Na, Ti, and Al) are diagrammatically represented in figure 41. At least four main fractionation trends or series are found in basaltic rocks:

I diopside → salite → hedenbergite

II diopside or calcic augite → ferroaugite or hedenbergite

III subcalcic augite → subcalcic ferroaugite

VI bronzite → hypersthene → ferrohypersthene *or* pigeonite → ferropigeonite

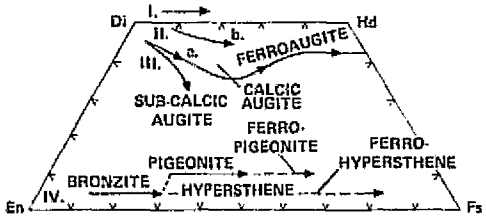

Figure 41.– Pyroxene quadrilateral diagram showing fractionation trends for various basaltic pyroxenes. Trend I is for pyroxenes of nephelinic or highly alkalic undersaturated magmas. Trend IIa is for pyroxenes of the Skaergaard layered intrusive complex. Trend IIb is for pyroxenes of alkalic basalts. Trend III is for pyroxenes of tholeiitic basalts. Trend IV is for pigeonite and orthopyroxenes that coexist with those of the clinopyroxene trends (I, II, and III) and are commonly observed in meteorite pyroxenes.

Some of the above pyroxene can be armored by more Fe-rich compositions through compositional zoning in more rapidly cooled effusive basaltic magmas; the fractionation trend shifts from Mg-pyroxenes to Fe-pyroxenes in the Ca-rich and Ca-poor series.

The various basaltic magmas can be characterized by their constituent pyroxenes and pyroxene compositional trends.

Pyroxene Trend I. Pyroxenes in undersaturated alkalic basalts are commonly diopside to salite (some to ferrosalite) compositions. In particular, the nephenlinic rocks of Hawaii and also the intrusive sills, Garbh Eilean and the Black Jack sill contain pyroxenes of this trend.

Pyroxene Trend IIa (diopside or augite → ferroaugite → hedenbergite). This trend is common in slowly cooled, highly fractionated plutonic rocks (Skaergaard, Bushveld, etc.) and saturated tholeiitic basalts, although pyroxenes in tholeiites rarely exceed Fs_{40} in Fe content. An additional characteristic of tholeiitic pyroxenes is the possible presence of coexisting pairs (Ca-rich pyroxene and Ca-poor pyroxenes at Trend IV). Other basalts rarely contain a second pyroxene.

Pyroxene Trend IIb (calcic augite → ferroaugite). The undersaturated alkali olivine basalts (alkalic suite) commonly contain calcic augite that may show fractionation to ferroaugite.

Pyroxene Trend III (subcalaic augite). This trend does not represent an equilibrium trend, but is typical of pyroxenes that formed rapidly in magmas that were supercooled to subsolidus temperatures. Thus, nonequilibrium conditions did not allow the separation of augite and hypersthene or pigeonite.

Pyroxene Trend IV (bronzite → hypersthene → ferrohypersthene or the pigeonite series). These pyroxenes by themselves are not representative of any basaltic magma, but are present as a fractionated series in equilibrium with augites and ferroaugites in plutonic rocks and some tholeiitic basalts.

Pyroxene trends of various basalts–

1. Hawaiian rocks. The three basaltic suites of Hawaii (tholeiitic, alkalic, and nephelinic) can be distinguished on the basis of pyroxene composition (fig. 42(a)).

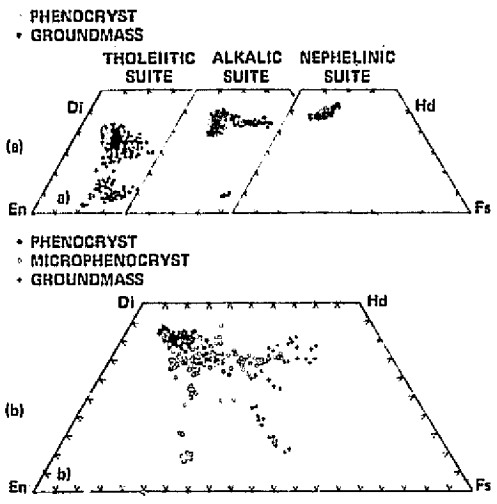

Figure 42.– (a) Pyroxene compositions in tholeiitic, alkalic and nephelinic basalts of Hawaii (Fodor et al. 1975). (b) Pyroxenes in oceanic ridge basalts of leg 34 rocks (Bunch and LaBorde 1976).

2. Oceanic-ridge basalts. Most of the oceanic basalts are tholeiitic and their constituent pyroxenes follow typical tholeiitic trends. Pyroxenes in Leg 34 basalts follow tholeiitic trends (fig. 42(b)), although they tend to extend further toward iron enrichment than other oceanic basalt samples (fig. 43).

3. Generalized pyroxene trends in other selected basalt occurrences are shown in figure 44.

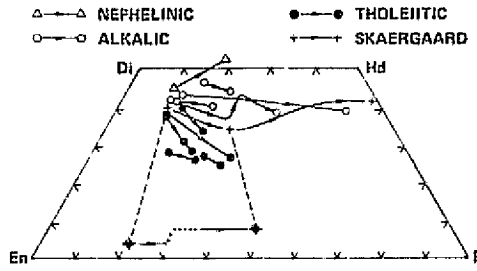

Figure 44.– Generalized pyroxene composition trends for different basaltic rocks.

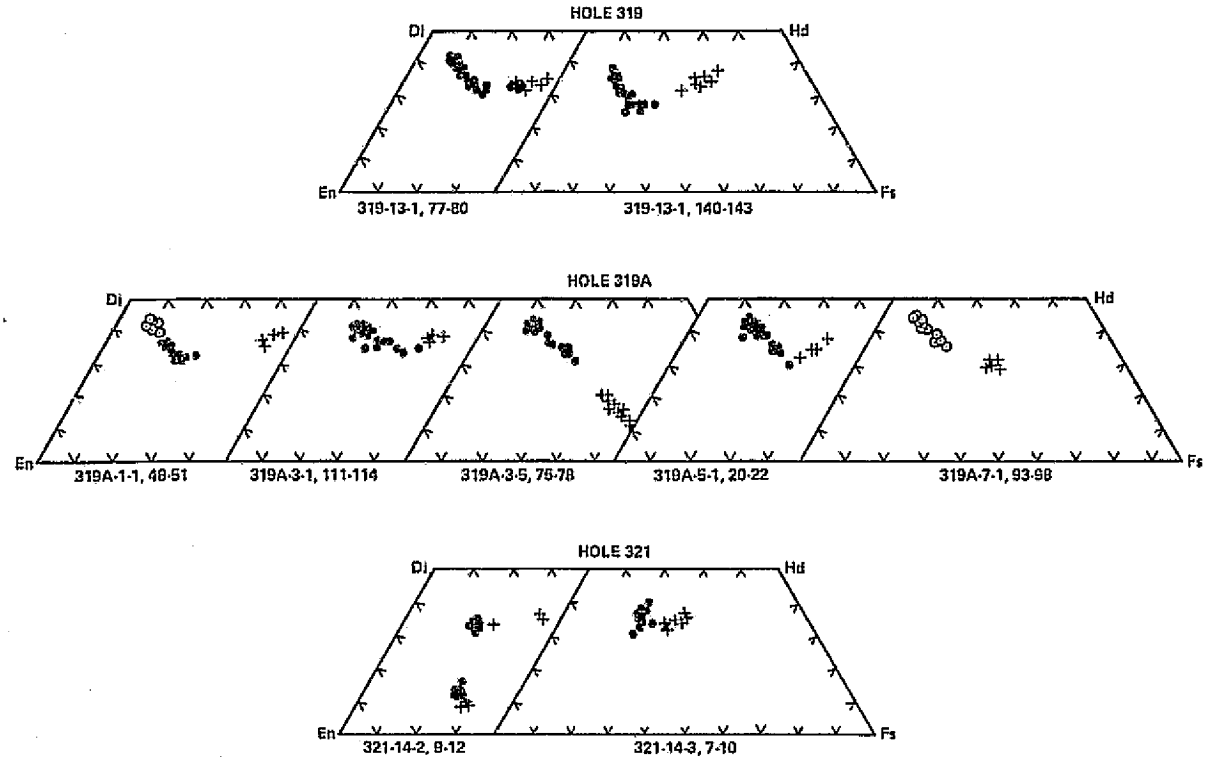

Figure 43.– Pyroxene compositions for individual samples of oceanic-ridge basalts of leg 34. Open circles = phenocrysts; filled circles = microphenocrysts; cross = groundmass and interstitial pyroxen (Bunch and LaBorde 1976).

1.4.3 Olivine

Olivine consists almost entirely of (Mg, $Fe)_2SiO_4$ with minor to trace amounts of Cr, Ni, Mn, and Ca. A complete diadochy exists between the Mg solid solution member forsterite (Mg_2SiO_4) or Fo and the Fe member, ferrosilite (Fe_2SiO_4) or Fs. When present, olivine (Fo_{90-80}) is usually the first mineral to crystallize.

Although olivine may be the first to crystallize as phenocrysts in a basaltic magma, it may also be totally or partly resorbed by the liquid, particularly in *saturated* tholeiites.

Olivine can be used to distinguish among tholeiitic, alkalic, and nephelinic basalts on the basis of increasing $FeO/(FeO + MgO)_{olivine}$ to $FeO/(FeO + MgO)_{cpx}$ ratios. In addition, the three suites may be separated by the amounts of minor element contents in their respective olivines. Nickel oxide (NiO) in olivine decreases from tholeiitic to alkalic to nephelinic basalts (Bunch et al. 1976).

1.4.4 Iron-Titanium Oxides

These minerals consist of two solid solution series: (1) the *spinel series* that includes the pair magnetite (Fe_3O_4) and ulvöspinel (Fe_2TiO_4) and (2) the *rhombohedral series* that includes the pair ilmenite ($FeTiO_3$) and hematite (αFe_2O_3). Compositions of each coexisting pair and their subsolidus textures provide significant petrographic information. Phase equilibrium studies in the system FeO-Fe_2O_3-TiO_2 (Buddington and Lindsley 1964) show that the temperature and oxygen fugacity (fO_2) of formation of coexisting titaniferous magnetite and ilmenite can be determined in many rocks. Figure 45(a) shows the major solid solution series ulvöspinel-magnetite ($Mt\text{-}Usp_{SS}$) and ilmenite-hematite ($Ilm\text{-}Hem_{SS}$) in the phase system FeO-Fe_2O_3-TiO_2.

Calculations for arriving at the desired formation temperature and fO_2 are simplified here and are as follows: (1) the spinel and rhombohedral minerals are recalculated into their end members, that is, TiO_2 in titanomagnetite is combined with sufficient FeO to form the end member Fe_2TiO_4, and the remaining component is Fe_3O_4 (other minor oxides are not considered here); and (2) for the rhombohedral phase, all FeO is combined with TiO_2 to form $FeTiO_3$ (ilmenite) and the remaining component is Fe_2O_3 (other minor oxides in the analysis and excess TiO_2 are not considered here). We now have the necessary data to plot on the fO_2-T graph of Buddington and Lindsley (1964).

Even without this graph, a fair idea of the formation environment can be obtained in two ways. First, since we have the end member compositions of the series members, we can plot them on the system diagram shown in figure 45(b) and connect both series compositions with a tie line. For example, tie line No. 2 in figure 45(b) represents a titaniferous magnetite with an equivalent amount of 44.9 percent ulvöspinel and a coexisting ilmenite with a calculated amount of 92.3 percent $FeTiO_3$ (the remaining constituents being 3.9 percent excess TiO_2 and 3.8 percent Fe_2O_3), which indicates a rather low oxidation state ($fO_2 = 10^{-16.4}$) and an estimated formation T of 860°C. (These values are taken from the fO_2-T graph not shown here). Compare this coexisting pair, which is present in the Skaergaard complex, with tie line No. 4 that represents a titaniferous magnetite with an equivalent amount of 22.3 percent ulvöspinel and coexisting ilmenohematite with a calculated amount of 86.4 percent $FeTiO_3$ (the remaining constituents being 3.2 percent excess TiO_2 and 10.4 percent Fe_2O_3), which indicates an oxidation state of $fO_2 = 10^{-15.8}$ and a T of 710°C.

Second, by knowing the amount of TiO_2 in titanomagnetite and converting it to equivalent

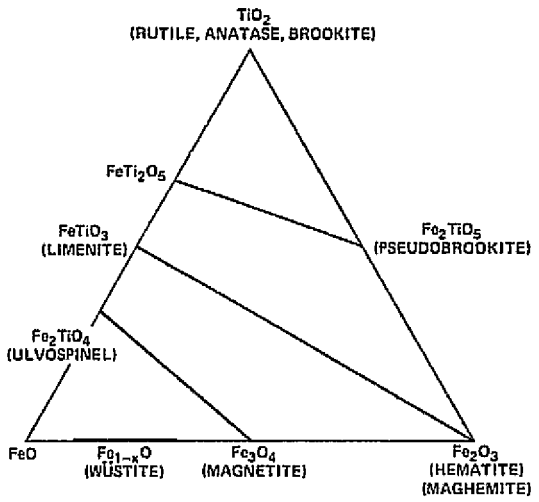

(a) Phases in the system FeO-Fe_2O_3-TiO_2 showing the major solid solution series (mole percent).

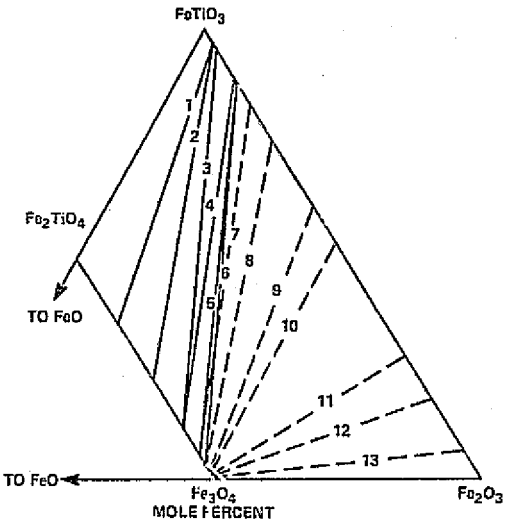

(b) Tie lines for coexisting magnetic-ulvospinel$_{ss}$ and the bulk composition of the corresponding members of the hematite-ilmenite$_{ss}$ series.

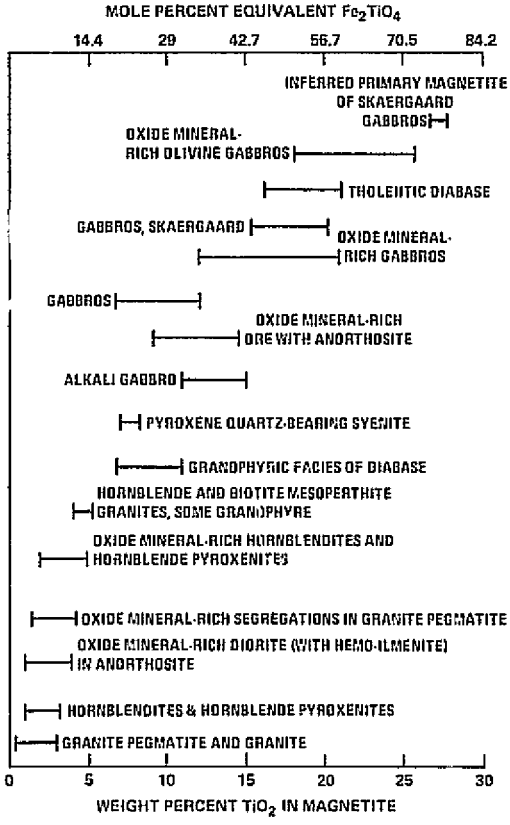

(c) Range of Tio_2 and equivalent Fe_2TiO_4 in magnetite of some terrestrial rocks.

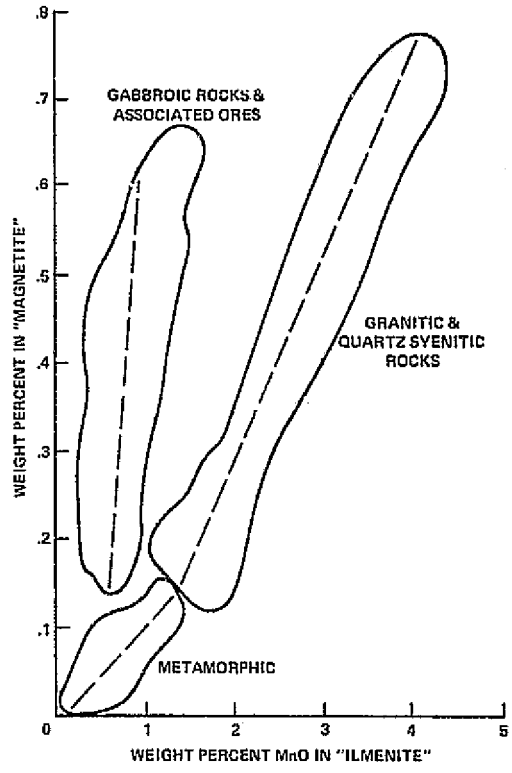

(d) Distribution of MnO between coexisting Ti-magnetite and ilmenite.

Figure 45.– Temperature of formation and environmental data for coexisting titaniferous magnetite and ilmenite.

Fe_2TiO_4, we can compare the formation environment of the co-existing oxide pair of interest to the environments of other rocks (fig. 45(c)), which show a trend of more oxidation and lower formation temperatures as the amount of TiO_2 in magnetite decreases and the amount of Fe_2O_3 in ilmenite increases (not shown).

In addition to Fe and Ti, the Fe-Ti oxides in basaltic rocks may also contain small amounts of MgO, Al_2O_3, MnO, and V_2O_3 and to a lesser degree, Cr_2O_3 and SiO_2. Vanadium and Mg are mainly concentrated in the spinel series relative to the rhombohedral series. Vanadium and Mg decreases in spinel with fractionation whereas the Fe^{2+}/Fe^{3+} ratio increases. Manganese is concentrated in the rhombohedral minerals relative to the spinel minerals and the distribution of Mn between the two series minerals can be used to infer relative formation temperatures. The ratio of MnO in ilmenite to MnO in 'magnetite' increases from basaltic, gabbroic and anorthositic rocks to intermediate values in granites and syenites to higher ratios in high-grade metamorphic rocks (fig. 45(d)) (Buddington, 1963).

1.5 METHODS OF CHEMICAL AND MINERAL EXPRESSION

Most of our so-called reasoning consists of finding arguments for going on believing as we already do.

J. H. Robinson

Mineral and bulk chemical analyses can be used to interpret formation environment, post-formational history, chemical exchange, and many other factors that aid in understanding the history of a particular rock. Listed below are several methods of making chemical calculations that can be used for basaltic rock interpretation together with methods of chemical data illustration.

1.5.1 Calculation Examples

1. Weight percent of oxides

2. Cation percentage:

$$\frac{\text{wt percent of oxide}}{\text{mol wt}} = \text{mol number}$$

$$= \frac{\text{cation number}}{\Sigma \text{ cation number}} \times 100 = \text{cation wt percent}$$

3. Molecular percent of a mineral:

if plagioclase = $Ab_{35}(An_{65})$, then

35 = mol prop or mol wt of sodic plagioclase

then

$$\frac{\text{mol prop (sodic)}}{\Sigma \text{ mol prop (sodic + calcic)}} \times 100$$

= total albite in bulk sample.

4. Mineral structural formula: Theoretically, minerals could exist in their pure form, that is, enstatite should be mostly $MgSiO_3$. Because a solid solution exists with $FeSiO_3$, the amounts of Mg and Fe will vary. In addition, minor amounts of other elements will also be present and these are important in understanding the rock's formation environment. Large amounts of Al, in part substituting for Si, may indicate a high-pressure environment. The amounts of Ca and Na in Ca-rich pyroxenes indicate whether the host basalt is alkalic, non-alkalic, or peralkalic (fig. 46). Moreover, the amount of Ti in

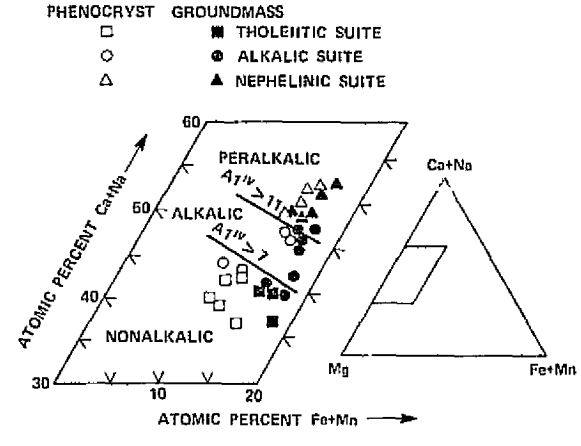

Figure 46.– Plot of high Ca-pyroxene compositions in rocks of tholeiitic, alkalic, and nephelinic suites of Hawaiian basalts (Fodor et al. (1975)).

ratio to Al^{VI} distinguishes between many kinds of basalts. Many other kinds of determinations are made from structural formulae calculations; an example is given below.

augite with the molecular formula of

$W_{1-p}(X, Y)_{1+p}Z_2O_6$

W = Ca, Na

X, Y = Mg, Fe, Al^{VI}, Ca, Mn, Cr

Z = Si, Al^{IV}

cation distribution based on 6 oxygens.

COMPOSITION AND METHOD

Composition	Column 1	2	3	4	Method
SiO_2	51.20	0.852	1.704	1.898	
Al_2O_3	3.01	.030	.090	$.102^{IV}$ $.030^{VI}$	2.000 = Z
TiO_2	.91	.011	.022	.025	
Fe_2O_3	2.46	.015	.045	.067	
MgO	15.48	.384	.384	.856	= 1.989 = W, X, Y (Theoretical = 2.000)
FeO	5.32	.074	.074	.165	
CaO	20.73	.370	.370	.824	
Na_2O	.34	.005	.005	.027	
K_2O	--	--	--	--	
			2.693		$\frac{6}{2.693} = 2.228$

Column 1 is wt percent from analysis
Column 2 is wt percent/mol wt
Example: FeO = 5.32/72 = 0.074 = mol percent
Column 3 is column 2 X number of oxygens
Column 4 is column 2 X the factor 6/2.693 = 2.228 or total of column 3 divided by number of oxygens

Note: always multiply this sum by the number of cations.
Example: TiO_2 = 0.011 X 2.228 = 0.0245 or 0.025.
Fe_2O_3 = 0.015 X 2.228 = 0.0334 X 2 for 2Fe = 0.067.

5. Mineral modes (vol. percent of minerals by point counting): To calculate wt percent of mineral A,

vol percent (X) S.G. = wt prop of mineral A

then

$$\frac{\text{wt prop of A}}{\Sigma \text{ wt percent}} = \text{wt percent of A}$$

6. CIPW Normative calculation: Part of the following example is through the courtesy of Prof. Walt Vennum of Sonoma State College.

In the CIPW classification system, the chemical analysis of an igneous rock is used to calculate the relative percentages of a group of standard or normative minerals that might hypothetically occur in such proportions in a rock of a given composition. These arbitrary normative minerals may or may not correspond to the actual or modal minerals that occur in the rock. A rock is classified according to its *norm*, the proportion of calculated normative minerals, rather than according to its *mode*.

The CIPW system is, then, fundamentally a geochemical classification scheme. From the chemical analysis, the proportions of a hypothetical group of minerals of simple composition are calculated according to an arbitrary procedure in such a way that all the rock constituents are accounted for. It is a particularly useful scheme because, once one is familiar with its workings, the norm of a rock forms the basis for a more rapid recognition of the petrologic affinities of a rock than does chemical analysis, unless a person has had considerable experience interpreting analyses. Calculation of a CIPW norm is an instructive procedure, for the normative mineral group was chosen so as to reveal as much significant petrologic information as possible. Consequently, in the process of making a calculation, one can gain insight into the way different rock-forming oxides are distributed among the different types of igneous minerals. To do this, it is not necessary to master all the intricacies of the calculations, which can become quite involved in the case of a rock of unusual composition. In all, there are more than 30 normative minerals used in the system. Of these, we

will need only those listed in Table 1 to deal with rocks of common occurrence.

TABLE 1.– NORMATIVE MINERAL MOLECULES

Mineral	Symbol*	Formula	Mol wt
Felsic group			
Quartz	q	SiO_2	60
Corundum	c	Al_2O_3	102
Orthoclase	or	$K_2O \cdot Al_2O_3 \cdot 6SiO_2$	556
Albite	ab	$Na_2O \cdot Al_2O_3 \cdot 6SiO_2$	524
Anorthite	an	$CaO \cdot Al_2O_3 \cdot 2SiO_2$	278
Leucite	lc	$K_2O \cdot Al_2O_3 \cdot 4SiO_2$	436
Nepheline	ne	$Na_2O \cdot Al_2O_3 \cdot 2SiO_2$	284
Kallophilite	kp	$K_2O \cdot Al_2O_3 \cdot 2SiO_2$	316
Mafic group			
Wollastonite	wo	$CaO \cdot SiO_2$	116
Enstatite	en	$MgO \cdot SiO_2$	100
Ferrosilite	fs	$FeO \cdot SiO_2$	132
Forsterite	fo	$2MgO \cdot SiO_2$	140
Fayalite	fa	$2FeO \cdot SiO_2$	204
Acmite	ac	$Na_2O \cdot Fe_2O_3 \cdot 4SiO_2$	462
Magnetite	mt	$FeO \cdot Fe_2O_3$	232
Hematite	hm	Fe_2O_3	160
Ilmenite	il	$FeO \cdot TiO_2$	152
Apatite	ap	$3(3CaO \cdot P_2O_5) \cdot CaF_2$	336
Pyrite	pr	FeS_2	120
Calcite	cc	$CaO \cdot CO_2$	100

*Upper or lower case first letter is used.

Here is another bead on the string of confusion.
W. Woodward

Procedure for calculation of CIPW norm– The molecular amount of each oxide constituent is determined from the chemical analysis by dividing the weight percentage by the molecular weight of the oxide. If the result is less than 0.002, it may be neglected. Lump the molecular amount of MnO with FeO and proceed as follows, using molecular amounts as calculated:

1. An amount of CaO equal to 3.33 that of P_2O_5 (or 3.00 P_2O_5 and 0.33 F, if the latter is present) is allotted for apatite.

2. An amount of FeO equal to that of the TiO_2 is allotted for ilmenite.

3. An amount of FeO equal to that of the Fe_2O_3 is allotted for magnetite.

4. Any excess Fe_2O_3 is calculated as hematite.

5. An amount of Al_2O_3 equal to that of the K_2O is allotted for orthoclase.

6. An excess of Al_2O_3 over that required for orthoclase is allotted to an equal amount of Na_2O for albite.

7. An excess of Al_2O_3 over that required for the alkali feldspars is allotted to equal amount of CaO for anorthite.

8. If there is still an excess of Al_2O_3 from steps 6, 7, and 8, it is calculated as corundum.

9. If there is an excess of CaO from step 8, it is first allotted to an equal amount of (Mg, Fe)O to form diopside, with MgO and FeO being allotted in such a way as to preserve their relative proportions existing after steps 2 and 3.

10. Excess (Mg, Fe)O over that required for step 10 is reserved for provisional hypersthene. Excess CaO over that required for step 10 is reserved for provision wollastonite. All oxides save SiO_2 have now been assigned.

11. Allot the necessary amount of silica to each mineral as follows (see mineral formulae given above):

a. to orthoclase (step 6)
b. to albite (step 7)
c. to anorthite (step 8)
d. to diopside (step 10)
e. to wallastonite (step 11)

12. If there is sufficient remaining SiO_2 to form the provisional hypersthene (step 11), it is assigned. If there is not, but there is enough SiO_2 remaining to exceed half the amount of (Mg, Fe)O of step 11, it is allotted to the (Mg, Fe)O of step 11 to form both hypersthene and olivine so that if

x = number of hy molecules
y = number of ol molecules
M = amount of (Mg, Fe)O available, and
s = amount of SiO_2 available

then

$x = 25 - M$ and $y = M - X$

Note also that constituents should be allotted to hypersthene and olivine in such a way that the ratio of MgO to FeO is the same in both minerals, namely that determined for step 10.

13. Any excess SiO_2 over that required for hypersthene is calculated as quartz.

14(a). If there is a deficiency of Si, minerals of a lower degree of silicification have to substitute, in part or wholly, for those minerals that were formed provisionally. In order to do that correctly, wollastonite, Wo, should be combined with an equal amount of (En + Fs) to form diopside (Di). In diopside and olivine the proportion FeO:MgO should be the same as in the provisionally formed pyroxenes.

14(b). The necessary amount of (En + Fs) remaining from 14(a) is converted into olivine (Fo and Fa) according to the equation:

$$4En = 3Fo + 1Q$$

14(c). If there still is not enough Si in the analysis, albite is turned into nepheline according to the equation:

$$5Ab = 3Ne + 2Q$$

14(d). Finally, if the analysis is very low in Si, orthoclase is in part or wholly converted into leucite:

$$5Or = 4Lc + 1Q$$

14(e). In rare cases there is not even enough Si to form leucite. Then kaliophilite is formed:

$$4Lc = dKp + 1Q$$

15. The mineral molecules so established are then calculated into their percentage weights by multiplying molecular amount times molecular weight (see list of mineral molecules above). A sample calculation is given in Table 2. If this calculation seems unduly complicated and time consuming, I have a computer program that can alleviate the frustrations.

TABLE 2.– CALCULATION OF NORM OF CALC-ALKALI GRANITE

Oxide	Wt percent	Mol amount
SiO_2	72.6	1.210 = 0.354 (or) + 0.300 (ab) + 0.046 (an) + 0.025 (hy) + 0.485 (Q)
TiO_2	0.4	0.005 = 0.005 (il)
Al_2O_3	14.0	0.137 = 0.059 (or) + 0.050 (ab) + 0.023 (an) + 0.005 (c)
Fe_2O_3	0.9	0.006 = 0.006 (mt)
FeO	1.7	0.024 = 0.005 (il) + 0.006 (mt) + 0.013 (hy)
MgO	0.5	0.012 = 0.012 (hy)
CaO	1.3	0.023 = 0.023 (an)
Na_2O	3.1	0.050 = 0.050 (ab)
K_2O	5.5	0.059 = 0.059 (or)

Mol	Mol amount	Wt percent
Quartz	0.485	29.1 q
Orthoclase (or)	0.059	32.8 or
Albite (ab)	0.050	26.2 ab
Anorthite (an)	0.023	6.4 an
Corundum (c)	0.005	0.5 c
$CaSiO_3$	--	--
$MgSiO_3$	0.012	1.2 hypersthene (hy)
$FeSiO_3$	0.013	1.7 hypersthene (hy)
Mg_2SiO_4	--	--
Fe_2SiO_4	--	--
Magnetite (mt)	0.006	1.4 mt
Ilmenite (il)	0.005	0.7 il

1.5.2 Diagrammatic Presentations

1. Variation diagrams: simple X to Y comparison

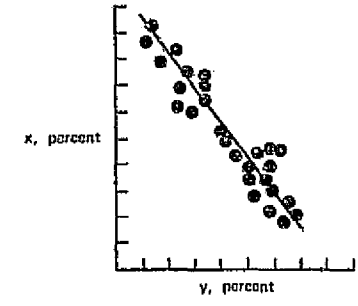

2. Ternary or triangular diagrams

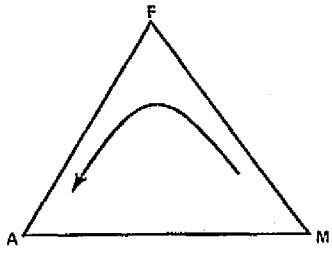

3. Harker diagram

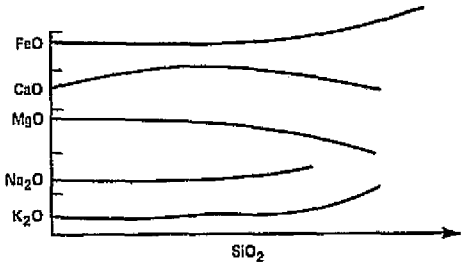

4. Larsen diagram (shows significant variations between felsic and basic rocks)

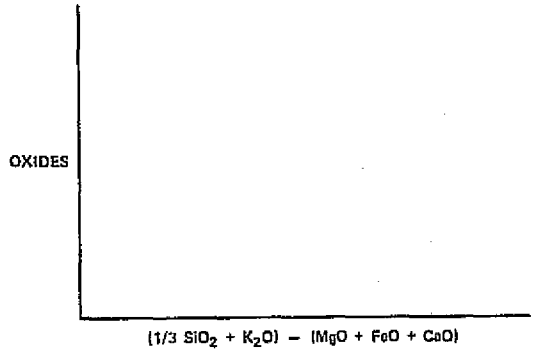

5. Solidification Index (Kuno, 1957)

$$S.I. = MgO/(MgO + FeO + Fe_2O_3 + Na_2O + K_2O) \times 100$$

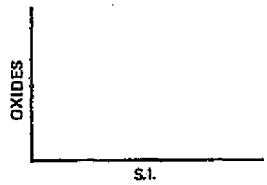

6. Alkali-Lime Index (Kuno, 1959)

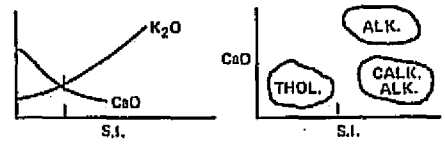

7. Alkali-Silica

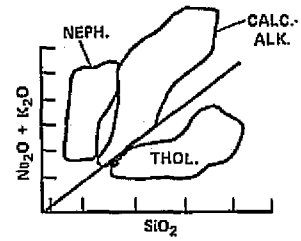

8. Al_2O_3 vs Σ alkalis (Kuno, 1960)

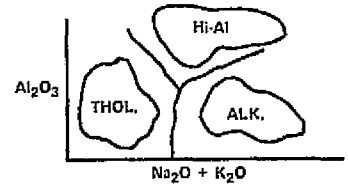

9. Differentiation Index (Thornton and Tuttle, 1960)

$$D.I. = Q + Ab + Or + Lc + Kp + Ne$$

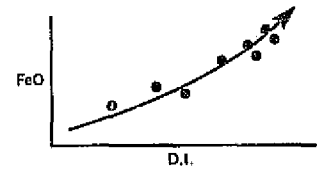

10. Crystallization Index (Poldervaart and Parker, 1964)

$$C.I. = An + Di + Fo + En + Sp$$

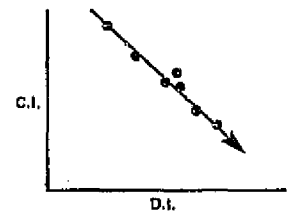

1.6 OUTLINE OF THE PETROGRAPHIC, NORMATIVE, AND CHEMICAL CHARACTERISTICS OF MAJOR BASALT GROUPS

1.6.1 Tholeiites

Normative and chemical characteristics–

1. Contain normative hypersthene and possibly quartz, although some may be olivine normative.

2. Silica content is commonly 48-51 percent.

3. Contain low K_2O content (< 0.4 for oceanic tholeiites; ≈ 0.9 for continental).

4. Low Fe_2O_4/FeO ratios.

5. Oceanic tholeiites are commonly consistent in chemical composition.

6. Continental tholeiites contain more alkalis than either oceanic-ridge or oceanic-island basalts.

Determination of tholeiites basalts in thin section–

1. May contain olivine phenocrysts but no olivine in groundmass. Olivine is commonly unzoned and may be mantled by pyroxene.

2. Pyroxene phenocrysts and microphenocrysts are less calcic than other basalts. Groundmass pyroxene may be augite, subcalcic augite, pigeonite, or, as in some oceanic tholeiites, ferroaugite. Hypersthene may occur in the groundmass or as phenocrysts. Pyroxene twinning, if present, is indicative of tholeiites.

3. Plagioclase is commonly labradorite.

4. Quartz may be present.

Other–

1. Ultramafic inclusions are not found in tholeiites.

2. Tholeiites are chemically transitional to high-alumina basalts and alkalic basalts.

3. Lunar and meteoritic basalts are mostly similar to terrestrial tholeiites.

1.6.2 Alkalic Basalts (Alkali Olivine Basalts)

Normative and chemical characteristics–

1. Normally contain normative nepheline.

2. Do not contain normative quartz.

3. Contain higher amounts of alkalis Cr, Ni, and trace elements than tholeiites.

4. Higher Fe_2O_3/FeO ratios (more oxidized than tholeiites).

Determination of alkali basalts in thin section–

1. Olivine present as phenocrysts and in groundmass; may be zoned.

2. Pyroxene is typically more calcic; may also contain high amount of Ti.

3. Alkali feldspars may mantle plagioclase or occur as individual grains.

4. Nepheline may be present.

Other–

1. Ultramafic inclusions are found in alkalic basalts.

2. Alkalic basalts older than late Paleozoic are unknown.

3. Alkalic basalts are unknown (*in situ*) from the ocean floor (at the time of this writing).

1.6.3 High-Alumina Basalts (Kuno, 1960)

Normative and chemical characteristics–

1. Contents of Al_2O_3 is > 17 percent.

2. May have small amounts of normative quartz or olivine.

3. Intermediate between tholeiites and alkalic basalts in composition and mineralogy.

Determination of high-alumina basalts in thin section–

1. Not easy; olivine may occur in phenocrysts or in groundmass, plagioclase is labradorite, and either quartz or alkali feldspars may occur.

2. Olivine phenocrysts may have inclusions of picotite spinel.

3. Pyroxene mostly limited to augite; pigeonite very rare.

1.7 PHASE EQUILIBRIA AND EXPERIMENTAL PETROLOGY

The whole is simpler than the sum of its parts.

W. Gibbs

1.7.1 Introduction

Field and laboratory observations led to the conclusion that igneous rocks contain consistent proportions of minerals in definite genetic sequences. This conclusion gave rise to the branch of petrology called experimental petrology which is concerned with understanding petrological processes. Laboratory studies include experiments dealing with physical and chemical properties of minerals, rocks, rock melts, vapors, and liquids that coexist with solid or molten materials. The pioneer and most dynamic experimental petrologist was N. L. Brown, whose book "The Evolution of the Igneous Rocks" is the most comprehensive work on the subject.

This section deals briefly with how phase equilibria experiments are performed, principles of phase equilibria, and some phase equilibria systems that deal directly with the understanding of igneous rocks.

1.7.2 Experimental Methods

Four stages are commonly employed to experimentally investigate a phase equilibria system: (1) synthesis of materials; (2) heating experiments; (3) determination of final products and phases; and (4) construction of phase equilibrium diagrams.

Synthesis of materials– Starting materials consist of analytical grade chemicals that are combined into the desired proportions. For example, if a starting composition of $An_{40}Di_{60}$ if desired, and 5 g are needed, then the following procedure is done: for each oxide in anorthite (CaO, Al_2O_3, SiO_2)

$$\frac{\text{mol wt of oxide}}{\text{mol wt of anorthite}} = \text{mol percent}$$

since An content = 40 or 40 percent of 5 g, then the correct weight percent of each oxide is calculated, weighed, mixed, and ground into a fine powder.

Example:

$$Al_2O_3 = \frac{101.94}{278.14} = 36.65 \text{ percent}$$

$$= 0.733 \text{ g or } 36.65 \text{ percent of } 2 \text{ g}.$$

The same procedure is done for Di_{60} (3 g). After thorough grinding, the powder is fused in a melting furnace, at a temperature at least 100°C above the melting temperature, and then quenched into a water bath. This melting procedure is repeated at least one more time to ensure homogeneity. The glass is examined optically to check for crystalline products and the index of refraction is checked for the desired composition (the above compound refractive index should be 1.590). We now have a glass (metastable liquid) that will be used in the quenching furnace technique.

Heating experiments– A vertical quenching furnace is used to determine the liquidus and solidus of the desired system. The furnace consists of a vertical ceramic tube that is externally wound by a heating element, usually made of platinum alloy, and both of these components are encased in a filled (commonly MgO) stainless steel container with both the top and bottom of the ceramic tube open. The glass or other starting material is put into a platinum crucible and lowered into the tube by means of a thin platinum wire. The furnace is heated to the desired temperature, which is read by a thermocouple, and the temperature is held for a predetermined period of time. To quench the sample, a high current is delivered to the platinum suspension wire and the crucible falls into a quenching bath (H_2O). This method has been simply described and more involved techniques are actually used or other methods can be

employed. A sketch of the furnace is shown below.

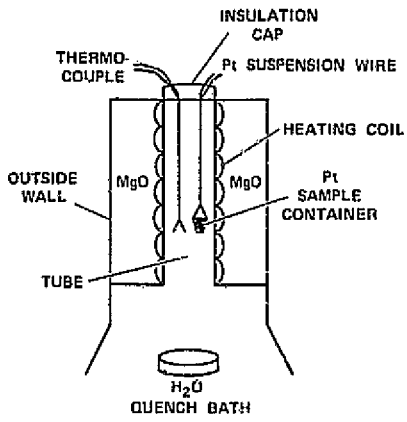

Determination of final products and phases– The products are checked for homogeneous distribution and phase compositions are determined by optical, x-ray, or electron microprobe methods.

Construction of phase equilibrium–

Diagrams: For simple systems, the above heating exercise is repeated for the same starting material until temperatures for the liquidus (glass + crystals) and solidus (all crystalline products) are determined. The entire operation is repeated for the next compositional increment.

Example: Diopside-anorthite system.

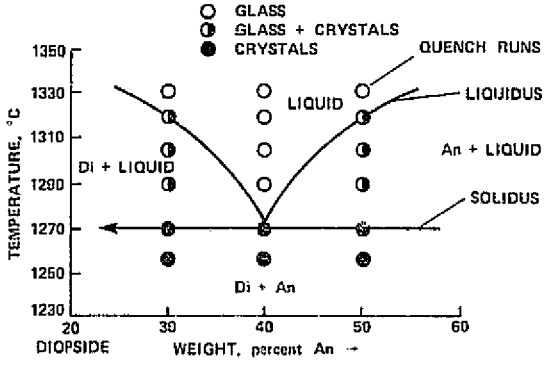

1.7.3 Phase Rule and Terminology

Phase– Physically distinct. Any portion of a system that is physically homogeneous within itself and bounded by a surface so that it is mechanically separable from other portions.

Component– The smallest number of independent variable constituents by which the composition of each phase taking part in equilibrium can be expressed as a chemical reaction:

$$CaCO_3 \rightleftharpoons CaO + CO_2$$

(two components; CaO and CO_2)

Degrees of freedom– The number of variable factors (temperature, pressure, concentration of components) that must be arbitrarily fixed in order that the condition of the system may be perfectly defined. A system is termed *invariant*, *univariant*, *divariant*, *trivariant*, etc., according to whether it possesses 0, 1, 2, or 3 degrees of freedom; some examples are:

1. Divariant: one phase present (vapor), P and T can change.

2. Univariant: two phases present (vapor + liquid); once one variable is changed the other is fixed.

3. Invariant: three phases present (vapor, liquid, and solid); T and P are fixed and there are no variables.

Phuse rule– For a system in equilibrium, the sum of the number of phases plus the number of degrees of freedom must equal the sum of the components plus two:

$$P + F = C + 2$$

where P is the phase, F are degrees of freedom, and C the components.

Each component has (P-1) equations; therefore, C(P-1) + number of equations

$$F = P(C-1) + C(P-1)$$

$$F = C - P + 2$$

Example for water:

1. ice (solid); F = 1 - 1 + 2; F = 2; P and T are variable.
2. ice and water (liquid); F = 1 - 2 + 2
3. ice plus water plus vapor; F = 1 - 3 + 2
   F = 0

1.7.4 One Component System (H_2O)

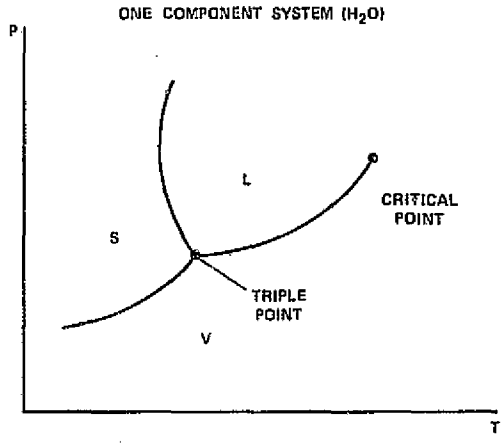

1. Variables: T or pressure
2. Phases = 3
3. F = C + 2 - P = 0 at triple point

Critical point– A point that represents a set of conditions (pressure, temperature, composition) at which two phases become indistinguishable. In a one component system, the T and P at which a liquid and its vapor become identical in all properties.

Triple point– An invariant point at which three phases coexist.

1.7.5 Two Component Systems

1. Three variables (P, T, or composition)
2. One of the following is held constant:
   T = isothermal
   P = isobaric
   X = isoplethal (composition)

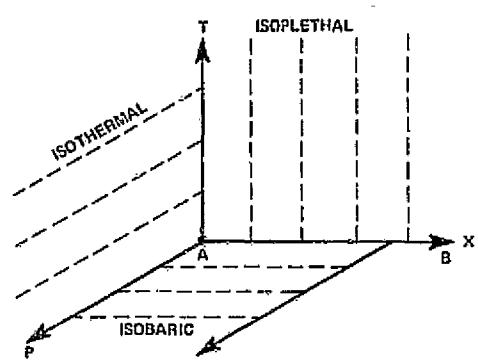

An isobaric two component (A+B) section is shown below.

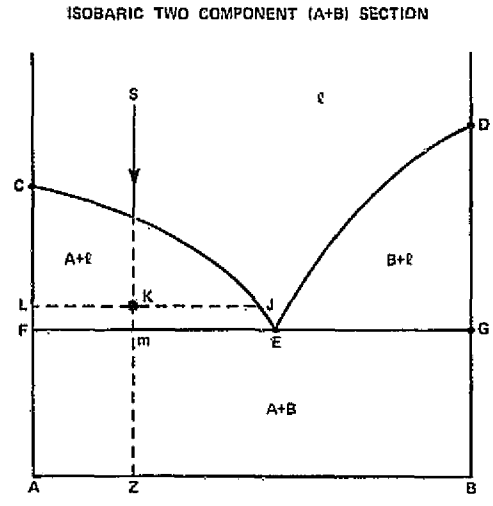

Eutectic (E)– Invariant point for the system. At the eutectic point an addition or removal of heat, increases or decreases the proportion of liquid to solid phases with change in temperature. The composition of liquid phases in equilibrium with solid phases can be expressed in terms of positive quantities of solid phases or the amount of one solid phase + liquid can also be determined: [A/J(liq)] = (JK/Kℓ) this ratio is called the *lever rule*. In more simple terms consider A_____C_____B where A and B are formed from C: The amount of AX length or AC = amount of BX length BC or A/B = BC/AC.

The amounts of the two phases are inversely proportional to their distances from the given composition. In the above diagram, when the crystallization course hits E then

$$\frac{A}{\text{liq } E} = \frac{ME}{MF}$$

This does not hold when B crystallizes or when ℓ disappears. Only B will crystallize (when starting composition is at S) when E is reached.

Note: The eutectic point is that point located at the intersection of two solubility curves in a binary system or the three soluability surfaces in a ternary system. It is the lowest melting point of any system.

Additional example: Solid Solution

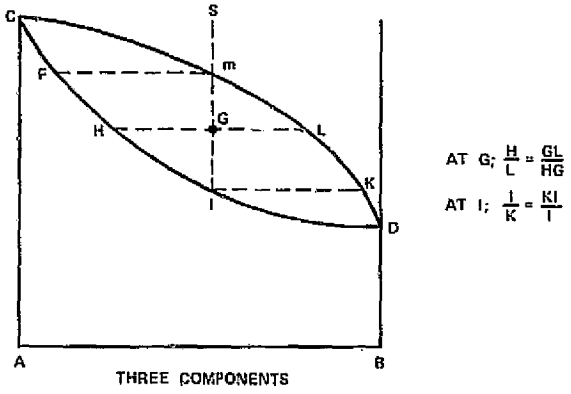

1.7.6 Three Component Systems

There are four independent variables (P, T, and two concentration variables) in a ternary system. Five coexisting phases produce an invariant system, four phases a univariant system, three phases a divariant system, etc. For example, in a three component system with four phases, the phase rule requires:

$$F = C + 2 - P \ , \quad F = 3 + 2 - 4 = 1$$

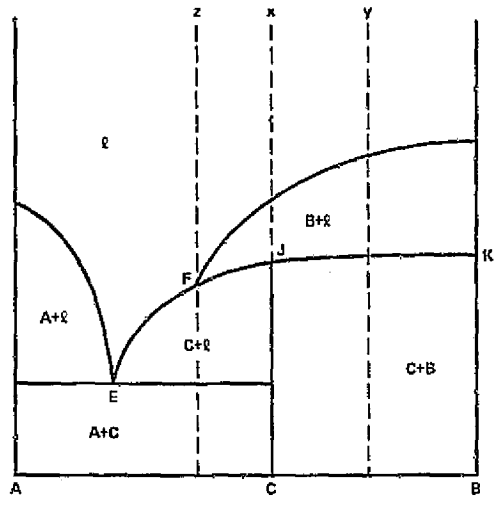

Three Component System With a Peritectic Point

Comp. X– B crystallizes to F (F-J-K plane) where there is the reaction B + liq F → C, thus 3 phases F, J, K and T is constant until all mixtures become one phase, C. Point F is a *peritectic point* or reaction point; that is, it is invariant and no independent changes of the system can be made. The composition of the liquid cannot be stated in terms of positive quantities of the solid phases. This is synonymous with *incongruent melting point*, which at a specified pressure the temperature where one solid phase transforms into another solid phase plus a liquid phase, all of which are different in composition from the original composition.

Comp. Y– B crystallizes to F (F-J-K plane) and B + liq F → C, but some B is left so the final composition is B + C.

Comp. Z– B + liq F → C, but some liq F is left. Crystallization continues down the curve to E. Final products will be A + C. From F to E, component C has its own primary field. C behaves in 2 ways: (1) a reaction product; (2) as a primary crystallization product.

Example: If B represents olivine, then B + (liq F) = C which is hypersthene.

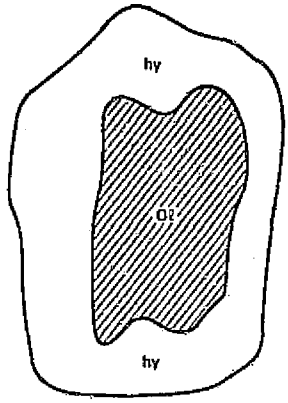

This is a rather common occurrence in igneous rocks where olivine has partially reacted with the liquid and is mantled with the reaction product, hypersthene:

"a corona structure (see fig. 3)"

Three component system (ternary) diagrams—

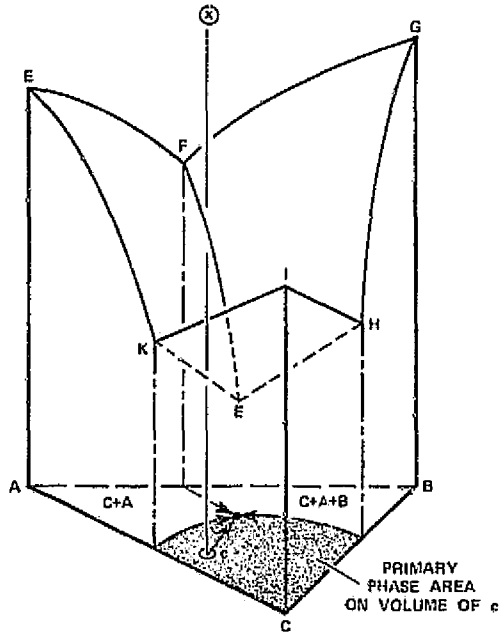

Comp. X intersects the liquidus surface in the primary phase field of C and continues until E, where A+B+C + liq coexist. At E, F = 1 which is fixed (P). When the liquid is used up, then T can drop.

The following diagram is a section cut through the above prism, parallel to the base; it shows the primary phase boundary surface or liquidus together with isotherms.

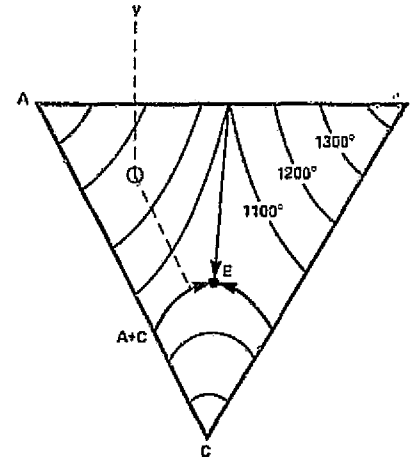

Comp. Y intersection of liquidus surface at D gives phase A + ℓ; A continues to crystallize until A-C boundary curve is reached where A+C+ℓ coexist. Crystallization of A+C continues to E where A+B+C+ℓ coexist.

1.7.7 Three Component Subsolidus System

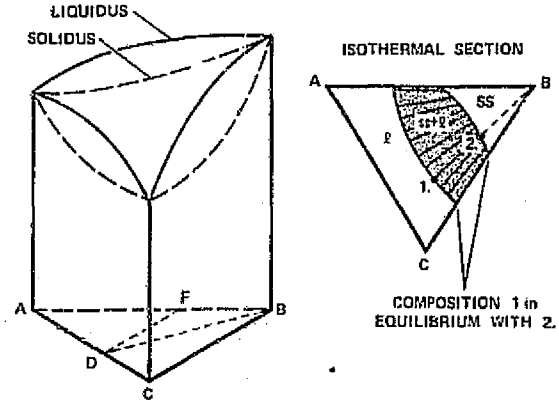

sections cut parallel along D-B and D-F

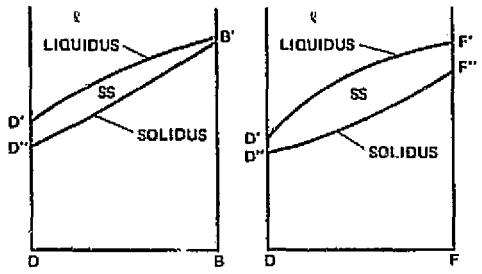

1.7.8 Application of the Lever Rule in a Ternary System

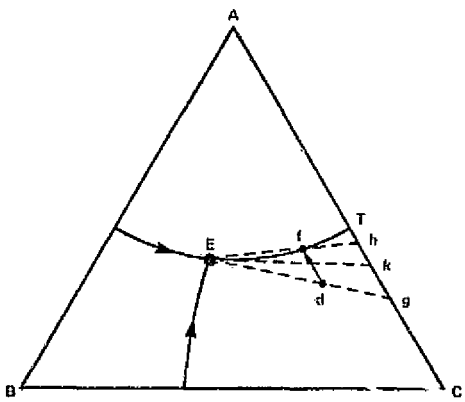

Composition projection hits principal phase volume C at d and crystallization of C continues to f (A-C boundary curve) where A+C crystallizes. Composition of f can be calculated by projecting a line from E (eutectic) through f to the A-C side (h), so that

$$f = \frac{C}{A} = \frac{Ah}{Ch}$$

Crystallization continues from f to E. Compositions along this curve (f to E) can be expressed by lines emanating from E thru the composition point on f-E to side A-C.

Example:

$$\frac{C}{A} = \frac{kA}{kC}$$

At E, B begins to crystallize, but A and C are expressed at g where the lever line emanates from E through d to A-C.

$$\frac{C}{A} = \frac{gh}{gC}$$

1.7.9 Plagioclase System – Equilibrium Solid Solution

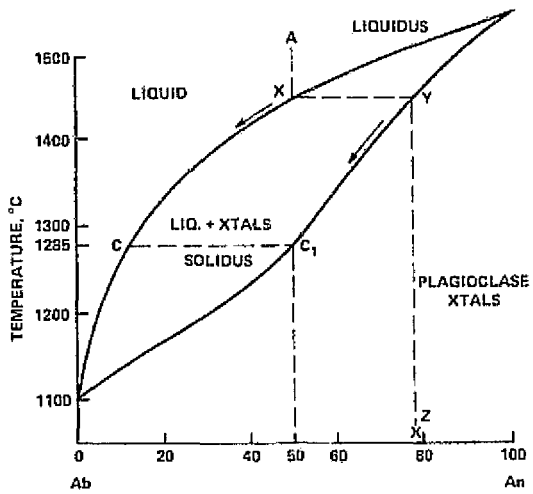

Initial composition = 50 percent Ab 50 percent An. Falling T to liquidus at X. Composition of first phase determined by line XYZ; comp. = An_{79}. Composition shifts down liquidus and solidus. Xtals are reacting continuously with the liquid when C-C' points are reached, the liquid is used up and the final composition is 50 percent Ab 50 percent An.

1.7.10 Plagioclase System – Disequilibrium (From Crystal Settling, Rapid Cooling, Zoning)

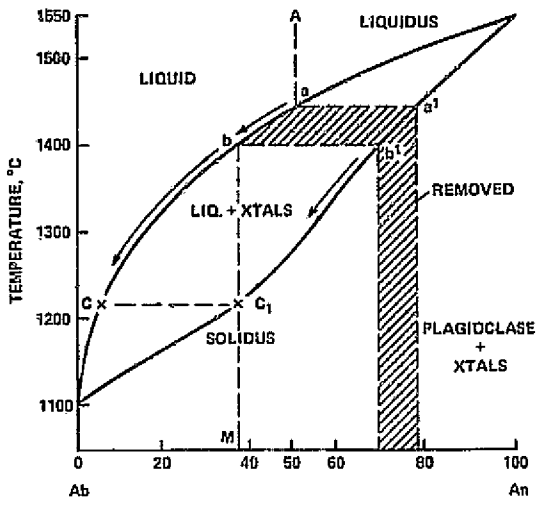

Initial composition = 50 percent Ab 50 percent An. Falling T to liquidus at *a*. a′-b′ removed from liquid by fractionation. Equilibrium begins again at b. To locate final composition drop a perpendicular from b to solidus (C_1) and continue on to M. Final solid composition is M = An_{38}. Last liquid composition at C.

1.7.11 Ternary System Forsterite – Diopside – Silica (Reaction Pair and Solid Solution Serie)

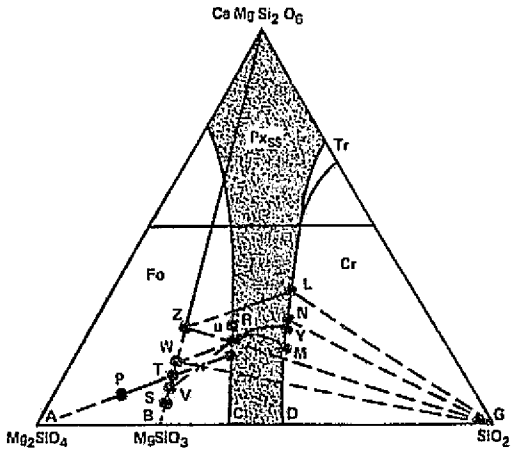

(Diagram distorted to show crystallization course.)

Comp. P– Fo crystallizes to point Q where Fo + liq = Px (pyroxene). Composition of Px shown at S. As crystallization shifts toward R, composition of pyroxene shifts towards V as it is changed by reaction with liquid. Point R is final point because original point P shows final composition of Px to be at T (line P-T-Q). Proportion of pyroxene: olivine is PA:PT.

Comp. X– Crystallization of Fo, course moves to U and Fo is used up. Px comp. here is read at V; therefore, no Fo (line V-X-U). Crystallization follows a curved path to Y where cristobalite crystallizes until point N is reached and all liquid is gone. Three phase triangle G-W-N gives final composition. Proportion of pyroxene:tridymite is XG:XW.

Comp. U– Similar to X. Only crystallization goes to L. Final composition is (A-Z-L).

Fractional crystallization– Crystallization would proceed on to tridymite field with 3-phase triangle giving changing composition along crystallization path.

1.7.12 Ternary System Incongruent Melting Point (Silica-Forsterite-Anorthite)

This ternary system is composed of three binary systems; fosterite-silica, anorthite-silica and forsterite-anorthite.

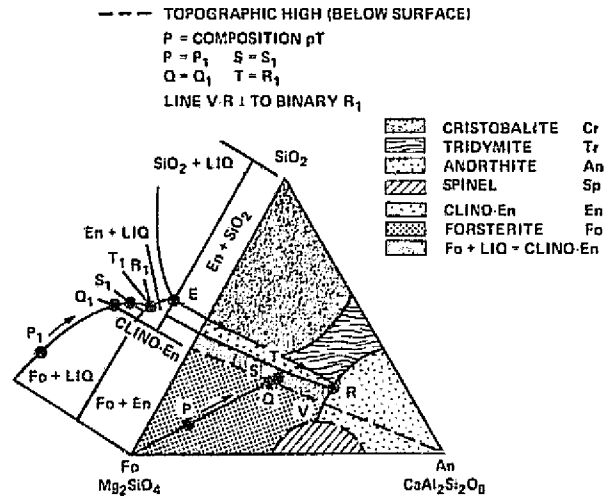

Comp. P– On falling temperature, moves to T, crystallizing Fo which in turn reacts with liquid to form clino-En at T. Liquid moves to R. At R. intersection of An boundary.

Final comp. = En + An + some Fo

Comp. Q (composition of clino-En)– Fo crystallizes between Q and T. T to R, liquid reacts with Fo to form En. At R, An crystallizes.

Final comp. = En + An, no Fo

Comp. S (lies within clino-En field)– Fo crystallizes from S to T. T to R, · Fo reacts with liquid to form En. An crystallizes at R and liquid is left over, course continues to E where tridymite crystallizes.

Final comp. = En + An + Tr

Comp. T– En forms by direct crystallization to point M where An crystallizes. Course continues to E where tridymite crystallizes.

Final comp. = En + An + Tr

Fractionation of Fo (with initial P comp.)– Fo crystallizes between P and Q, with Fo fractionating from the system. System behaves as if starting point was Q. Any system is a function of starting composition and cooling history. Composition P is undersaturated, composition Q is slightly saturated, and compositions S and T are saturated. In natural systems, olivine may be prevented from reacting with the liquid by pyroxene mantling.

1.8 PETROGENESIS OF MAJOR BASALTIC MAGMAS

Even when the experts all agree, they may well be mistaken.

B. Russell

Many hypotheses have been presented concerning the origin of basalts. Until the last 20 years most hypotheses were based on observations with little experimental data. Since Osborn's classic work in 1957, an explosion of experimental work on basalt petrogenesis has occurred, although no hypothesis is clearly accepted. This section outlines many of these hypotheses; a summary of Osborn's experimental work, which has had such great bearing on petrogenetic theory, is summarized first.

1.8.1 Osborn (1957)

Osborn emphasized the importance of the role of the partial pressure of O_2 (fO_2) in the crystallization trends of basaltic magmas. His work indicates that fO_2 is the chief determinant of whether liquids move toward higher SiO_2 and lower iron oxide content (calc-alkalic trend) or toward higher iron oxide and lower SiO_2 content (tholeiites). The accompanying diagram summarizes some of the important conclusions of his work.

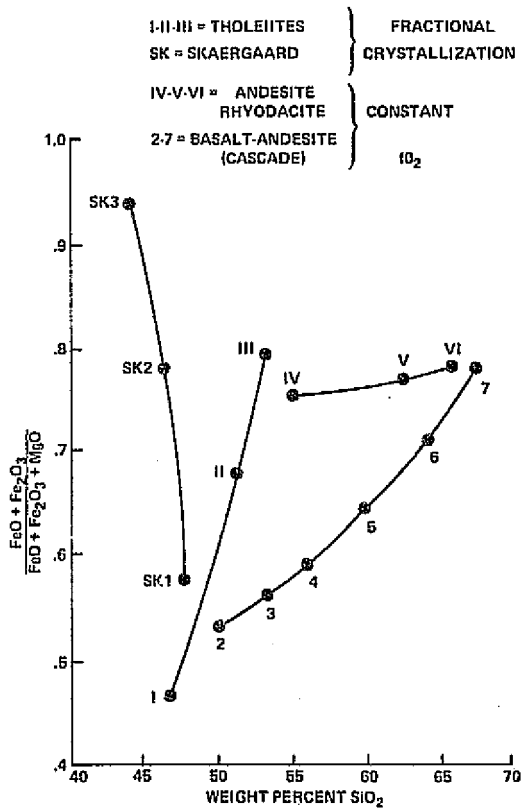

With fractional crystallization:

1. If fO_2 decreases, then trends I-III and SK occur.

2. If fO_2 remains constant, or increases during fractional crystallization, then trends 2-7 and IV-VI occur (basalt-andesites of orogenic belts).

An increase in fO_2 probably comes from added H_2O from sediments in orogenic belts; this helps to explain that "explosive" basalts (highly charged with H_2O) are confined to orogenic belts.

If plagioclase fails to separate in expected proportions, then high-Al basalts form.

1.8.2 Yoder and Tilley (1962)

Tholeiitic and alkalic basalts are primary; they result from partial melting of a garnet peridotite mantle at a depth of 100-150 km. Tholeiites differentiate in shallow magma chambers soon after initial melting, whereas alkalic basalts differentiate in a magma chamber at or near the point of melting in the mantle. Basalts, gabbros, pyroxenites and eclogites, are derivatives of a more primitive source. If eclogite is the basalt parent then tholeiites and alkalic basalts similarly originate from different depths (tholeiitic basalts, lower pressure or shallow depths, alkalic basalts, higher pressure, or deeper depths).

1.8.3 Kuno (1960, 1962)

The primary basaltic magmas: *tholeiites* result from partial melting in the mantle above 200 km; *high-Al basalts* result from partial melting of the mantle at 200 km; and *alkalic basalts* result from partial melting of the mantle below 200 km. Separation of olivine from the magma increases SiO_2 content in remaining liquid. In addition, the amount of Fe relative to SiO_2 is controlled by the amount of magnetite and olivine that separates from the magma. Kuno supported Osborn (1957) in that higher fO_2 causes oxidation of $FeO \rightarrow Fe_2O_3$ so that more magnetite and less ferrous silicates form.

1.8.4 A. E. J. Engel et al. (1965), G. A. Macdonald, and Their Coworkers (Summary)

Tholeiite is the only primary magma and is formed by partial melting of the upper mantle ($\approx$ 60 km in Hawaii). Alkalic basalt is derived from tholeiite by fractional crystallization (olivine and pyroxene settling) and gaseous transfer of alkalis. Differentiation occurs in shallow magma chambers in the crust. (Experimental evidence does not show differentiation of alkali basalts at low pressures.)

1.8.5 Green and Ringwood (1967)

Tholeiites and alkalic basalts are primary and are the result of different degrees of partial melting in the mantle. Tholeiites result when about 5 percent melting occurs and alkalic basalts form after 30 percent partial melting. Orthopyroxene replaces olivine as the liquidus phase in an olivine tholeiite at 13-18 kb (the orthopyroxene is rich in Al_2O_3). Extraction of this pyroxene gives a direct fractionation trend from olivine tholeiite to a derivative alkali olivine basalt magma; thus a direct fractionation trend exists from olivine and hypersthene normative tholeiitic basalt to olivine and nepheline normative alkali olivine basalt by separation of a simple phase.

They suggest that the source material of partial melting is a pyroxene-olivine rock called pyrolite (SiO_2 = 45 percent; Al_2O_3 = 3.5 percent; FeO^* = 9.0; MgO = 37.5 percent; CaO = 3.0 percent; and alkalis, 0.7 percent). Melting of this rock occurs at $<$ 100 km in the stability field of olivine $\pm$ aluminous orthopyroxene. From their calculated melting curve for pyrolite, Green and Ringwood show that at 60-75 km (seismic activity for Kilauea, Hawaii) partial melting of pyrolite yields an olivine tholeiite magma that rises rapidly to shallow levels to give an early tholeiite series. Tholeiites would continue to form if the process were sufficiently

rapid. With a slowdown in activity, the magma ascent is slower and the olivine tholeiitic magmas change to alkali olivine basalts to nepheline-bearing basalts (nephelinites) near the last stage.

The above hypothesis is based mainly on major element contents. Alkalic basalts contain high amounts of rare-earth elements and incompatible elements (U, Th, Ba, Cs, Rb, Sr, Zr, Hf) which are unable to substitute in major phases of the upper mantle. Green and Ringwood theorize that these elements are incorporated into the magma through reaction with the wall rock during slowly rising shallow magmas, whereas tholeiites are rapid rising, deep-sourced magmas.

1.8.6 O'Hara (1965)

Liquids that form from partial or total melting equal primary magmas. The magma type depends on the temperature, pressure, and degree of partial melting in the mantle and on the amount of differentiation that occurs during the magma's ascent to the surface. Thus surface compositions may not be a reliable guide to liquid compositions at depth.

1.8.7 Ito and Kennedy (1973)

Tholeiites, olivine tholeiites, and alkalic basalts may come from partial melting of eclogite at different depths. Alkalic basalts probably originate at shallow depths based on:

1. High vesiculation in alkalic basalts.
2. Alkalic basalts erupt explosively (high H_2O and volatiles).
3. Alkalic basalts are rich in nodules of stratiform type that form in bottoms of magma reservoirs.
4. Eruptions occur from tops of volcanoes, never as flows on ocean floor.
5. Accumulation of volatiles comes from higher levels in magma chamber, not at depth.

The Law of Perversity of Nature: You cannot successfully determine beforehand which side of the bread to butter.

Make three correct guesses consecutively and you will establish a reputation as an expert.

L. Peter

REFERENCES

Bowen, N. L. (1928). The evolution of the igneous rocks. Princeton Univ. Press, Princeton, N.J.

Buddington, A. F. (1963). Distribution of MnO between coexisting ilmenite and magnetite, in Advancing Frontiers in Geolcgy and Geophysics, A. P. Subramamiam, ed., Indian Geophysical Union, Hyderabad, India, pp. 233-248.

Buddington, A. F. and D. H. Lindsley (1964). Iron-titanium oxide minerals and synthetic equivalents. J. Petrol., vol. 5, pp. 310-357.

Bunch, T. E. and Laborde (1976). Mineralogy and composition of selected basalts from DSDP Leg 34. Initial Report Deep Sea Drill Project 34. In press.

Bunch, T. E., K. Keil, and R. Fodor (1976). Contributions to mineral chemistry in Hawaiian lavas: V olivine phenocrysts and groundmass olivine in lavas from Haleakala volcano. Contri. Mineral. Petrol. In press.

Engel, A. E. J., C. G. Engel and R. G. Havens (1965). Chemical characteristics of oceanic basalts and the upper mantle. Bull. Geol. Soc. Am., vol. 76, pp. 719-734.

Fodor, R., K. Keil, and T. E. Bunch (1975). Contributions to mineral chemistry of Hawaiian lavas: IV pyroxene phenocrysts and groundmass pyroxene in lavas from Haleakala volcano. Contr. Mineral. Petrol., vol. 50, pp. 173-197.

Green, D. H. and A. E. Ringwood (1967). The genesis of basaltic magmas. Contr. Mineral. Petrol., vol. 15, pp. 103-190.

Ito, K. and G. C. Kennedy (1973). The composition of liquids formed by partial melting of eclogites at high temperatures and pressures. J. Geol., vol. 82, pp. 383-393.

Keil, K., R. Fodor, and T. E. Bunch (1972). Contributions to the mineral chemistry of Hawaiian lavas: II Feldspars and Interstitial Material in Rocks from Haleakala and West Maui Volcanoes, Maui, Hawaii. Contri. Mineral. Petrol., vol. 37, pp. 253-276.

Kuno, H. (1959). Origin of Cenozoic petrographic provinces of Japan and surrounding areas. Bull. Volcanologique, sec. II, vol. 20, pp. 37-76.

Kuno, H. (1960). High-alumina basalt. J. Petrol., vol. 1, pp. 121-145.

Kuno, H. (1962). Frequency distribution of rock types in oceanic, orogenic, and kratogenic volcanic associations: The crust of the Pacific Basin. Am. Geophys. Union Geophys. Mon., vol. 6, pp. 133-139.

Macdonald, G. A. (1968). Composition and origin of Hawaiian lavas. Geol. Soc. Am. Mem. No. 116, pp. 477-522.

Macdonald, G. A. and T. Katsura (1964). Chemical composition of Hawaiian lavas. J. Petrol., vol. 5, pp. 82-133.

O'Hara, M. J. (1965). Primary magmas and the origin of basalts. Scottish J. Geol., vol. 1, pp. 19-40.

Osborn, E. F. (1957). Role of oxygen pressure in the crystallization and differentiation of basaltic magma. Am. J. Sci., vol. 259, pp. 609-647.

Poldervaart, A. and A. B. Parker (1964). The crystallization index as a parameter of igneous differentiation in binary variation diagrams. Am. J. Sci., vol. 262, pp. 281-289.

Thornton, C. P. and O. F. Tuttle (1960). Chemistry of igneous rocks: Part I, Differentiation index. Am. J. Sci., vol. 258, pp. 664-684.

Yoder, H. S. and C. E. Tilley (1962). Origin of basaltic magmas: An experimental study of natural and synthetic rock systems. J. Petrol., vol. 3, pp. 342-532.

Additional Reading

Clague, D. A. (1974). The Hawaiian-Emperor seamount chain: Its origin, petrology, and implication for plate tectonics. Ph.D. dissertation, Univ. of California, San Diego, Calif.

Findlay, A. (1903). Phase rule and its application. Edited and revised by A. N. Campbell and N. O. Smith (1951). Dover Publ. Co., New York, N.Y.

Hess, H. H. and Arie Poldervaart (1967) Basalts: The Poldervaart Treatise on Rocks of Basaltic Composition, vols. 1 and 2, Interscience Publ., New York.

McBirney, A. R. and H. Williams (1969). Geology and petrology of the Galapagos Islands. Geol. Soc. Am. Mem. No. 118.

Williams, H., F. J. Turner, and C. M. Gilbert (1954). Petrography – An introduction to the study of rocks in thin sections. W. H. Freeman and Co., San Francisco, Calif.

2. STRATIFORM IGNEOUS ROCKS

The test of a first rate intelligence is the ability to hold two opposed ideas in mind at the same time and still retain the ability to function.

F. S. Fitzgerald

2.1 INTRODUCTION

Ultramafic rocks in stratiform intrusions are formed by crystal settling in much the same way that sedimentary rocks form; that is, the resulting texture and structures reflect sedimentary processes controlled by gravity, densities, viscosity, grain shapes and sizes, and currents. Many of these igneous sedimentary piles (cumulates) have been studied thoroughly and are summarized by Wager and Brown (1967) and by Jackson (1967, 1971). Because of the coverage provided in these three sources, there is no need to make a lengthy presentation here; therefore, only an outline of layered rock or stratiform complex characteristics will be given. Additional attention will be given to petrographic characteristics of typical rocks of the Skaergaard Intrusion, Greenland, and the Stillwater Complex, Montana.

2.2 STRUCTURAL CHARACTERISTICS

Stratiform complexes commonly have the structural form of a lopolith, although the Skaergaard intrusion is shaped like an inverted funnel. The layered rocks dip, slightly (5°–25°) toward the center of the intrusion. The end-differentiate does not necessarily occur at the very top; rather it is usually located near the top because of simultaneous crystallization from the bottom (settling) and top (chilling of magma).

The most famous layered intrusions include the Skaergaard, Greenland; Stillwater, Montana; the Rhum, Scotland; the Bushveld, South Africa; the Great Dyke, South Africa; and the Muskox, Canada.

2.3 CHEMISTRY

1. Chemical variation trends – MgO and CaO decrease continuously with differentiation; SiO_2 remains constant in early stage and increases markedly during late stage; Na_2O and K_2O behave in a manner similar to SiO_2. Total Fe gradually increases until late stage where a sharp increase occurs; TiO_2 and P_2O_5 increase gradually until early late-stage, when sharp increases occur, and then decrease in the final stage.

2. AMF diagram – Early stages show continual increase of iron until the time of iron oxide crystallization when the trend shifts towards rapid increase of alkalis.

2.4 TERMINOLOGY (modified from Wager et al. 1960 and Jackson 1971)

1. Cumulus phases – Phenocrysts that have settled out of a liquid magma, and have been packed into some sort of sedimentary pile; "sediment" minerals at the bottom of the liquid.

2. Layering – Form of stratification of sheet-like structures in igneous rocks.

3. Rhythmic layering – Conspicuous banding of cumulate minerals rhythmically repeated.

4. Adcumulus or adcumulate – Postcumulus overgrowth by material of same composition as cumulus mineral.

5. Orthocumulate – Cumulate rock where intercumulus trapped material (pore space filling material) has the overall composition of the contemporaneous magma. For example, pore material will consist of poikilitic pyroxenes, olivine, and magnetite in Skaergaard rocks of cumulus plagioclase.

6. Heteradcumulate – Intercumulus material which does not have the overall composition of the magma. For example, cumulus bronzite and interstitial postcumulus plagioclase.

7. Oikocrysts – Poikilitic phases that enclose cumulus minerals (Note: see photomicrographs

and petrographic descriptions of Skaergaard and Stillwater rocks for examples of terminology.)

2.5 MINERALOGY

A large variety of rock types are found in large layered intrusions, although the great bulk of the intrusions are composed essentially of plagioclase-rich rocks, norite, and anorthositic members. Rock layers lower in the intrusions tend to have fewer numbers of phases and some are even monomineralic (bronzitites and dunites). The number of phases in the upper member rocks increase (ferrogabbros and granophyres).

Major minerals are listed below.

1. Pyroxenes – Early in the crystallization sequence, both Ca-rich and Ca-poor phases are present. The major chemical variation is increase of Fe content (Fs) as crystallization proceeds. When the pyroxene composition reaches about Fs_{50}, crystallization of the Ca-poor phase ceases and only the Ca-rich phase continues to crystallize (only this phase is in equilibrium with the magma). Most of the Ca-poor clinopyroxene inverts to orthopyroxene on cooling. Prior to inversion, lamellae of Ca-rich pyroxene exsolve; exsolution also takes place in the Ca-rich pyroxene. (See fig. 44, chapter 1 for Skaergaard pyroxene trends.)

2. Plagioclase – Composition changes from high-calcium contents $< An_{80}$ to sodic varieties with increasing structural height. Plagioclase occurs as cumulus: orthocumulus, adcumulus, and postcumulus phases. Adcumulus = border growth composition same as core which implies that border growth in upper level of sediment.

3. Olivine – Mg-rich olivine in lower rocks which became progressively more Fe-rich with differentiation. Crystallization of olivine ceased at about Fo_{53} and a gap exists until later crystallization of olivine starts at about Fo_{40}. Olivine may continue to crystallize until pure fayalite composition is reached.

4. Others – Chromite crystallized in early lower stages and magnetite commonly occurs in the middle to late stages. Apatite crystallized during middle to late stage and may be a cumulus mineral in some intrusions (Skaergaard). Quartz is common as intercumulus phase in late stages together with alkali feldspars and Fe-rich olivine. Other minerals, micas, and amphiboles formed as reaction phases.

2.6 THE SKAERGAARD LAYERED INTRUSION

The Skaergaard layered intrusion was discovered by Professor L. R. Wager in 1930. The complex is situated on the southeastern coast of Greenland and is Tertiary in age. The margins of the intrusion are referred to as the marginal border group (MBG) and consists of fine-grained gabbros which are the result of chilling of the magma against the country rock. The present thickness of the layered rock is approximately 2500 m. Theory predicts that layered rocks persist below the lowest rocks presently exposed and these are referred to as the *hidden layered series* or *hidden zone* (HZ). The exposed rocks can be subdivided into layered zones on the basis of the entrance or discontinuance of cumulus minerals. The *lower zone* (LZ) contains cumulus Mg-olivine in abundance, the *middle zone* (MZ) contains no olivine, and the *upper zone* (UZ) contains cumulus olivine again although it is more iron-rich (Fa_{60}) relative to the most iron-rich olivine in the lower zone (Fa_{47}). Plagioclase shows a continuous increase in Na content from the lower zone through to the upper zone and clinopyroxene becomes progressively enriched in Fe relative to Mg (see fig. 44). Magnetite is mostly absent in the lower zone and apatite does not appear until the upper zone rocks formed. The marginal and upper border groups (mostly absent in exposures) were formed from the same fractionating magma as the layered series. The *tranquil division* and the *banded division* belong to the marginal border

group. The last rocks to crystallize are situated in a thin layer between those rocks that formed the upward growing layered series (LZ, MZ, UZ) and the downward growing series (UBG); this zone is referred to as the *sandwich zone*. The reader is referred to Wager and Brown (1967) for a more complete description of the Skaergaard.

2.6.1 Skaergaard Sample Descriptions

The following is a description of Skaergaard hand specimens and their sections that closely follows the original descriptions made by members of the geology staff at the University of Oregon. The samples were collected by the University of Oregon Expedition to the Skaergaard Intrusion in 1974.

The samples are arranged in descriptive order A through X; this order corresponds to the labeling scheme of Western Minerals Inc., from whom samples were obtained. An additional designation is made by a number for each sample which corresponds to those made by the geologists in the field.

A. (Oregon no. 9) *Lower Zone A*

Rock – An olivine gabbro containing cumulate olivine and plagioclase in a matrix of intercumulate poikilitic clinopyroxene and accessory magnetite. This sample was collected along Uttentals Sund in the northwest corner of the intrusion.

Thin Section – Olivine (Fo_{65}) and labradorite are large granular crystals that formed as cumulates. Poikilitic pyroxene (px) grew around the cumulate phases but was not a primary precipitate at this level. Magnetite occurs as an accessory mineral which crystallized from the trapped intercumulate liquid. Biotite (bt) formed between magnetite and plagioclase (pl) as a result of reaction with volatiles escaping from the underlying gneiss. (See fig. 47, p. 48.)

B. (Oregon no. 10) *Lower Zone B*

Rock – An olivine gabbro with cumulate olivine, plagioclase, and clinopyroxene in a matrix of poikilitic clinopyroxene and minor amounts of magnetite. It was collected along the northern shore of Uttentals Sund at the site of the 1965 drilling attempt of the Skaergaard intrusion.

Thin Section – Olivine, labradorite, and augite are cumulus phases at this level. Poikilitic pyroxene and accessory magnetite fill in the intercumulate areas. Note the exsolution textures in the pyroxene. (See fig. 48, p. 48.)

C. (Oregon no. 11) *Lower Zone C*

Rock – An olivine gabbro with cumulate olivine, plagioclase, clinopyroxene, and magnetite with intercumulate poikilitic clinopyroxene and abundant anhedral magnetite. The sample was collected from the eastern edge of Kramers Island.

Thin Section – Magnetite is abundant at all levels above the base of this zone and probably precipitated as a cumulus phase. Note the reaction rims between magnetite and pyroxene: this is thought to be the result of subsolidus reduction of magnetite and desilication of adjacent pyroxene to produce an iron-rich olivine. Feathery intergrowths of pyroxene and spinel formed near the edges of some of the plagioclase, possibly through locally concentrated water, which favored a shift of the plagioclase to a more Na-rich composition. Plagioclase at this level is strongly oriented. (See fig. 49, p. 49.)

D. (Oregon no. 25) *Middle Zone*

Rock – A coarse-grained gabbro with cumulate clinopyroxene, plagioclase, and magnetite. Interstitial minerals include clinopyroxene and magnetite. Olivine is generally absent from this zone but rare crystals do exist. Collected from the southeast corner of Kramers Island.

Thin Section – At this level olivine ceased to crystallize as a primary phase but is still present in small amounts due to late reactions between magnetite and pyroxene. Plagioclase is now about An 50 and the pyroxene is intermediate between iron and magnesium end-members. (See fig. 50, p. 49.)

E. (Oregon no. 23) *Upper Zone A*

Rock – A ferrodiorite with cumulate olivine, plagioclase, clinopyroxene, and magnetite. The intercumulate material is primarily poikilitic clinopyroxene and anhedral magnetite. Collected 0.5 km south of Forbindels glacier along Uttentals Sund.

Thin Section – Olivine (hortonalite) reappeared as a cumulus phase at the base of the upper zone and became increasingly iron-rich upwards. Pyroxenes (px) have a brownish color and high RI because of their high iron content. (See fig. 51, p. 50.)

F. (Oregon no. 21) *Upper Zone B*

Rock – A ferrodiorite with cumulate olivine, plagioclase, clinopyroxene, and apatite. Intercumulate minerals include plagioclase, clinopyroxene, and magnetite. Collected from the south side of Home Bay.

Thin Section – About 100 m above the base of the upper zone, apatite (ap) is present as a cumulate mineral. This rock contains about 2.7 percent P_2O_5. Olivine and pyroxene (px) are very iron-rich and often show exsolved magnetite along fractures. (See fig. 52, p. 50).

G. (Oregon no. 26) *Upper Zone C*

Rock – A ferrogabbro containing cumulate olivine, plagioclase, magnetite, and apatite. The original intercumulate wollastonite has inverted to a patchy pyroxene during cooling. Collected along Skaergaard Bay near the foot of Basisglacier.

Thin Section – Near the top of the upper zone the pyroxenes are almost pure hedenbergite. They crystallized initially as a Fe-wollastonite but with a small amount of cooling they entered the stability range of clinopyroxene. Olivine is essentially pure fayalite, but the plagioclase is still only andesine. Scattered patches of granophyre have crystallized from the trapped liquid. (See fig. 53, p. 51.)

H. (Oregon no. 28) *Sandwich Horizon*

Rock – A ferrogabbro containing cumulate crystals of olivine, plagioclase, apatite and inverted wollastonite. This horizon also contains dendritic magnetite and myrmekitic quartz. The sandwich horizon represents the final product of the layered series differentiation and is believed to have formed from residual liquids trapped between the layered series and the Upper border group. Collected from the eastern slopes of Basistoppen.

Thin Section – This is thought to be the last rock to crystallize as the layered sequences of the reef and the floor converged. It is very rich in residual components, including high concentrations of excluded trace elements. Note that the silica mineral apparently crystallized originally as quartz (q). (See fig. 54, p. 51.)

I. (No hand specimen available) *Upper Border Group* γ

Thin Section – The last of the rocks of the upper border group that crystallized from the reef downward have many of the features of the main layered series, but tend to be richer in plagioclase and to have been hydrothermally altered by gases that streamed up through them. This rock, which comes from just above the sandwich horizon, crystallized tridymite (tr) as the initial silica phase, but crystallized quartz as the rock cooled. The needle-like quartz crystals

are pseudomorphs of tridymite. The tridymite-quartz transition occurred at about 980° C at this pressure level. (See fig. 55, p. 52.)

J. (Oregon no. 29) *Upper Border Group*

Rock – Is a medium-grained plagioclase-rich gabbro containing cumulate plagioclase, clinopyroxene, and olivine. Alteration introduced quartz, chlorite and zeolite. The rocks of the upper border group are often altered from having formed above the cooling Skaergaard magma. Collected approximately 0.5 km north of the southern margin of the intrusion near the entrance of Skaergaard.

Thin Section – This section shows the type of alteration typical of much of the upper border group. Quartz, chlorite, and zeolite are the typical alteration minerals. Note the myrmekitic intergrowths of quartz in plagioclase. Hydrothermal fluids from the layered series also deposited anomalously high amounts of trace elements in the upper border group. Small zircon crystals are also present. (See fig. 56, p. 52.)

K. (No hand specimen available) *Upper Border Group α*

The highest levels of the upper border group contain large laths of labradorite with a composition similar to plagioclase of the lowest exposed part of the layered series. Poikilitic pyroxene has grown between the plagioclase laths and comprises a large portion of the rock. Graphic magnetite crystals and rare interstitial quartz crystallized from the trapped liquid.

L. (Oregon no. 7) *Chilled Margin*

Rock – This fine-grained basalt formed when the Skaergaard magma was chilled against the country rock. This rock contains uniformly sized grains of olivine, plagioclase, magnetite, and clinopyroxene. Collected along the northwest margin of the intrusion on the north side of Uttentals Sund.

Thin Section – In most places close to the contact, the chilled margin rocks have a fine-grained granular texture and commonly show a strong orientation of plagioclase. Olivine may or may not be present depending on the amount of assimilation of silica from the wall rocks. Small fragments of gneiss are common in the chilled margin. (See fig. 57, p. 53.)

M. (Oregon no. 8) *Gabbro Picrite*

Rock – This particular rock is closer to a feldspathic peridotite than a gabbro but the name applied by Wager is widely accepted. Blocks of the composition are found near the margin of the intrusion along the northern boundary where the lowest levels of the intrusion are exposed. Olivine is the most Mg-rich in the intrusion. Presumably the blocks were carried up to their present level from a deeper horizon, perhaps in the feeding channel.

Thin Section – A medium-grained olivine-rich gabbro contained as blocks on the marginal zone of the intrusion along its northern contact. The rock contains abundant euhedral olivine crystals in a matrix of plagioclase, magnetite, and poikilitic pyroxene. The olivine is Fo_{81} and is the most magnesium-rich in the intrusion collected from the marginal border group on Uttentals Plateau. (See fig. 58, p. 53.)

N. (Oregon no. 4) *Perpendicular Feldspar Rock*

Rock – A medium-grained olivine gabbro containing elongated feldspar crystals. The plagioclase crystals contain cores of An 72 and rims of An 77 and are elongated parallel to their c axis. These plagioclase crystals grew perpendicular to the intrusion contact in what is called the tranquil division of the marginal border group. The groundmass contains euhedral to subhedral crystals of olivine, plagioclase, magnetite, and orthopyroxene enclosed in poikilitic crystals of clinopyroxene.

Thin Section – Many rocks within the marginal border group contain slender plagioclase crystals oriented normal to the contact which give the rock a comb or crescumulate texture. Small cumulate olivines and poikilitic pyroxene occur between the elongated feldspar crystals. (See fig. 59, p. 53.)

O. (Oregon no. 5) *Coarse Clot Material*

Rock – A coarsely crystalline olivine gabbro from the marginal border zone of the intrusion. It is composed of large intergrown crystals of plagioclase and clinopyroxene with included euhedral crystals of olivine and anhedral magnetite. These clot bands, which occur at irregular intervals within the Marginal Border Group, are often partially altered to chlorite minerals. Collected approximately 50 m from the intrusion margin on Mellamo Island.

Thin Section – Many bands of coarsely crystalline clots are present within the marginal border group. Although the exact mechanism for their formation is unknown they are believed to have formed from very volatile rich liquids. These clots contain large crystals of olivine, plagioclase, pyroxene, apatite, and magnetite. Biotite is now largely altered to chlorite. Magnetite and chlorite often replaced olivine. Quartz occurs as a late alteration product and sphene is an accessory mineral. (See fig. 60, p. 54.)

P. (Oregon no. 30) *Melanogranophyre*

Rock – This rock, originally called a hedenbergite granophyre by Wager, has a coarse, graphic texture with perthitic alkali feldspars and iron-rich pyroxene. The melanogranophyre occurs as isolated bodies within the upper border group and is believed to represent an immiscible liquid which separated from the main Skaergaard magma at the late stage in its differentiation history.

Thin Section – This sample is a granophyne that contains quartz, plagioclase, orthoclase and abundant magnetite and pyroxene. The quartz forms myrmekitic intergrowths with orthoclase and the pyroxene occurs as dendritic needles which give the rock a streaky appearance. Melanogranophyre bodies occur as disseminated masses in much of the lower portion of the upper border group. Collected from the south side of Basistoppen. (See fig. 61, p. 54.)

Q. (Oregon no. 27) *Transgressive Granophyre*

Rock – A medium-grained granophyre with anhedral crystals of quartz and orthoclase, euhedral crystals of plagioclase, and accessory hornblende and biotite; it comes from one of the many post-Skaergaard granophyre dikes that cut through the layered series. Collected 0.5 km south of Forbindelses glacier along Uttentals Sund.

Thin Section – The transgressive granophyres cut the layered series as sills and dikes. These acid granophyres are composed primarily of quartz, orthoclase, and plagioclase. Accessory apatite, hornblende, and biotite indicate that the granophyre was volatile rich.

R. (Oregon no. 16) *Tinden Sill*

Rock – An acid granophyre containing plagioclase, orthoclase and quartz crystals and areas of myrmekitic intergrowths of quartz and orthoclase. The sill represents the most differentiated rock in the Skaergaard complex. Collected from the north side of Tinden peak near Brodretoppen glacier.

Thin Section – This acid granophyre forms a large sill intruded into the upper part of the Skaergaard intrusion; it is the most silica-rich rock in the complex. Strontium isotope studies indicate that this sill is the product of melting of the surrounding gneiss. The granophyre contains alkali feldspars and quartz.

S. (Oregon no. 1) *Contact Gneiss*

Rock – A recrystallized feldspathic gneiss that shows a slight remnant foliation. The rock is composed primarily of quartz, orthoclase, and plagioclase, and contains the accessory minerals biotite, chlorite, and magnetite. The intrusion is in contact with Precambrian gneiss along its western and northern margins. Collected approximately 1 m west of the contact on Mellamo Island.

Thin Section – This sample was collected less than 1 m from the Skaergaard contact and is surprisingly unaltered, although there has been some recrystallization. Minerals include quartz, cloudy feldspar, biotite, chlorite, epidote, and magnetite.

T. (Oregon no. 2) *Foliated Gneiss*

Rock – A strongly foliated feldspathic gneiss of Precambrian age. The lighter bands are composed primarily of quartz, orthoclase, and plagioclase, and the darker bands are composed of magnetite, clinopyroxene, and quartz with only scattered feldspar crystals. Collected from the western end of Mellamo Island approximately 100 m from the intrusion.

Thin Section – This specimen of strongly foliated feldspathic gneiss was collected 100 m from the intrusion contact. It consists of a mosaic of quartz and feldspar with granular aggregates of hypersthene, magnetite, and deeply embayed biotite. Some of the plagioclase has clear untwinned rims surrounding a cloudy interior.

U. (Oregon no. 6) *Fused Gneiss*

Rock – This sample comes from a partially melted gneiss block included in the marginal border zone of the intrusion. The rock has a mottled appearance caused by darker bands of Skaergaard material surrounding lighter areas of fused gneiss. The darker bands contain crystals of olivine, plagioclase, magnetite, and clinopyroxene; the lighter areas are composed of cores of fused gneiss surrounded by lighter reaction rims of euhedral quartz. The rock also contains scattered blebs of chalcopyrite. (Collected from the marginal border group on Uttentals Plateau.)

Thin Section – The darker bands contain olivine, plagioclase, magnetite, and clinopyroxene. The lighter bands contain a larger proportion of plagioclase and accessory biotite and clinozoisite. The lighter areas represent partially fused gneiss and the darker areas the Skaergaard magma. Most of the original quartz has been consumed in reaction with the olivine gabbro.

V. (Oregon no. 3) *Basaltic Dike*

Rock – This sample was collected from a fine-grained, post-Skaergaard, basaltic dike approximately 0.5 m in width. Post-Skaergaard dikes ranging from a few centimeters to many meters in width are very abundant in the southern portion of the intrusion. (Collected on Mellamo island near the western contact of the intrusion.)

Thin Section – The rock originally contained microphenocrysts of augite, plagioclase, and olivine in an intergranular groundmass of plagioclase, pyroxene, magnetite, and glass that was hydrothermally altered (olivine was altered to serpentine).

W. (Oregon no. 24) *Altered Basalt*

Rock – A fine-grained basalt which was altered to a granular hornfels by the Skaergaard intrusion. (Collected on the east side of the intrusion near Miki's Fiord.)

Thin Section – The section contains rounded aggregates of coarse pyroxene in a fine-grained matrix of granular pyroxene and anhedral plagioclase. Olivine was completely altered and magnetite recrystallized to elongated blebs and irregular clots. Secondary biotite is intimately

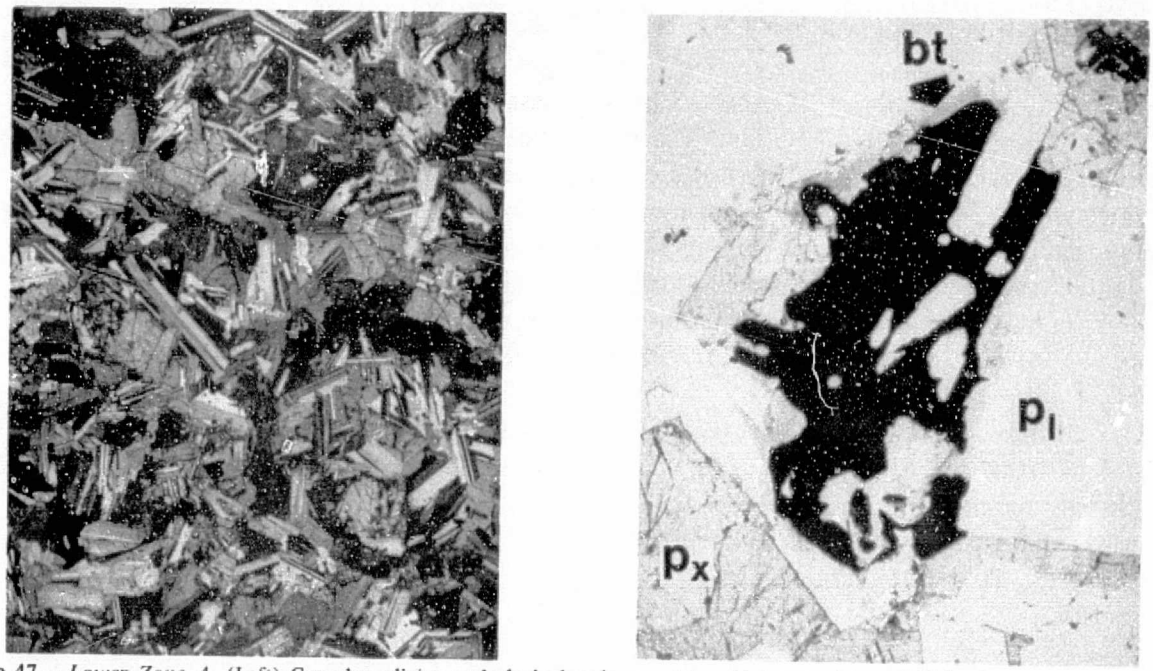

Figure 47.– *Lower Zone A.* (Left) Cumulus olivine and plagioclase in a matrix of intercumulate poikilitic clinopyroxene. Photomicrograph, field width = 15 mm. (Right) Reaction relationship of biotite (bt) and magnetite (dark), field width = 0.35 mm. (Cross polarized light.)

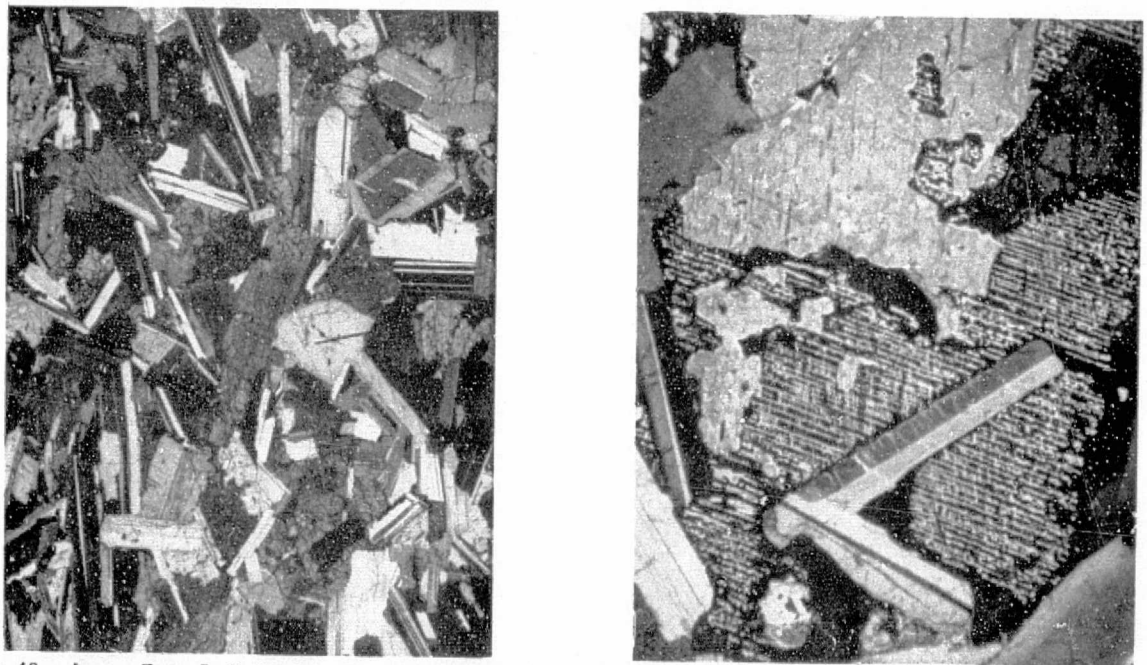

Figure 48.– *Lower Zone B.* (Left) Cumulus olivine, plagioclase, and clinopyroxene in a matrix of late poikilitic clinopyroxene. Photomicrograph, field width = 15 mm. (Right) Exsolution texture in poikilitic pyroxene, field width = 0.9 mm. (Plane polarized light.)

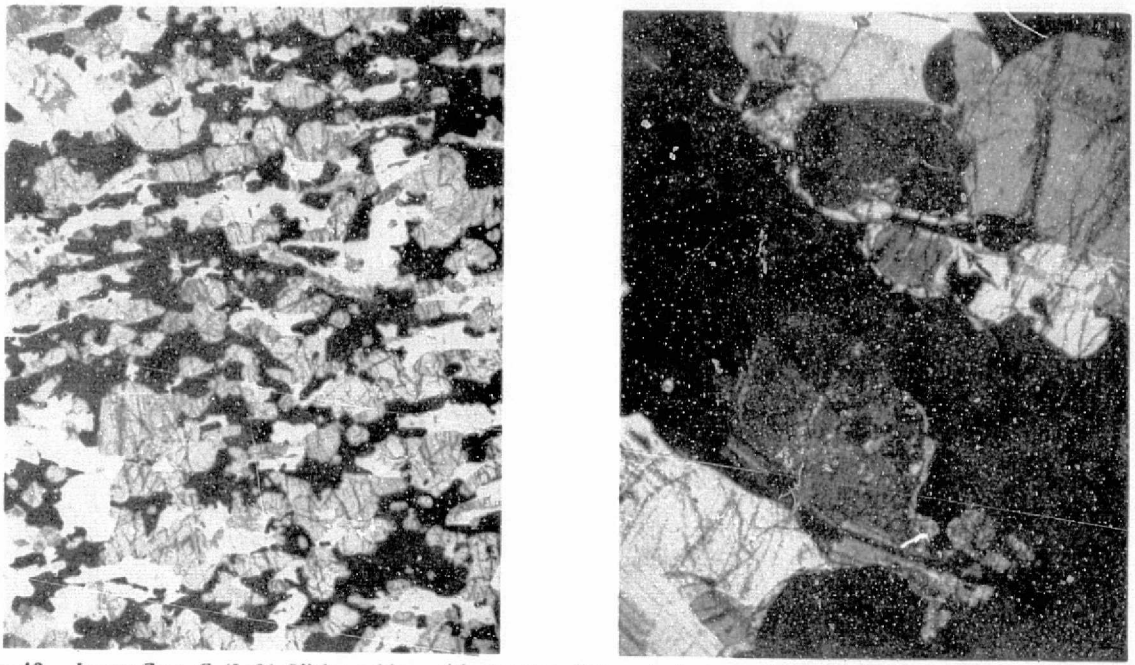

Figure 49.– *Lower Zone C.* (Left) Olivine gabbro with cumulus olivine, plagioclase, clinopyroxene, and magnetite. Note preferred orientation of plagioclase laths (layering). Field width = 15 mm. (Right) Arrow points to iron-rich olivine from reaction-reduction of magnetite and pyroxene. Field width = 0.35 mm. (Cross polarized light.)

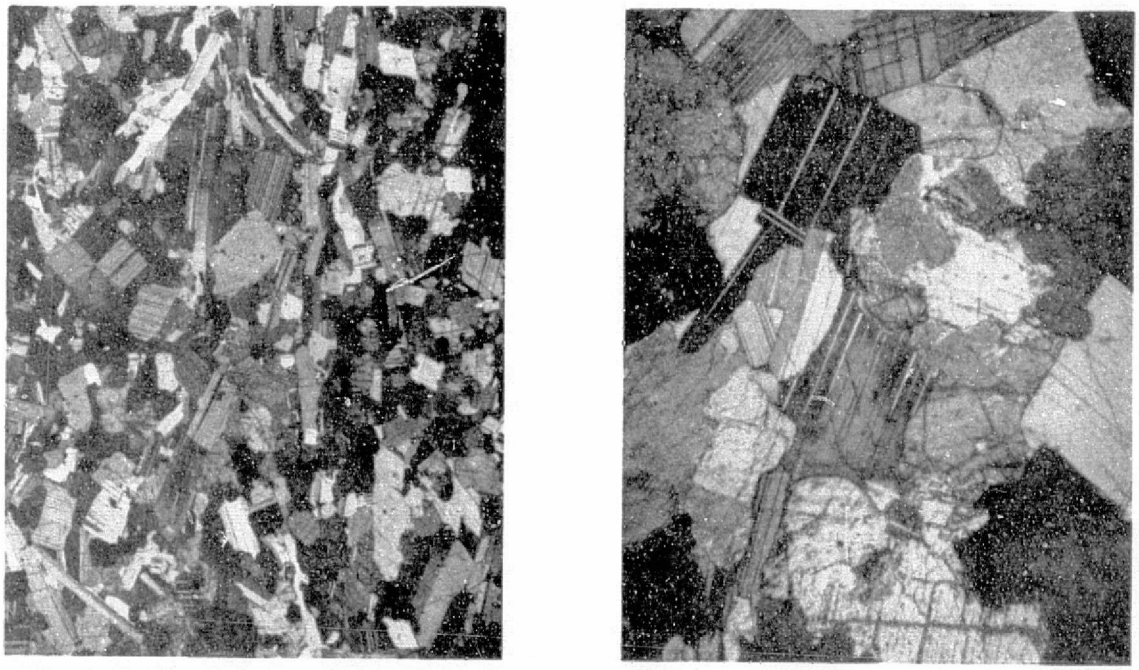

Figure 50.– *Middle Zone.* (Left) Cumulus plagioclase, clinopyroxene and magnetite (olivine is absent). Field width = 15 mm. (Right) Enlargement showing grain boundary relationship of cumulus phases. Field width = 0.9 mm. (Cross polarized light.)

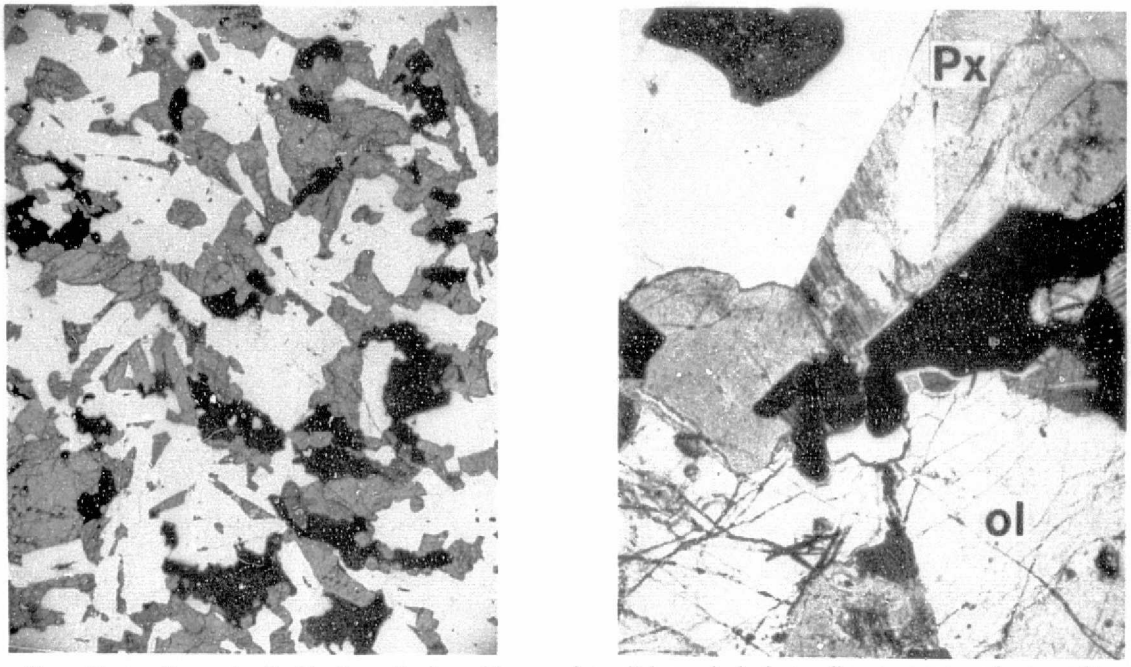

Figure 51.– *Upper Zone A.* (Left) Ferrodiorite with cumulus olivine, plagioclase, clinopyroxene and magnetite. Field width = 15 mm. (Right) Thin border of reaction-formed Fe-olivine. Px = clinopyroxene with exsolved orthopyroxene, Ol = olivine. Field width = 0.9 mm. (Cross polarized light.)

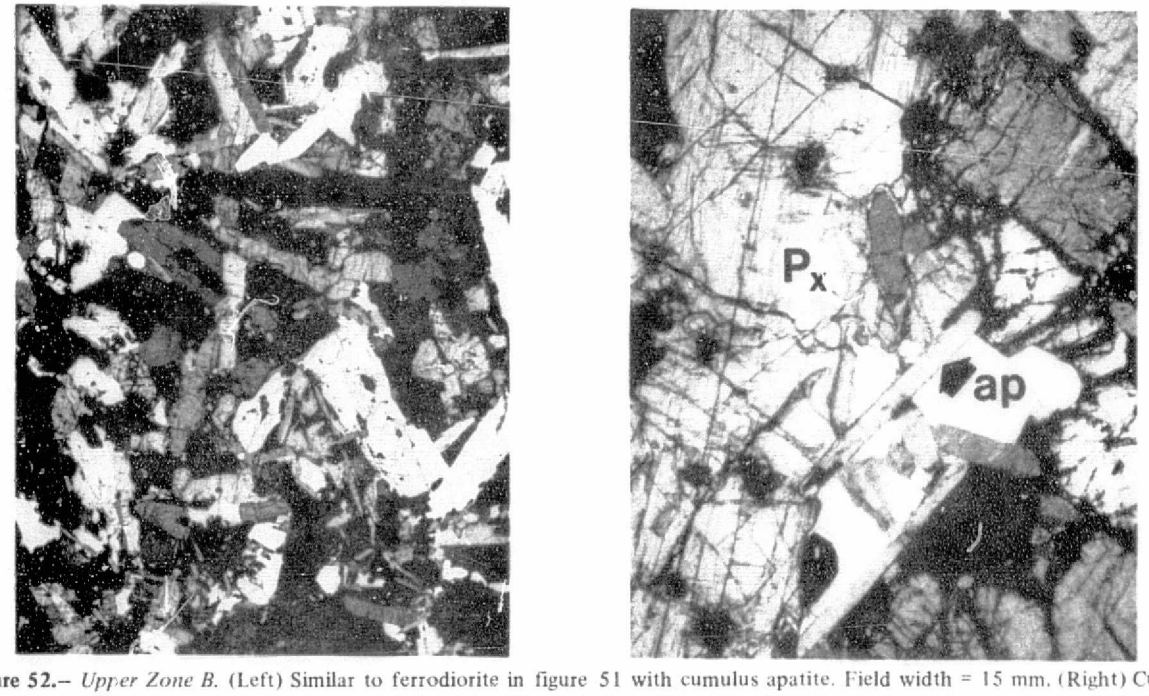

Figure 52.– *Upper Zone B.* (Left) Similar to ferrodiorite in figure 51 with cumulus apatite. Field width = 15 mm. (Right) Cumulus apatite (ap) showing a cross-cutting relationship with plagioclase. Magnetite along fractures of olivine in upper right. Field width = 0.9 mm. (Cross polarized light.)

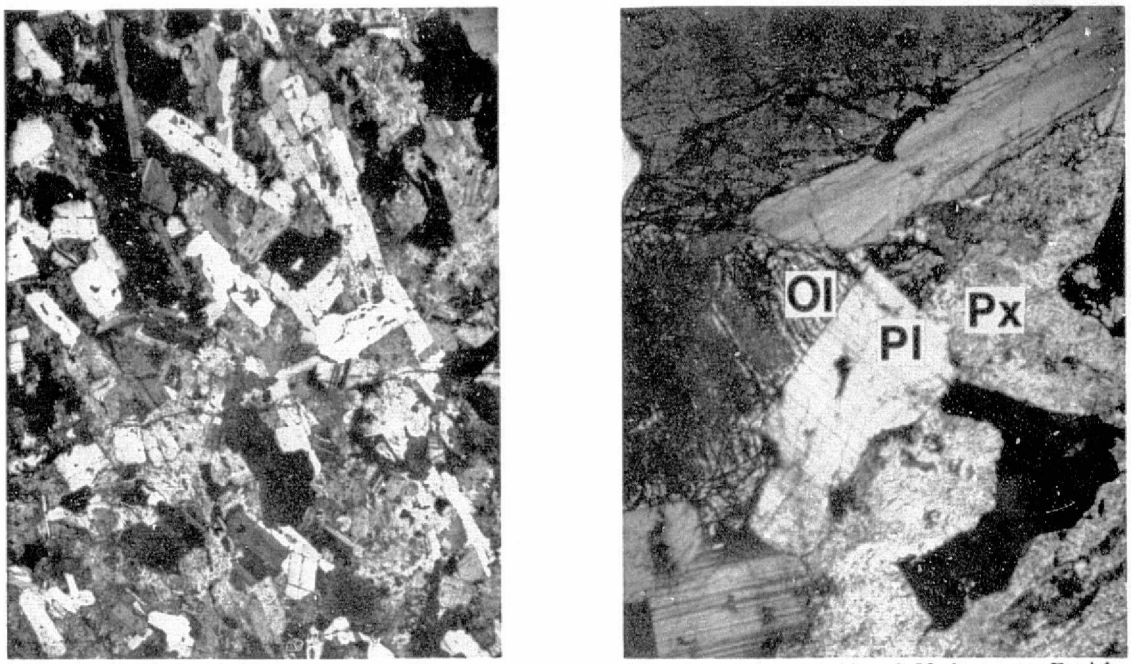

Figure 53.– *Upper Zone C.* (Left) An additional ferrogabbro similar to those in figures 51 and 52, but more Fe-rich. Field width = 15 mm. (Right) Both olivine (fayalite) and clinopyroxene (hedenbergite) are near their respective Fe end-member compositions. Olivine in thin section shows considerable amount of fine included magnetite. Field width = 0.9 mm. (Cross polarized light.)

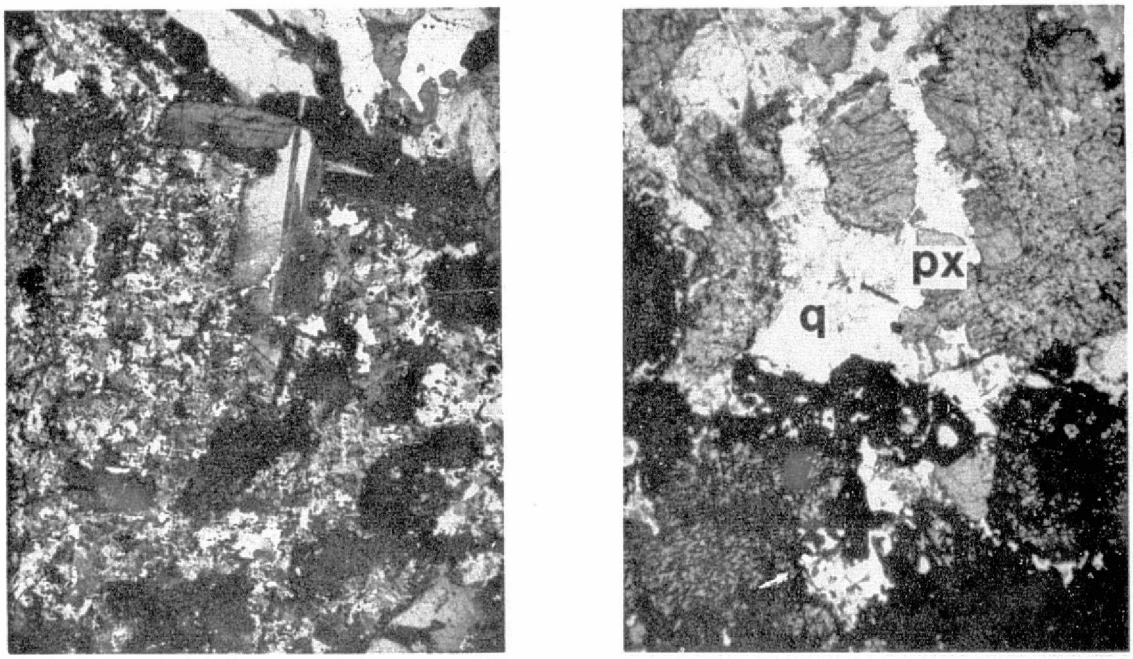

Figure 54.– *Sandwich Horizon.* (Left) Final rock formed from residual liquids (a ferrogabbro). Field width = 15 mm. (Right) Section contains large amounts of interstitial quartz and iron oxides. Field width = 0.9 mm. (Cross polarized light.)

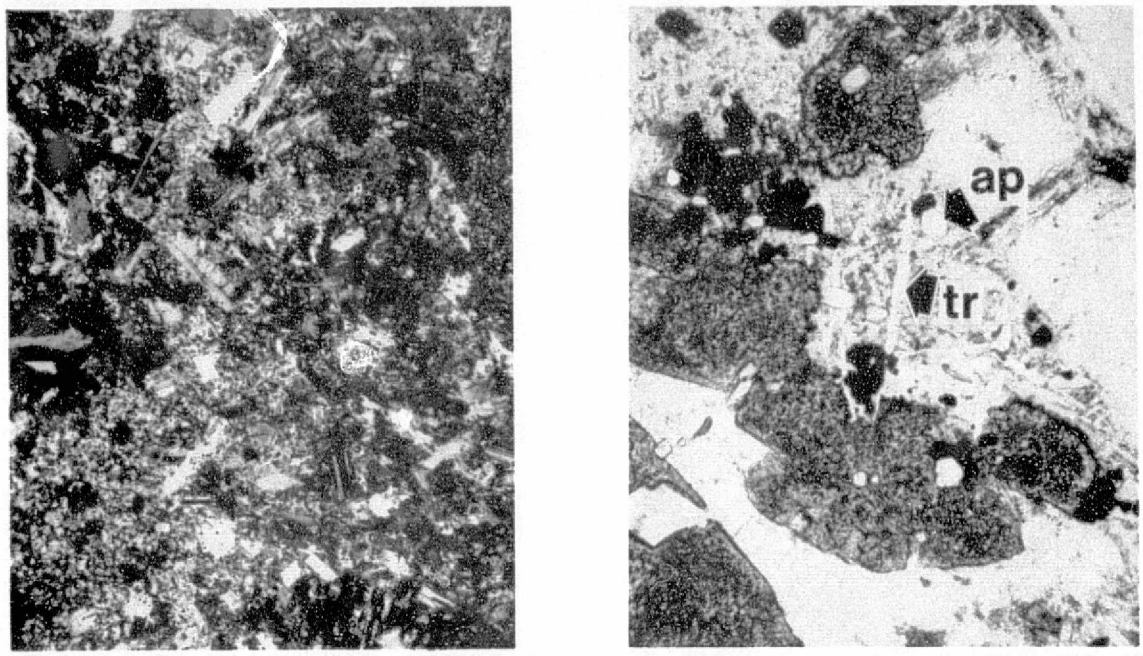

Figure 55.– *Upper Border Group* γ. (Left) Rock in thin section shows substantial hydrothermal alteration. Field width = 15 mm. (Right) Note crystals of tridymite (tr) and apatite (ap). Field width = 0.35 mm. (Cross polarized light.)

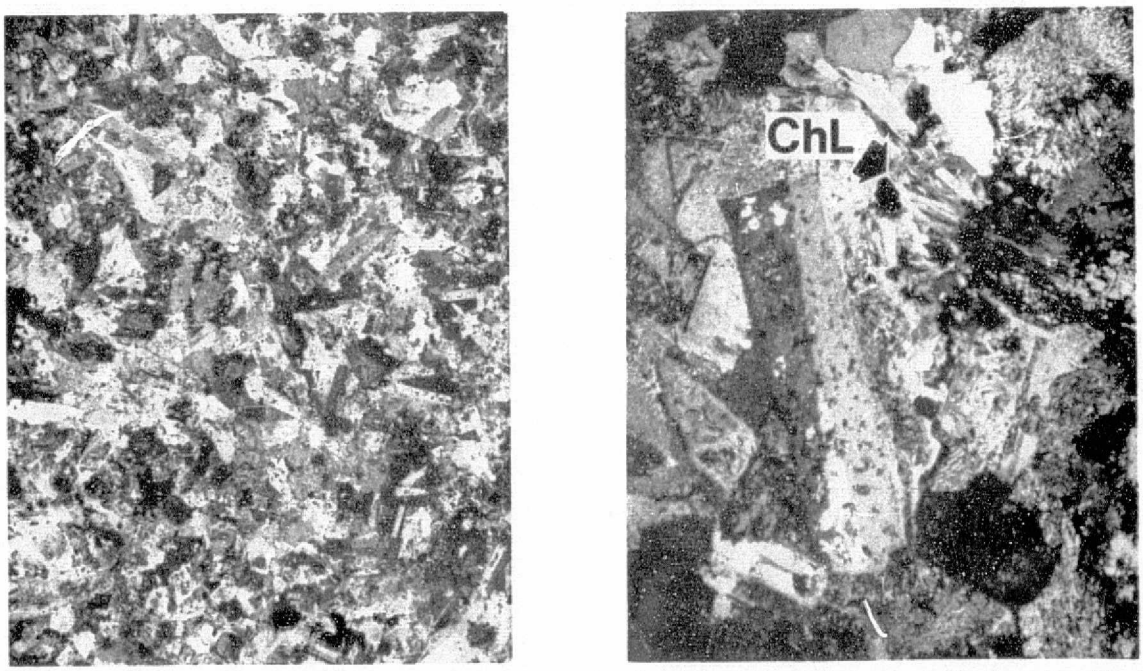

Figure 56.– *Upper Border Group.* (Left) Another altered gabbro that shows extensive development of chlorite and zeolites. Field width = 14 mm. (Right) Note fibrous chlorite (arrow) and myrmekite (upper right). Field width = 0.35 mm. (Cross polarized light.)

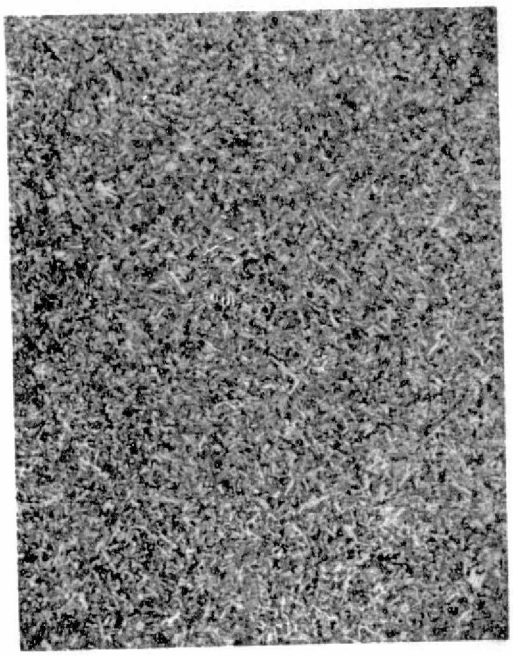

Figure 57.– *Chilled Margin.* Fine-grained intergranular basalt. Field width = 0.9 mm. (Cross polarized light.)

Figure 58.– *Gabbro Picrite.* Cumulate gabbro with poikilitic pyroxene. Field width = 15 mm. (Cross polarized light.)

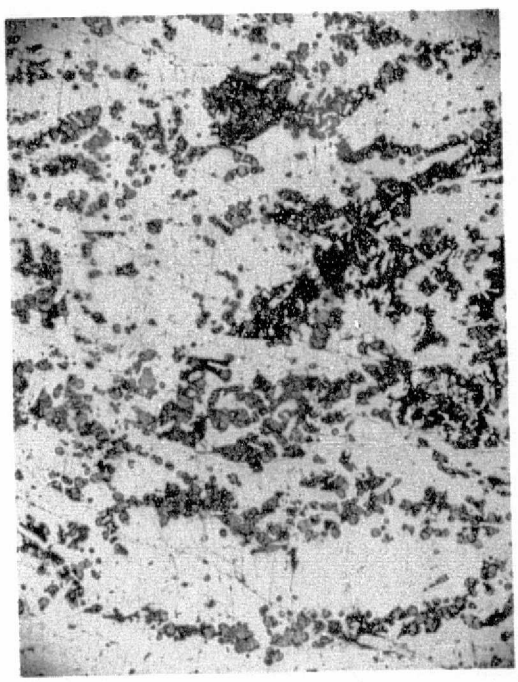

Figure 59.– *Perpendicular Feldspar Rock.* (Left) Strong preferred orientation of plagioclase with interstitial granular olivine and magnetite. Note poikilitic orthopyroxene in right center. Field width = 15 mm. (Right) Same. (Plane polarized light.)

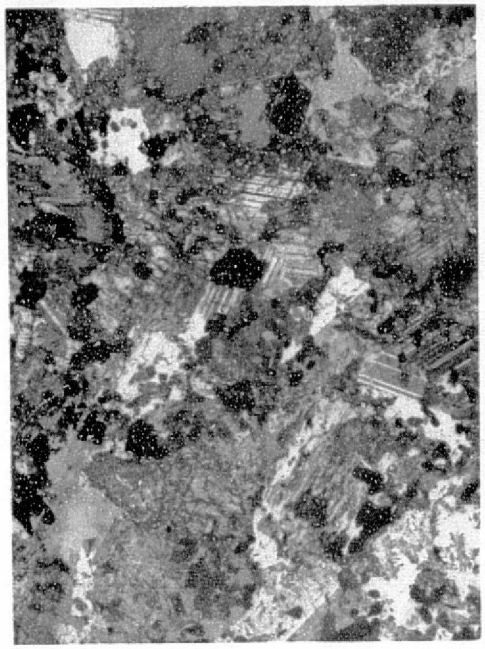

Figure 60.– *Coarse Cpt Material.* Large crystals of plagioclase and clinopyroxene with the latter partly converted to chlorite. Field width = 14 mm. (Cross polarized light.)

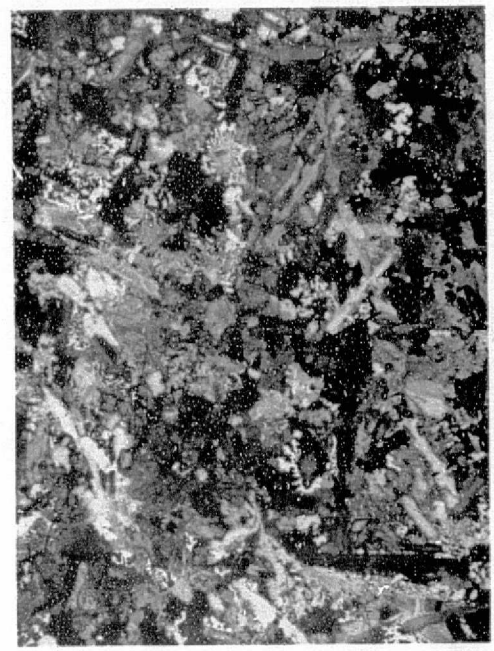

Figure 61.– *Melanogranophyre.* Residual granophyre that contains abundant myrmekitic intergrowths of quartz and orthoclase. Field width = 15 mm. (Cross polarized light.)

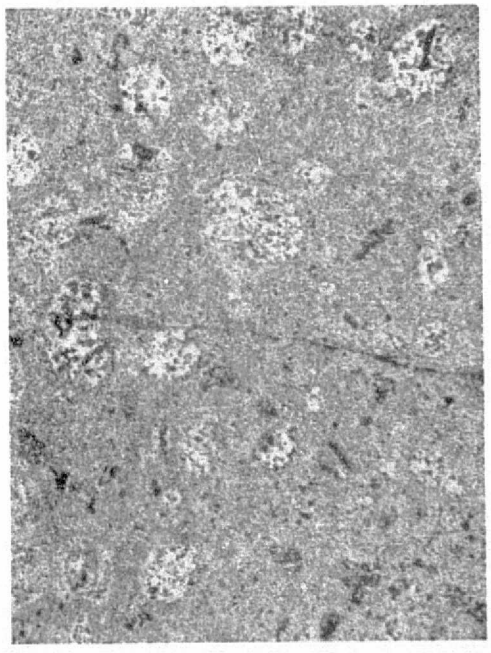

Figure 62.– *Altered Basalt.* Rounded structures are altered aggregates of pyroxene. Rock has a granular hornfels texture. Field width = 15 mm. (Cross polarized light.)

Figure 63.– *Basistoppen Sill.* Cumulus plagioclase with altered interstitial pyroxenes. Field width = 15 mm. (Cross polarized light.)

associated with magnetite and apatite is an abundant accessory mineral. (See fig. 62, p. 54.)

X. (Oregon no. 22) *Basistoppen Sheet*

Rock – A spotted gabbro containing plagioclase, orthopyroxene, and magnetite. The Basistoppen sheet is a large differentiated basic sill in the southern portion of the intrusion. Mafic minerals in the sill, which are often altered, gives the rock its characteristic mottled or spotted appearance. (Collected from Skillenunatak along Skaergaard Bay.)

Thin Section – The thin section contains orthopyroxene and clinopyroxene that has partially altered to chlorite. Other minerals include plagioclase and graphic magnetite. Although this sill is believed to be later than the Skaergaard intrusion it tends to be more altered. The alteration of the mafic minerals in this rock gives it a characteristic spotted appearance. (See fig. 63, p. 54.)

2.7 STILLWATER LAYERED INTRUSION COMPLEX

The Stillwater complex is located in southern Montana in portions of Stillwater, Grass, and Park counties, and lies almost completely within national forest land. Radiometric dating in the basal portions of the intrusive indicate an age of at least 3200 m.y.; it is intrusive into older sediments which it has metamorphosed to hornfels and is in turn intruded by younger Precambrian granite. The upper surface of the complex is an erosional unconformity largely covered by Cambrian and younger sediments. Though complexly faulted, the layered rocks generally dip steeply to the north or northeast (Wager and Brown, 1967, Jackson, 1967).

Crystal deposition on the floor of the magma chamber was the prime factor responsible for the layered structure, textures, and cryptic layering. Hess (1960) and Jackson (1961) believe that the layered features originated as semi-horizontal structures that were tilted to the north and in some cases overturned by later tectonic events.

The Stillwater complex can be divided into two "zones": the lower, or ultramafic, zone which is characterized by the presence of cumulus olivine, orthopyroxene, and chromite and by the absence of cumulus plagioclase; and the upper, or banded and upper, zone which is characterized by the first appearance and continued presence of cumulus plagioclase. Typical textures are shown in figures 64–73.

REFERENCES

Hess, H. H. (1960). Stillwater igneous complex, Montana, Geol. Soc. Am. Mem., no. 80.

Jackson, E. D. (1961). Primary textures and mineral association in the ultramafic zone of the Stillwater complex, Montana. U.S.G.S. Prof., Paper 358, pp. 1–106.

Jackson, E. D. (1967). Ultramafic cumulates in the Stillwater, Great Dyke and Bushveld intrusions. In: Ultramafic and Related Rocks, P. J. Wyllie, ed. New York, John Wiley and Sons, pp. 20–38.

Jackson, E. D. (1971). The origin of ultramafic rocks by cumulus processes. Fortschs. Mineral., vol. 48, pp. 128–174.

Wager, L. R. and G. M. Brown (1967). Layered Igneous Rocks, Oliver and Boyd, London.

Wager, L. R., G. M. Brown, and W. J. Wadsworth (1960). Types of igneous cumulates, J. Petrol., vol. 1, pp. 73–85.

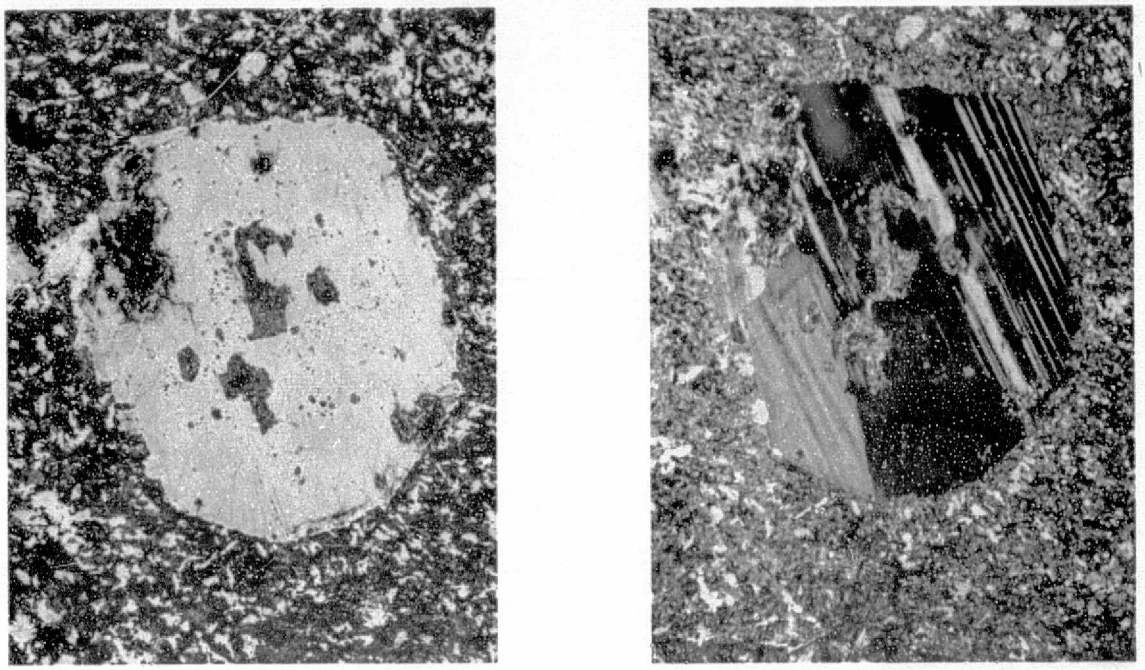

Figure 64.– (Left) Cordierite-orthopyroxene-biotite hornfels (diamictite). Plagioclase pebble set in matrix of cordierite-orthopyroxene-biotite. Collected from Moat Nickel mine, Mountain View area. (Photomicrograph, plane light.) (Right) Same, crossed nicols.

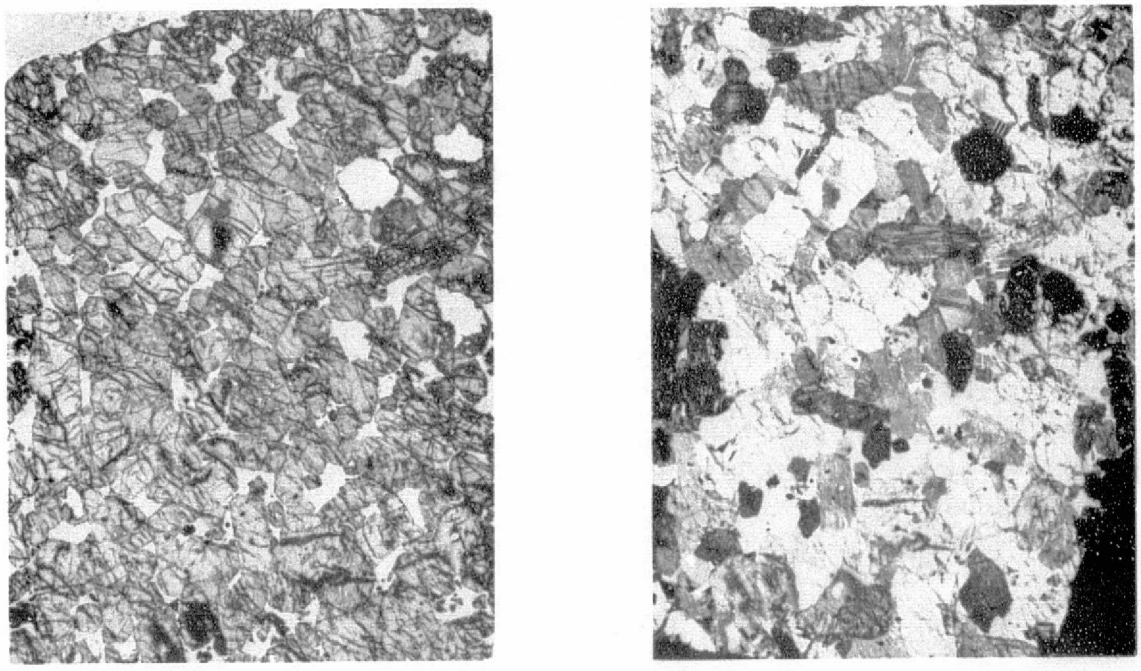

Figure 65.– (Left) Poikilitic bronzite. Automorphic bronzite with interstitial poikilitic plagioclase. Collected at lower chromite mine, Mountain View area. (Photomicrograph, plane light.) (Right) Same, crossed nicols. Bronzite contains exsolution lamellae of clinopyroxene oriented || (100). Closely-spaced exsolution lamellae of this type that extend to grain margins are typical of cumulus bronzite.

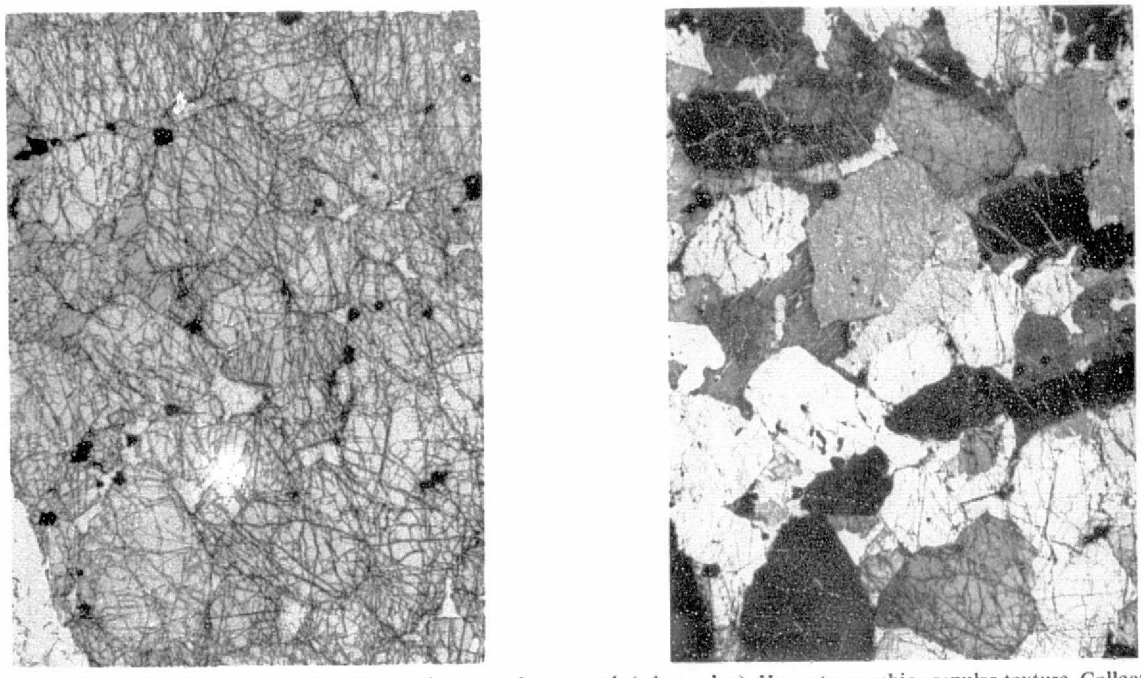

Figure 66.– (Left) Poikilitic harzburgite affected by secondary growth (adcumulus). Hypautomorphic granular texture. Collected at lower chromite mine, Mountain View area. (Photomicrograph, plane light.) (Right) Same, crossed nicols. Note deformation lamellae in olivine.

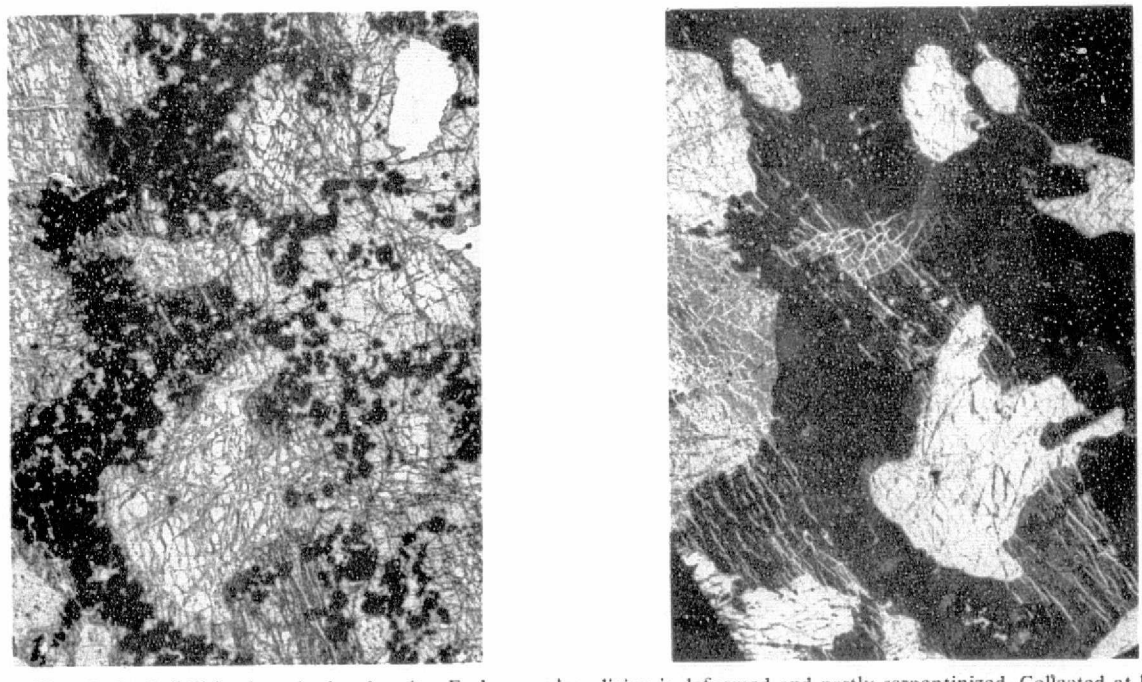

Figure 67.– (Left) Poikilitic chromite harzburgite. Early cumulus olivine is deformed and partly serpentinized. Collected at lower chromite mine, peridotite member, Mountain View area. (Photomicrograph, plane light.) (Right) Same, crossed nicols. Note bronzite oikocryst at extinction which contains both chromite and olivine.

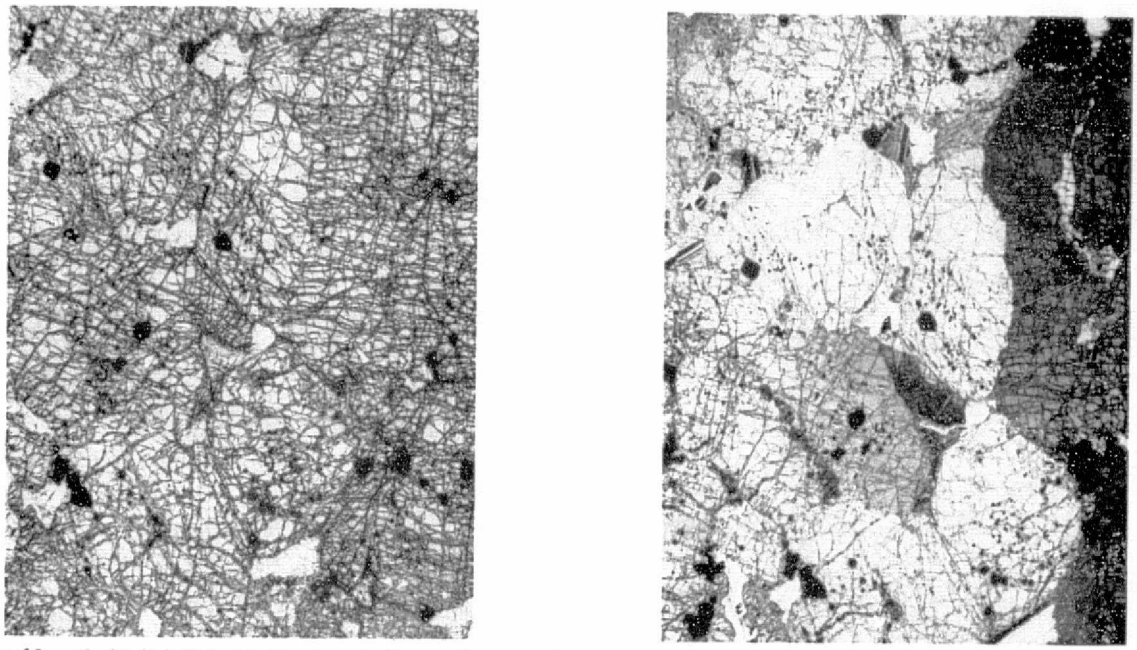

Figure 68.– (Left) Poikilitic harzburgite, similar to figure 3. Note twinning in post-cumulus plagioclase. (Photomicrograph, plane light.) (Right) Same, crossed nicols.

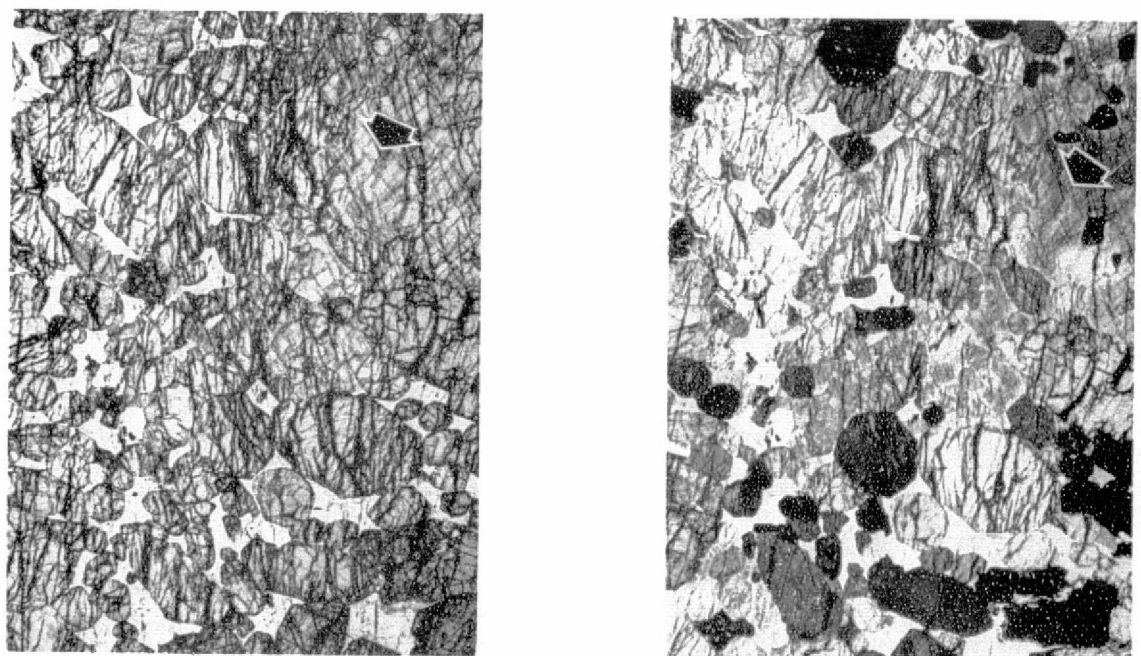

Figure 69.– (Left) Poikilitic bronzitite. Cumulus bronzite with post-cumulus poikilitic plagioclase and augite (arrow). Collected at upper mine area (bronzitite member of ultramafic zone), Mountain View area. (Photomicrograph, plane light.) (Right) Same, crossed nicols.

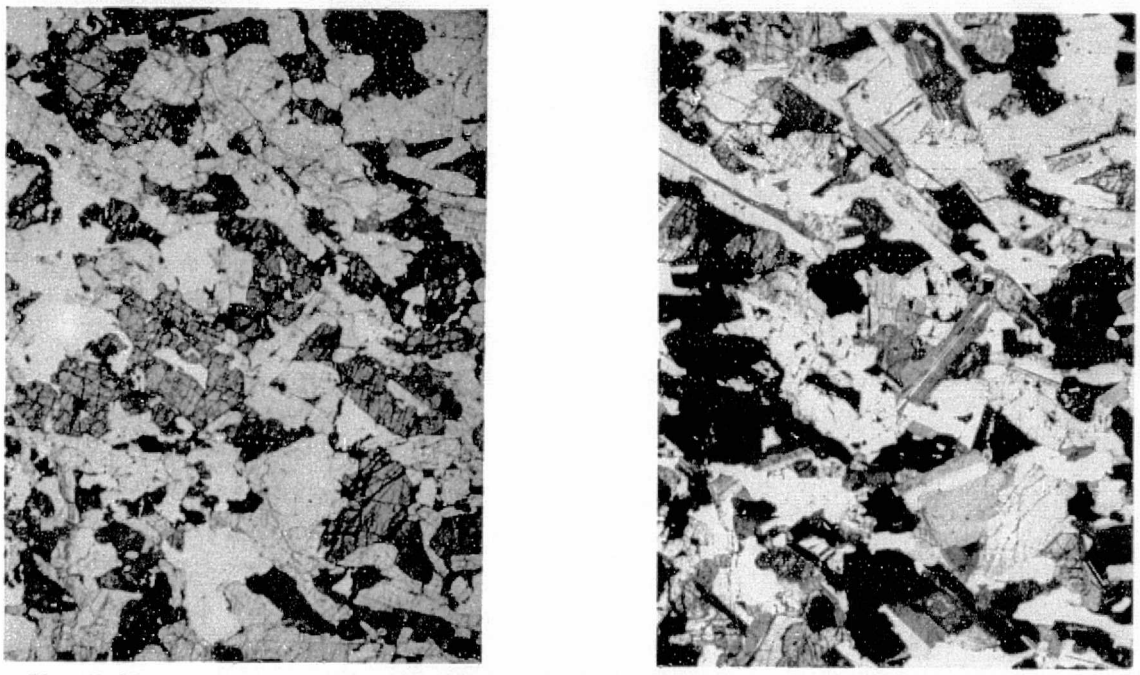

Figure 70.– (Left) Two-pyroxene gabbro collected from Banded and Upper Zone. Simultaneous crystallization of orthoclinopyroxenes and plagioclase. (Photomicrograph, plane light.) (Right) Same, crossed nicols.

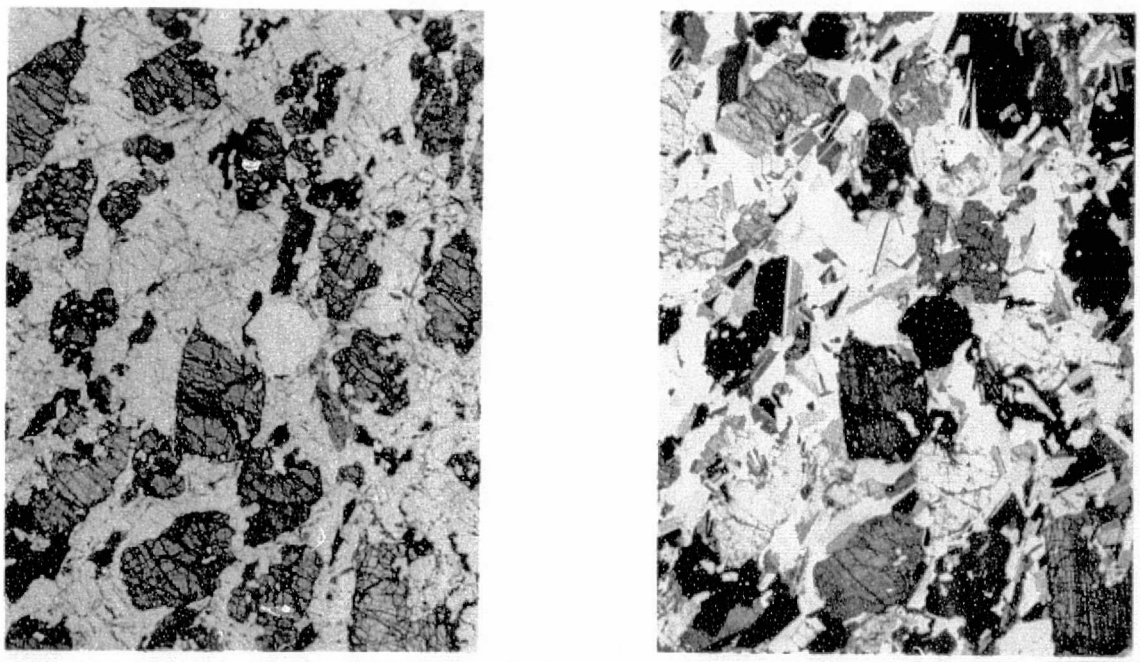

Figure 71.– (Left) Norite (gabbro) collected from Banded and Upper Zone. Crystallization of plagioclase slightly preceded pyroxenes. Note small included plagioclase grains in orthopyroxene. (Photomicrograph, plane light.) (Right) Same, crossed nicols.

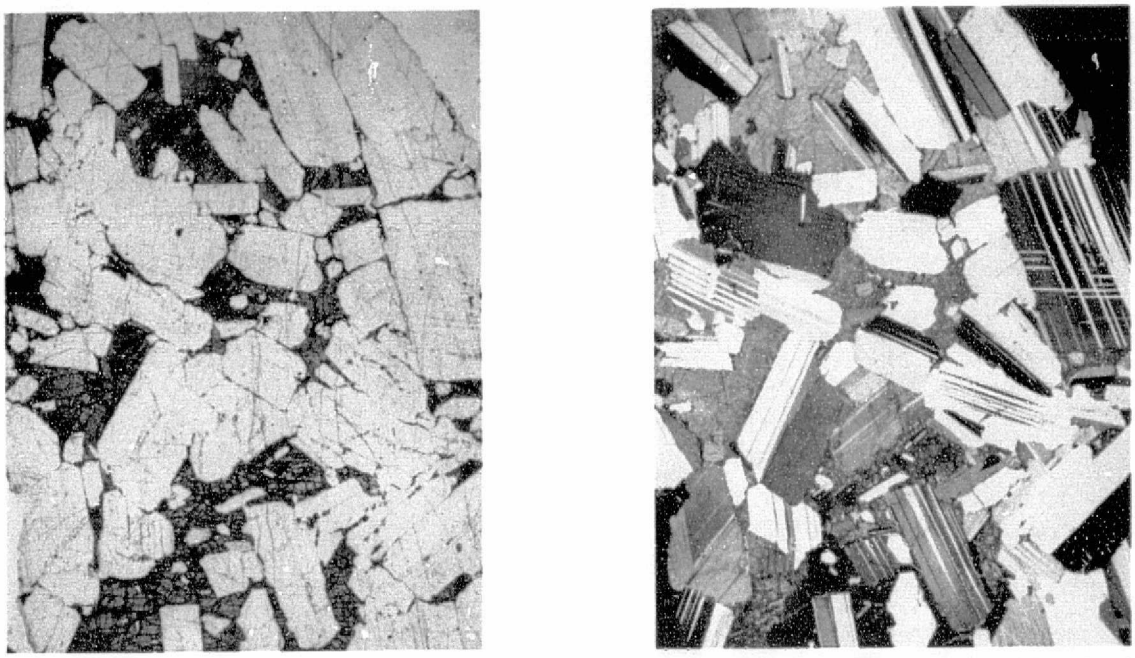

Figure 72.– (Left) Poikilitic norite. Cumulus plagioclase and post-cumulus oikocryst of hypersthene. Collected from Banded and Upper Zone, Mountain View area. (Photomicrograph, plane light.) (Right) Same, crossed nicols.

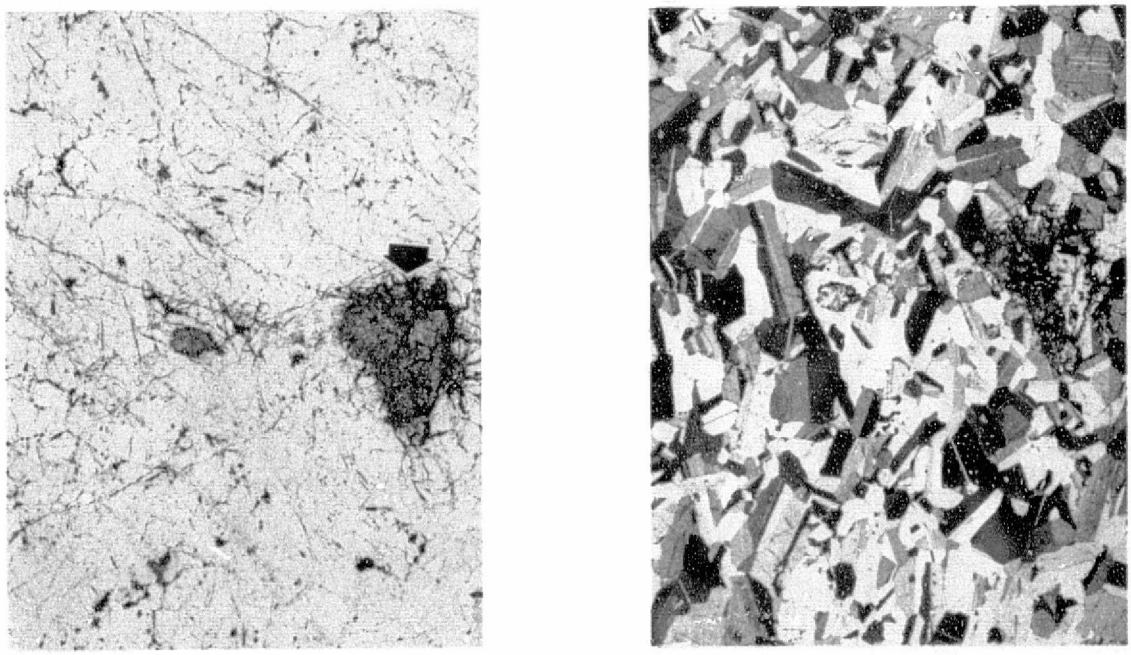

Figure 73.– (Left) Anorthosite. Arrow points to altered pyroxene. Collected from Picket Pin Mt. (Photomicrograph, plane light.) (Right) Same, crossed nicols.

3. EXTRATERRESTRIAL BASALTS AND LAYERED ROCKS (CUMULATES)

A final philosophy of earth [and planetary] history must be largely founded upon the unshakable facts known about igneous rocks.

R. A. Daly

3.1 LUNAR BASALTS AND LAYERED ROCKS

Apollo moon missions provided scientists with a wealth of interesting basalts and cumulate rocks that eventually changed our concept of lunar geology. Studies show that the Moon does not have great extents of granitic rocks, nor are there large areas of ash flows. The surface and near-surface rocks consist almost exclusively of basalts and rocks of the anorthositic suite (anorthosites, troctolites, norites); many samples of the latter group show cumulate textures. The Moon contains an aluminous-rich, refractory crust (lunar highlands) and a Fe-Mg-rich mantle that is the source region for many of the mare (basin filling) basalts. The bulk Moon composition is neither meteoritic nor Earth-like and is best shown by ratios of volatile and refractory elements. The K/U ratios for lunar samples range between 1300 and 2300, between 7000 and 20,000 for terrestrial rocks, and between 30,000 and 80,000 for meteorite chondrites. Geochemical models of the Moon imply that rare earth elements are enriched in the bulk Moon by a factor of between 5 to 20 times relative to chondrites. In addition, the Moon is depleted in volatile siderophile elements.

Basalts collected from the moon are difficult to classify because of the lack of field data and because of a wide variation in texture, mineralogy and chemistry; nevertheless, attempts have been made to classify basalts from each mission by various combinations of these criteria (Warner 1975). Lunar mare basalts are similar to their terrestrial counterparts, although the lunar basalts are more enriched in LIL elements (acronym for large-ion lithophile; Ba, Th, Zr, U, etc.) and more depleted in volatile elements. Other chemical differences include higher FeO (17-23 wt percent), lower alkalis ($Na_2O + K_2O < 1.0$ wt percent), and lower plagioclase contents (modes range from 15 to 36 percent). Warner (1975) uses the elements Ti, Al, and K to define mare basalt groupings: low vs. high TiO_2 (2-4 vs. 10-13 wt percent); low vs. high Al_2O_3 (7-11 vs. 11-14 wt percent); and low vs. high alkalis ($K_2O < 0.1$ vs. 0.3-0.4 wt percent). The mare basalts can then be divided into four groups: (1) half the Apollo 11 and all the Apollo 17 basalts contain high TiO_2 and low alkalis and Al_2O_3; (2) the half of Apollo 11 basalts contain high TiO_2 and alkalis and low Al_2O_3; (3) all but one Apollo 12 and all Apollo 15 basalts contain low TiO_2, alkalis, and Al_2O_3; and (4) the remaining Apollo 12, two Apollo 14 and all the Luna 20 basalts contain low TiO_2 and alkalis, and high Al_2O_3. Most of the Apollo 17 mare basalts are similar to the high TiO_2 Apollo 11 basalts. Taylor (1974) divides the mare basalts into: (1) olivine normative; (2) quartz normative; (3) high K_2O, TiO_2; (4) low K_2O, TiO_2; and (5) aluminous mare basalts.

Major minerals in mare basalts are clinopyroxene, calcic plagioclase, olivine, and ilmenite. Minor minerals include silica minerals, Cr-spinels, ulvöspinel, Ni-Fe metal, troilite, and phosphates. Pyroxferroite, ($Fe_{0.8}$ $Ca_{0.6}$ SiO_3), armalcolite ($Fe_{0.5}$ $Mg_{0.5}$ Ti_2O_5), and tranquillityite ($Fe_8(Zr+Y)_2Ti_3SI_3O_{24}$) are new minerals found in some of the mare basalts. The presence of metallic Ni-Fe, FeS, and the absence of ferric Fe in the mare basalts imply formation in a highly reduced environment; estimate of oxygen fugacity in 1150° C is $\sim 10^{-13}$. Compared with terrestrial basalts, this value is at least 3-4 orders of magnitude less, although it is similar to fO_2 of formation for meteoritic basalts.

Many of the basalts display textures that suggest rapid cooling and were probably extruded onto the surface as a liquid. Experimental interpretation of mare basalt major element chemistry suggests that many of the basalts found at each landing site formed from liquids at shallow depths through fractionation of olivine or spinel (e.g., Compton et al. 1970). This process is similar to the origin of some terrestrial oceanic ferrobasalts by Clague and Bunch (1976). Even though some fractionation has occurred, changes in the bulk compositions are small compared with the highly fractionated terrestrial basalts. In terrestrial lavas, phenocrysts in a fine-grained matrix indicate that crystallization began well before eruption. Many mare basalts probably formed by a single-stage monotonic cooling at rates equally 10° C/hr. Some mare basalts possibly crystallized intact with little or no fractionation of the original magma. Many of the mare basalt textures are shown in figures 74–78 and 81–83.

Evidence of cumulate rocks from the lunar highlands (anorthositic suite) has been given by several Apollo investigators. These rocks probably originated at great depth through crystal settling during the primary lunar differentiation and crustal formation (e.g., Dymek et al. 1975). See figures 86, 87, 91–93 for lunar cumulate examples.

Sattingley's Law: It works better if you plug it in.

3.2 METEORITES, METEORITIC BASALTS AND LAYERED ROCKS

Meteorites provide tangible samples of solar system material that has undergone compositional changes through differentiation and chemical fractionation. These changes probably occurred before and during emplacement of matter around the Sun, in the course of condensation of primitive solids from the early solar nebula gas cloud, and during changing magmatic and metamorphic processes in a parent body. Collisional shock events have also aided in altering the compositions of small planetary bodies.

3.2.1 Classification

Generally speaking, meteorites are classified on the basis of bulk chemistry and mineralogy (Table 3). Further division of Table 3 classes into subtypes is commonly based on textural differences and minor and trace element differences.

Meteorites are classically grouped into stones, irons, and stony-irons. Among the stones, a major distinction is made between the chondrites, which contain chondrules (rounded supercooled mixtures of silicates and glass) to a greater or lesser extent, and achondrites, which do not contain them. The most abundant of the chondrites, called ordinary chondrites, fall into three subtypes based on the amount of metallic Fe-Ni alloy present and the Fa (fayalite, Fe_2SiO_4) and Fs (ferrosilite, $FeSiO_3$) contents of the constituent olivine and pyroxene, respectively: the H (high metal) group, the L (low metal) group, and the LL (very low) metal group. The main mineral constituents of all these are olivine, low Ca pyroxene, metal, high albite, troilite, and minor chromite. An additional subdivision into petrographic subgroups is based on texture (degree of metamorphism) (Van Schmus and Wood 1967). Ordinary chondrites with delicate chondrules, nonequilibrium assemblage, glass, etc., are designated 3 (least metamorphosed); those where the chondrules are recrystallized, with an equilibrium assemblage and no glass are designated 6 (H6, L6, or LL6) and are most metamorphosed.

The nonordinary chondrites consist mainly of enstatite chondrites and carbonaceous chondrites. The former are composed of an extremely reduced assemblage consisting mainly of clino-enstatite (Fs = O; ferrosilite, $FeSiO_3$), Fe-Ni alloy, and troilite with a host of minor and trace phases that reflect extremely low oxidation conditions (e.g., sinoite (Si_2ON_2), oldhamite (CaS), osbornite (TiN), etc.) (Keil 1969).

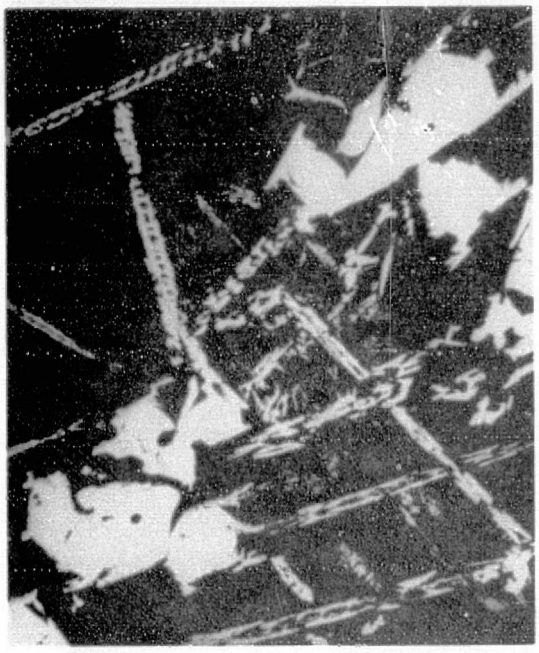

Figure 74.– Olivine vitrophyre (microlitic). Apollo 12 No. 12008. Skeletal grains of olivine in a microcrystalline glassy groundmass. Texture implies rapid cooling at or near the surface. Plane light, field width = 2.1 mm.

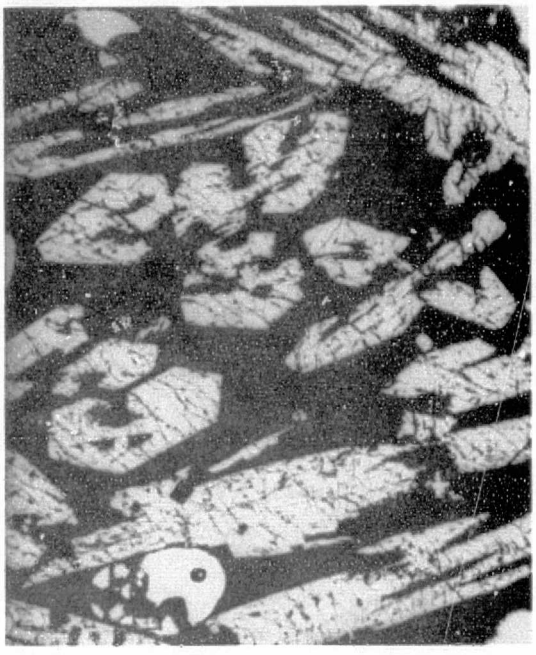

Figure 75.– Vitrophyric basalt, Apollo 15 No. 15485. Contains zoned Mg-pigeonite (cores) zoned to hedenbergite in the grain margins. The glass matrix contains normative plagioclase more sodic than most mare basalt samples. Plane light, field width = 5 mm.

Figure 76.– Porphyritic picritic basalt, Apollo 12 No. 12002. Feathery to acicular pyroxene and plagioclase matrix surrounding rounded phenocrysts of olivine. Crossed nicols, field width = 1.07 mm.

Figure 77.– Variolitic basalt, Apollo 12 No. 12052. Phenocrysts of pigeonite cores rimmed by ferroaugite set in a matrix of radiating (plumose) calcic plagioclase. Crossed nicols, field width = 2.08 mm.

Figure 78.– Ophitic basalt, Apollo 12 No. 12047. Plagioclase (white) partly enclosed by zoned Ca-rich clinopyroxene. Long dark grains are ilmenite. Plane light, field width = 2.08 mm.

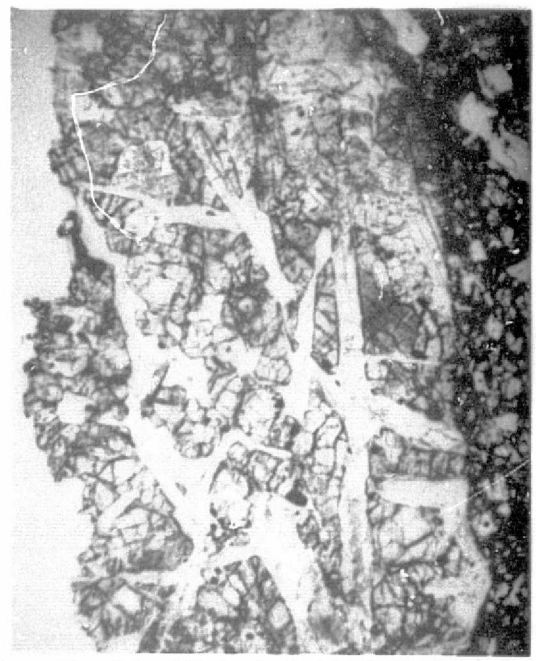

Figure 79.– Subophitic basalt clast in the Jodzie brecciated meteorite (howardite). Calcic plagioclase encloses ferropigeonite. Plane light, field width = 2.08 mm.

Figure 80.– Subophitic basalt clast in the Jodzie brecciated meteorite (howardite). Crossed nicols, field width = 3.0 mm.

Figure 81.– Variolitic basalt, Apollo 17 No. 70215. Hollow microphenocrysts of calcic plagioclase and acicular ilmenite set in a matrix of fine-grained pyroxene and plagioclase (rapid cooling). Plane light, field width = 3.6 mm.

Figure 82.– Granular gabbro, Apollo 12 No. 12035. Olivine and pyroxene enclosed poikilitically by plagioclase. Possible cumulate rock. Crossed nicols, field width = 2.08 mm.

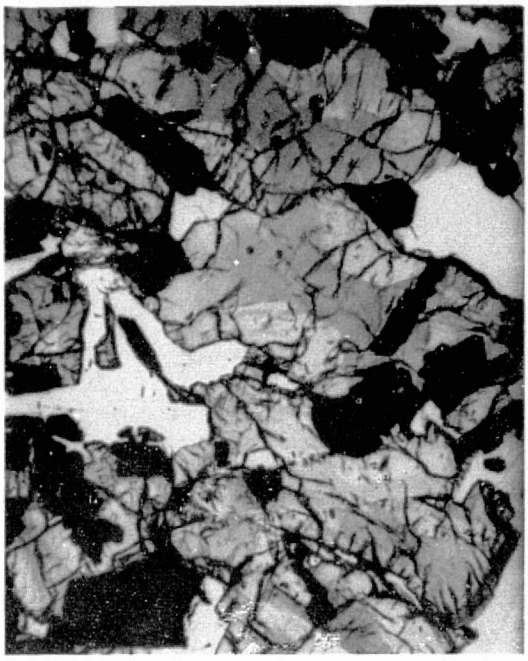

Figure 83.– Granular basalt, Apollo 17, No. 70185. Coarse-grained ferrobasalt with pyroxene cores of augite, zoned to ferroaugite at the margins. Ilmenite is enclosed by pyroxene and plagioclase, pyroxene is enclosed by plagioclase; mineral sequence is ilmenite → pyroxene → plagioclase. Plane light, field width = 3.2 mm.

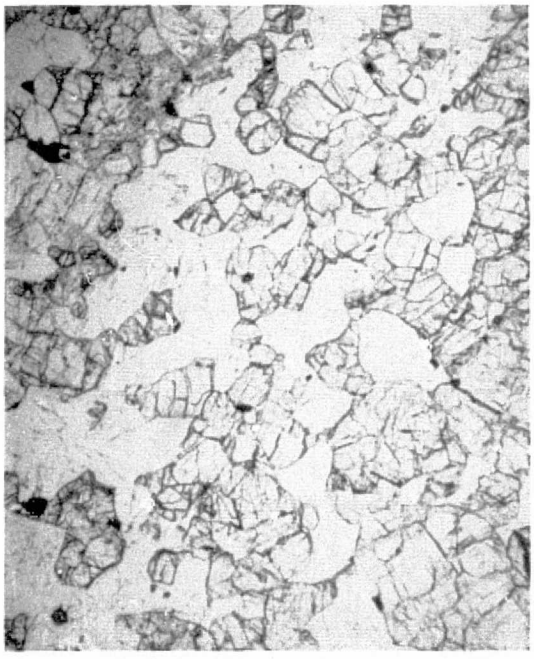

Figure 84.– Granular gabbro clast in the Jodzie brecciated meteorite (howardite). Pigeonite and calcic plagioclase have preferred orientation indicating a cumulate rock. Texture similar to Stillwater cumulate norite (fig. 43). Plane light, field width = 5.0 mm.

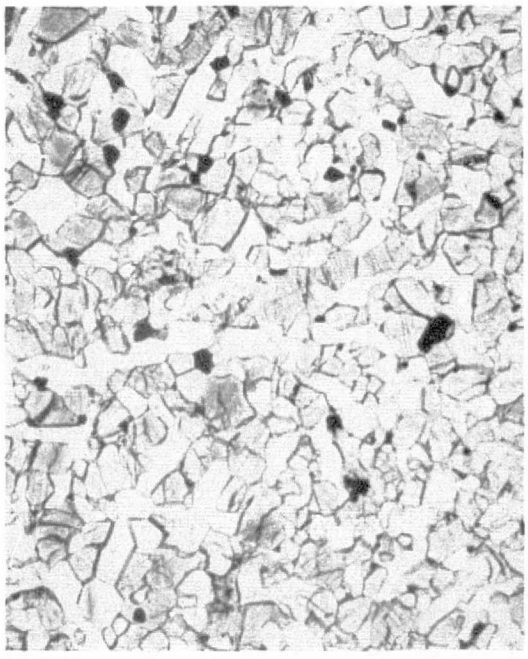

Figure 85.– Granular basalt clast, Washougal brecciated meteorite (howardite). Equalgranular to mosaic texture of pyroxene, ilmenite, and plagioclase indicating at least partial recrystallization. Plane light, field width = 1.05 mm.

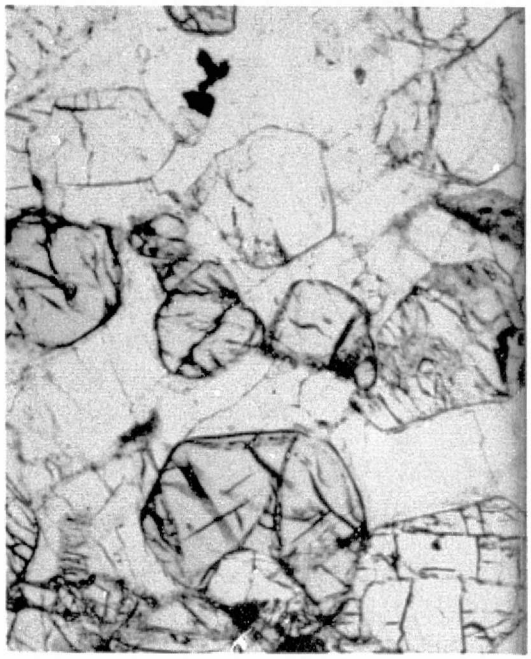

Figure 86.– Pink spinel troctolite cumulate rock Apollo 16 No. 67435. Cumulate spinel and olivine poikilitically enclosed by calcic plagioclase. Classic cumulate texture. Plane light, field width = 4 mm.

Figure 87.– Same as figure 86, crossed nicols. Spinels appear black; note optical continuity of plagioclase oikocrysts.

Figure 88.– Nakhla meteorite (cumulate). Cumulus pyroxene and olivine crystals with fibrous interstitial, post-cumulus plagioclase. Plane light, field width = 3.0 mm.

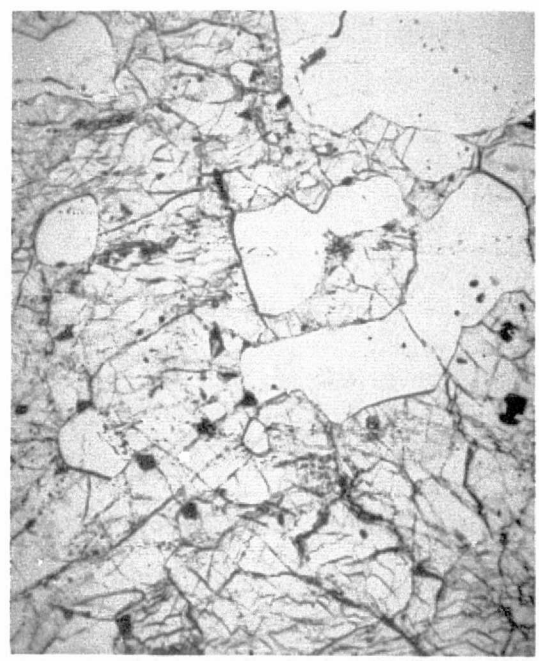

Figure 89.– Moore Co. basaltic achondrite. Well-known cumulate texture described by Hess and Henderson (1949). Pyroxene has preferred orientation. Plane light, field width = 4.0 mm.

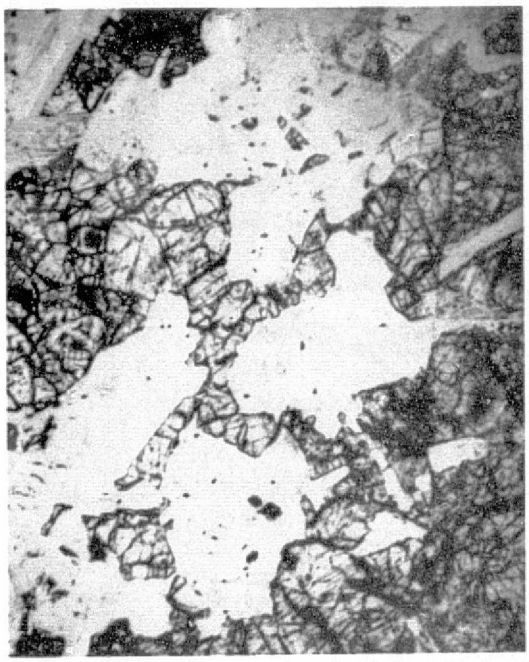

Figure 90.– Gabbro (cumulate) clast, Jodzie brecciated meteorite (howardite). Plane light, field width = 4.0 mm.

Figure 91.– Anorthositic gabbro, highly shocked, Apollo 16 No. 67915. Similar texture to that shown in figure 90. Plane light, field width = 4.0 mm.

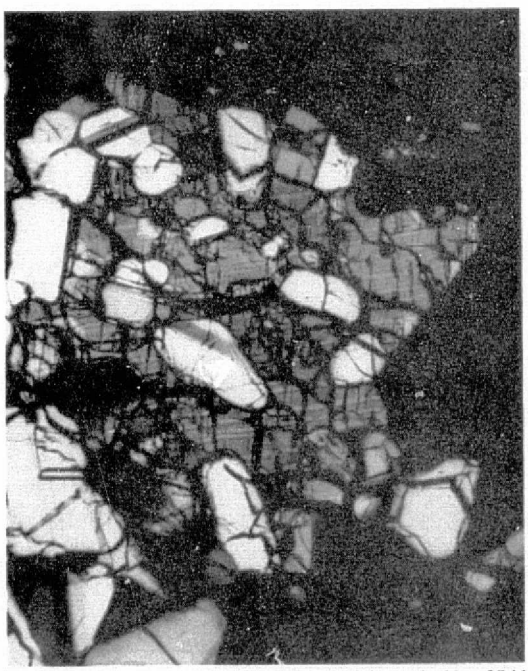

Figure 92.– Poikilitic clast in Apollo 16 breccia No. 67415. Pyroxene poikilitically encloses plagioclase grains. Crossed nicols, field width = 2.08 mm.

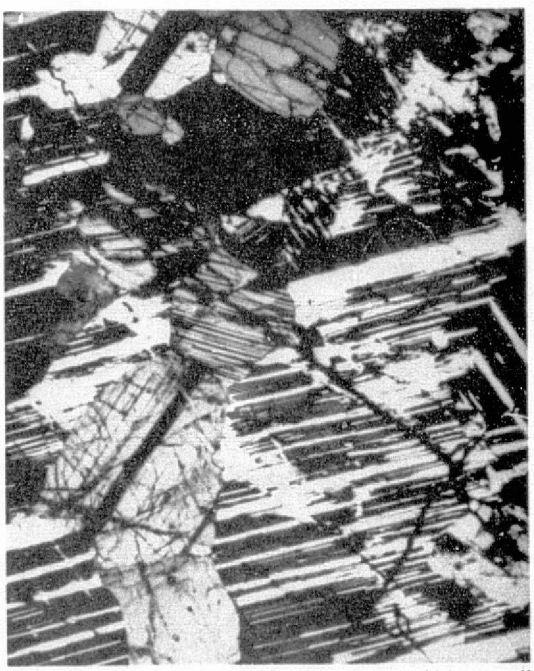

Figure 93.– Anorthosite, Apollo 15 No. 15415, so-called genesis rock. Partly recrystallized and well-twinned plagioclase with minor orthopyroxene. Crossed nicols, field width = 5.0 mm.

TABLE 3.– SIMPLIFIED CLASSIFICATION OF MAJOR METEORITE TYPES AND SUBTYPES

	Type	Major minerals
A.	Stone meteorites	
	Ordinary chondrites (H, L, LL)	Olivine, orthopyroxene, clinopyroxenes, metal, troilite, albitic plagioclase, chromite
	Enstatite chondrites	Enstatite (ortho- and clino-), metal, troilite, ± plagioclase
	Carbonaceous chondrites	
	Cl C = 3.5; H_2O = 20.1	Ferric chamosite, magnetite
	C2 C = 2.5; H_2O = 13.4	Ferric chamosite, olivine, enstatite, troilite
	C3 C = 0.5; H_2O = 1.0	Olivine, enstatite, pentlandite, troilite
	Achondrites	
	Enstatite achondrites	
	Bronzite achondrites	
	Olivine achondrites	
	Olivine-pigeonite achondrites	
	Augite achondrites	
	Diopside achondrites	
	Orthopyroxene-pigeonite-plagioclase achondrites } Pigeonite-plagioclase achondrites }	Basaltic achondrites
B.	Iron meteorites	
	Hexahedrites	Metal (≤ 7% Ni), troilite
	Octahedrites (coarse, medium, fine)	Metal (6.5-18% Ni), troilite, graphite
	Ni-rich ataxites	Metal (12-25+% Ni), troilite, schreibersite
	Irons with silicate inclusions (IWSI)	Metal, schreibersite, troilite, orthopyroxene, clinopyroxene, plagioclase, ± olivine, ± graphite
C.	Stony-iron meteorites	
	Pallasites	Metal, olivine
	Mesosiderites	Metal, orthopyroxene, olivine, troilite

The carbonaceous chondrites are commonly divided into three subtypes – C1, C2, and C3. The three are distinguished primarily by their carbon and water contents. The C1 meteorites are considered the most primitive meteoritic objects known and are the least fractionated chemically. They consist mainly of a very fine-grained layer-lattice silicate, ferric chamosite, and minor magnetite. The C2 meteorites consist of a matrix (52 percent on the average) of ferric chamosite and inclusions (aggregate clusters and some chondrules) (48 percent on the average) of forsterite, enstatite, spinel, and minor Fe-Ni-Cr-Co alloy metal. The C3 meteorites have no chamosite but consist mainly of a matrix of fine-grained olivine (~Fa 50) containing inclusions of mainly forsterite, enstatite, and spinel along with a minor amount of high Co (0.1–7 percent) Fe-Ni-Co-Cr alloy.

Achondrites consist of eight main subtypes whose major mineralogies are adequately described by their names alone (table 3).

Iron meteorites can be grouped into a moderately large number of subtypes; the octahedrites

(coarse, medium, fine) have 6.5–18 percent Ni; the hexahedrites have ⩽7 percent Ni; and the Ni-rich ataxites have 12 to over 25 percent Ni. These irons commonly contain nodular to lamellar inclusions of graphite, troilite, schreibersite, and cohenite. Graphite and troilite inclusions contain within them, in many cases, minor assemblages of silicates (or phosphates), some of which are Cr-rich. These are referred to later as "silicates in ordinary irons" or SOI meteorites (Bunch and Olsen 1975); this serves to distinguish them from an unusual group of iron meteorites that contain major irregular masses of silicate, troilite, ± phosphate, ± chromite assemblages, sometimes comprising 25–35 volume percent of the meteorite; these are called irons-with-silicate-inclusions, or simply IWSI.

The stony-iron meteorites consist principally of two subtypes: (1) pallasites, which have olivine (Fs = 10-20) in a matrix of Fe-Ni alloy; and (2) mesosiderites, which are mainly half Fe-Ni alloy and about half of an assemblage consisting of orthopyroxene (Fs = 29-30), anorthite (An = 87-97), olivine (Fa = 9-10), and troilite.

3.2.2 Mineralogy

Over 80 minerals (table 4) have been confirmed in meteorites of which 24 are unique to meteorite assemblages. Many of these unique minerals define unusual, if not extreme, formation environments. For example, many sulfides (CaS, Cr_2S_4, MgS, $K_3CuFe_{12}S_{14}$) indicate low partial pressures of oxygen (high reducing conditions). Brezinaite (Cr_3S_4) has been found in only one meteorite, the iron Tucson. The apparent oxidation state of Tucson was sufficiently low to reduce virtually all Fe and Ni and some Si and Cr to the elemental form and to change V and most Cr from lithophile to chalcophile character. Other minerals indicate high shock pressure environments (diamonds, C, and majorite, $Mg_3(MgSi)Si_3O_{12}$). High temperature minerals (grossular, melilite, and spinel), found in carbonaceous chondrites, support the high-temperature condensation theory for meteorite origin. In addition, many common minerals in meteorites have unusual compositions or textures that aid the reconstruction of meteorite origin, thermal history, and chemical environment. An example of this application is that the petrography and composition of C2 meteoritic metal is different from other meteorite types. Metal occurs dominantly as submicron-sized beads, rarely larger than 5 μ, poikilitic within Mg-rich forsterite (and enstatite) crystals (Fuchs et al. 1973). The crystals are often euhedral or fragments of euhedral crystals. Metal in ordinary chondrites occurs interstitial to silicates, is generally ragged and irregular, and often conforms to the external shapes of silicate grains. In the C2 meteorites, the petrographic relations indicate that the metal beads preceded forsterite formation and may have acted as nuclei for euhedral forsterite crystals. During the direct condensation of a solar nebula gas at $P(H_2) = 10^{-3}$ atm, metal alloys with the Fe, Ni, Cr, and Co contents observed in the metal beads of these carbonaceous chondrites (5–7 percent Ni, 0.3–0.5 percent Co, around 0.6 percent Cr) condense directly from 1445°-1370 K.

3.2.3 Geological and Planetary Significance of Meteorites

Two types of meteorites are important to this discussion: (1) carbonaceous chondrites, which contain organic compounds, inclusions composed of refractory elements, and water; and (2) basaltic achondrites, which have textures and mineralogy closely akin to lunar and terrestrial basalts and imply magmatic crystallization. The refractory element inclusions in carbonaceous chondrites may be an important clue to the condensation of the solar nebula. In discussing conditions of the solar nebula gas cloud, it is assumed that the composition of the cloud was heterogeneous; that is, the highest temperature refractory elements were concentrated closer to

TABLE 4.– METEORITE MINERALS

I. The minerals of meteorites, up to 1962 (an asterisk indicates those not known to occur in terrestrial rocks). Table modified from Mason (1972).

Name	Formula
Kamacite	α-(Fe,Ni)
Taenite	γ-(Fe,Ni)
Copper	Cu
Diamond	C
Graphite	C
Sulfur	S
Schreibersite	$(Fe,Ni)_3P$
Cohenite	$(Fe,Ni)_3C$
*Osbornite	TiN
Troilite	FeS
*Oldhamite	CaS
Pentlandite	$(Fe,Ni)_9S_8$
*Daubreelite	$FeCr_2S_4$
Chalcopyrite	$CuFeS_2$
Pyrite	FeS_2
Sphalerite	(Zn,Fe)S
*Lawrencite	$(Fe,Ni)Cl_2$
Magnesite	$(Mg,Fe)CO_3$
Calcite	$CaCO_3$
Dolomite	$CaMg(CO_3)_2$
Quartz	SiO_2
Tridymite	SiO_2
Cristobalite	SiO_2
Ilmenite	$FeTiO_3$
Spinel	$MgAl_2O_4$
Magnetite	Fe_3O_4
Chromite	$FeCr_2O_4$
Chlorapatite	$Ca_5(PO_4)_3Cl$
Whitlockite	$Ca_9MgH(PO_4)_7$
*Farringtonite	$Mg_3(PO_4)_2$
Gypsum	$CaSO_4.2H_2O$
Epsomite	$MgSO_4.7H_2O$
Bloedite	$Na_2Mg(SO_4)_2.4H_2O$
Olivine	$(Mg,Fe)_2SiO_4$
Orthopyroxene	$(Mg,Fe)SiO_3$
Clinopyroxene	$(Ca,Mg,Fe)SiO_3$
Plagioclase	$(Na,Ca)(Al,Si)_4O_8$
Serpentine (or chlorite)	$(Mg,Fe)_6Si_4O_{10}(OH)_8$

II. Minerals discovered in meteorites since 1962 (an asterisk indicates those not known to occur in terrestrial rocks).

Name	Formula
Awaruite	Ni_3Fe
*Lonsdaleite	C
Chaoite	C
*Haxonite	$Fe_{23}C_6$
*Barringerite	$(Fe,Ni)_2P$
*Perryite	$(Ni,Fe)_5(Si,P)_2$
*Carlsbergite	CrN
*Sinoite	Si_2N_2O
Pyrrhotite	$Fe_{1-x}S$
Mackinawite	FeS_{1-x}
Heazlewoodite	Ni_3S_2
*Niningerite	(Mg,Fe)S
Alabandite[1]	(Mn,Fe)S
*Brezinaite	Cr_3S_4
Djerfisherite	$K_3CuFe_{12}S_{14}$
*Gentnerite[2]	$Cu_8Fe_3Cr_{11}S_{18}$
Rutile	TiO_2
Hercynite	$(Fe,Mg)Al_2O_4$
Hibonite	$CaAl_{12}O_{19}$
Perovskite	$CaTiO_3$
Whewellite	$CaC_2O_4.H_2O$
*Stanfieldite	$Ca_4(Mg,Fe)_5(PO_4)_6$
*Brianite	$CaNa_2Mg(PO_2)$
Graftonite	$(Fe,Mn)_3(PO_4)_2$
*Panethite	$(Ca,Na)_2(Mg,Fe)_2(PO_4)_2$
Sarcopside	$(Fe,Mn)_3(PO_4)_2)$
*Ringwoodite	$(Mg,Fe)_2SiO_4$
*Majorite	$Mg_3(MgSi)Si_3O_{12}$
Woolastonite	$CaSiO_3$
*Ureyite	$NaCrSi_2O_6$
Potash feldspar	$(K,Na)AlSi_3O_8$
Nepheline	$NaAlSiO_4$
Sodalite	$Na_8Al_6Si_6O_{24}Cl_2$
*Merrihueite	$(K,Na)_2Fe_5Si_{12}O_{30}$
*Roedderite	$(K,Na)_2Mg_5Si_{12}O_{30}$
*Yagiite	$(K,Na)_2(Mg,Al)_5(Si,Al)_{12}O_{30}$
Richterite	$Na_2CaMg_5Si_8O_{22}F_2$
Melilite	$Ca_2(Mg,Al)(Si,Al)_2O_7$
Zircon	$ZrSiO_4$
Grossular	$Ca_3Al_2Si_3O_{12}$
Andradite	$Ca_3Fe_2Si_3O_{12}$
Rhonite	$CaMg_2TiAl_2SiO_{10}$.
Cordierite	$Mg_2Al_4Si_5O_{18}$
*Krinovite	$NaMg_2CrSi_3O_{10}$
Monticellite	$Ca(Mg,Fe)SiO_4$
*Buchwaldite	$NaCaPO_4$

the proto sun and decreased in abundance with increasing distance away from the Sun. Necessarily, the temperature gradient fell from highest temperature near the Sun to low temperatures near the outer portions of the primitive solar system. Because of the temperature gradient and the heterogeneous distribution of elements, it follows that all elements were completely in the vapor state. Theoretical models and observational considerations imply that the individual planets change in composition from high concentrations of refractory and transitional elements close in to the Sun (terrestrial planets) to high concentrations of light, volatile elements in the colder environments now occupied by the Jovian planets.

The presence of organic compounds in carbonaceous chondrites also indicates that low-temperature processes must have been involved during certain phases of the history of these meteorites. The distribution of hydrocarbons, amino acids, and fatty acids suggests that these compounds have been formed by random, abiotic, chemical processes (Kvenvolden et al. 1974). Stereochemical considerations of amino acids and fatty acids have now confirmed the idea that the processes were random and that the compounds do not result from extraterrestrial life.

A sequence of mineral condensation during cooling of the nebular gas cloud has been calculated from thermodynamic data (Grossman and Larimer 1974) and is consistent with meteorite compositions, particularly refractory element inclusions in carbonaceous chondrites. In essence, the results suggest that the Ca-Al-rich inclusions are aggregates of highest temperature condensates. These condensates were followed, at lower temperatures, by crystallization of nickel-iron, forsterite (Mg_2SiO_4) and enstatite ($MgSiO_3$). With increasing oxidation state, iron substituted for magnesium in these minerals in ordinary chondrites. Thus, the oxidation-state and trends of abundance of siderophile elements appear to reflect formation at monotonically differing distances from the Sun. The refractory condensates may have been transported by solar radiation pressure to other parts of the solar system before lower temperature condensation. This theory may account for the admixture of both high and low temperature fractions in meteorites and for the inferred refractory element concentration of the Moon. Heterogeneous accumulation models may account for the apparent stratified nature of the Earth and possibly other terrestrial planets, where planetary interiors are enriched in refractory elements and iron, with the more volatile materials concentrated in the outer layers.

Lunar studies strongly infer a post-accretional surface melting and differentiation stage that separated the Moon into an outer layer of refractory material (anorthositic rocks) and an underlying residuum that subsequently gave rise to massive basalt flows through partial melting. These events may not have been restricted to the Moon, but may have occurred on some or all of the terrestrial planets by rapid buildup of heat from concentration of extinct radionucleides or an exterior heating event during the T-Tauri solar wind (Sonett et al. 1968) or the highly luminous Hayashi phase of the early Sun. The meteorite record shows that basaltic achondrites have magmatic textures and probably originated through partial melting of parent body materials.

Basaltic achondrites breccias (howardites) contain fragments of anorthositic composition, in addition to many kinds of basaltic fragments (Bunch 1975). Crystallization ages for two basalt fragments were determined by Papanastassiou et al (1974) and they correspond to crystallization events of 3.6×10^9 and 3.9×10^9 yr, events that are distinctively younger than ages for simple basaltic achondrites samples that average 4.4×10^9 yr. These "young" magmatic events, together with textural studies, suggest that the parent body was geologically active for

at least 1 AE after accretion. The Nakhla meteorite is a highly differentiated rock that has an inferred crystallization age of 1.34×10^9 yr (Papanastassiou et al. 1974). Nakhla also shows evidence of magmatic crystal settling and partial alteration by water (Bunch and Reid 1974, and Reid and Bunch 1975). These conditions are similar to terrestrial processes and dissimilar to those of other extraterrestrial bodies, as we know them. From these cases we can see that meteorite parent bodies have been geologically active for considerable periods of time, and we can gain tremendous insight into planetary processes by continued study of the many meteorite samples that are available.

Recent spectral reflectivity measurements of asteroids (McCord and Chapman 1975) show that many of the meteorite classes are represented in the surface materials. Most of the larger asteroids appear to have a lunar-like regolith. Meteorite breccias also appear to be similar to the lunar regolith and suggest that the parent bodies suffered severe surface modifications through impact events and mixing of materials. In addition, petrographic studies of these breccias (chondrite and achondrite breccias) indicate that each meteorite compositional and petrologic class probably originated as separate bodies because fragments of different meteorite classes are not found within other meteorite breccias; that is, H-group chondrites are not found in L-group chondrite breccias and ordinary chondrite fragments are not found in achondrite breccias as would be expected if these meteorites originated from the same parent body.

3.2.4 Igneous Rock Textures

Igneous processes, similar to those that occur in the Earth, have been evoked to account for many textures observed in meteorites, particularly the basaltic achondrites. These meteorites show textures that include ophitic, subophitic, variolitic, vitrophyric, granular, gabbroic, and cumulate (figs. 79, 80, 84, 85, 88–90) and imply various cooling rates and conditions similar to terrestrial and lunar equivalents; for example, vitrophyric meteoritic basalts probably cooled rapidly on extrusion onto the parent body surface. Moreover, cumulate textures imply crystal settling in a magma chamber in an environment of sufficient gravity to allow for short-time separation of crystals of slightly less density than the magma. By studying these textures and using terrestrial and lunar analogies, we can piece together the history of various meteorites and reconstruct their parent body or bodies.

We have learned that the ordinary chondrite and basaltic achondrite parent bodies had a surface regolith (loose soil and breccias) similar to that of the Moon. In addition, textural and compositional data strongly imply large-scale (at least sub-lunar) planetary differentiation, magma generation, formation of cumulate and gabbroic rocks, which together argue for at least an early, vigorous period of surface melting and differentiation for the basaltic achondrite parent body.

To err is human, but when the eraser wears out ahead of the pencil, you're overdoing it.

J. Jenkins

REFERENCES

Bunch, T. E. (1975). Petrography and petrology of the basaltic achondrite polymict breccias (howardites). Proc. 6th Lunar Sci. Conf. Geochim Cosmochim Acta, pp. 469–492.

Bunch, T. E. and E. Olsen (1975). Distribution and significance of Cr in meteorites. Geochim. Cosmochim. Acta, vol. 39, pp. 911–927.

Bunch, T. E. and A. M. Reid (1975). The Nakhlites: Part I: petrography and mineral chemistry. Meteorites, vol. 10, pp. 303–315.

Chapman, Clark R. (1975). The nature of asteroids. Scientific Amer., vol. 232, no. 1, pp. 24–33.

Clague, D. and T. E. Bunch (1976). Formation of ferrobasalts at east mid-ocean spreading centers. J. Geophy. Res. In press.

Compston, W., B. W. Chappell, P. A. Arriens, and M. J. Vernon (1970). The chemistry and age of Apollo 11 lunar material. Proc. Apollo 11 Lunar Sci. Conf., Geochim. Cosmochim Acta, Suppl. 1, vol. 2, pp. 1007–1027.

Dymek, R. F., A. L. Albee, and A. A. Chodos (1975). Comparative petrology of lunar cumulate rocks of possible primary origin: Dunite 72415, troctolite 76535, norite 78235, and anorthosite 62235. Proc. 6th Lunar Sci. Conf., Geochim. Cosmochim. Acta, Suppl. 6, vol. 1, pp. 301–341.

Fuchs, L. H., E. Olsen and K. J. Jensen (1973). Mineralogy, mineral chemistry and composition of the Murchison (C2) meteorite. Smithson. Contrib. Earth Sci., vol. 10, pp. 1–39.

Grossman, L. and J. W. Larimer (1974). Early chemical history of the Solar System, Revs. Geophys. Space Phys., vol. 12, pp. 71–101.

Hess, H. H. and E. Henderson (1949). The Moore Co. meteorite: a further study with comment on its primordial environment. Amer. Mineral., vol. 34, pp. 494–507.

Ito, K. and G. C. Kennedy (1974). The composition of liquids formed by partial melting of eclogites at high temperatures and pressures. J. of Geol., vol. 82, pp. 383–392.

Keil, K. (1969). Meteorite composition. Handbook of Geochemistry, K. H. Wedepohl, ed. Springer, Berlin-Heidelberg, vol. 1, pp. 78–115.

Kvenvolden, K. A. (1974). Amino and fatty acids in carbonaceous meteorites. In: The Origins of Life and Evolutionary Biochemistry, ed. K. Dose, et al., Plenum Publishing Corp.,

Mason, B. (1972). The mineralogy of meteorites, Meteoritics, vol. 7, pp. 309–326.

McCord, T. B. and Clark R. Chapman, (1975). Asteroids: Spectral reflectance and color characteristics: The Astrophysical Jour., vol. 195, pp. 553–562.

Papanastassiou, D. A., R. S. Rajan, J. C. Huneke, and G. J. Wasserberg (1974). Rb-Sr ages and lunar analogs in a basaltic achondrite; implication for early Solar System chronologies. In: Lunar Science – VI, pp. 583–585, Lunar Science Institute, Houston, Texas.

Reid, A. M. and T. E. Bunch (1975). The Nakhlites: Part II: Where, when and how. Meteoritics, vol. 10, pp. 317–324.

Sonett, C. P., D. S. Colburn, and K. Schwartz (1968). Electrical heating of meteorite parent bodies and planets by dynamo induction from a pre-main sequence T Tauri "solar wind." Nature, vol. 219, pp. 924–926.

Taylor, S. R. (1975). Lunar Science: A Post-Apollo View, Pergamon Press, Elmsford, N.Y., p. 372.

Van Schmus, W. R. and J. A. Wood (1967). A chemical-petrological classification for the chondritic meteorites, Geochim. Cosmochim Acta, vol. 31, pp. 747–765.

Warner, J. (1975). Mineralogy, petrology and geochemistry of the lunar samples, Rev. of Geophys. and Space Phys., vol. 13, no. 3, pp. 107–113.

Acknowledgments: My thanks are due to Profs. Kenzo Yagi and Ed Lidiak for their inspiring lectures when I was a graduate student at the University of Pittsburgh, a short decade ago. Thanks are also due to many of my students for their thought-provoking questions and innocent insight into my sometimes hurried lectures.